

FINAL REPORT ~ FHWA-OK-14-07

PORTABLE WEIGH-IN-MOTION FOR PAVEMENT DESIGN - PHASES 1 AND 2

Hazem Refai, Ph.D.
Ahmad Othman, M.Sc.
Hasan Tafish
School of Electrical and Computer
Engineering
College of Engineering
The University of Oklahoma

September 2014



DISCLAIMER

The contents of this report reflect the views of the author(s) who is responsible for the facts and the accuracy of the data presented herein. The contents do not necessarily reflect the views of the Oklahoma Department of Transportation or the Federal Highway Administration. This report does not constitute a standard, specification, or regulation. While trade names may be used in this report, it is not intended as an endorsement of any machine, contractor, process, or product.

PORTABLE WEIGH-IN-MOTION FOR PAVEMENT DESIGN – PHASES 1 AND 2

FINAL REPORT ~ FHWA-OK-14-07
ODOT SP&R ITEM NUMBER 2240

Submitted to:

John R. Bowman, P.E.
Planning & Research Division Engineer
Oklahoma Department of Transportation

Submitted by:

Dr. Hazem Refai, Ph.D.
Ahmad Othman, Graduate Student
Hasan Tafish, Graduate Student
School of Electrical and Computer Engineering (ECE)
The University of Oklahoma



October 2014

TECHNICAL REPORT DOCUMENTATION PAGE

1. REPORT NO. FHWA-OK-14-07	2. GOVERNMENT ACCESSION NO.	3. RECIPIENT'S CATALOG NO.	
4. TITLE AND SUBTITLE Portable Weigh-In-Motion for Pavement Design		5. REPORT DATE Oct 2014	
		6. PERFORMING ORGANIZATION CODE	
7. AUTHOR(S) Hazem Refai, Ph.D. Ahmad Othman Hasan Tafish		8. PERFORMING ORGANIZATION REPORT The University of Oklahoma 202 W. Boyd St., Room 104 Norman, OK. 73019-0631	
		9. PERFORMING ORGANIZATION NAME AND ADDRESS School of Electrical and Computer Engineering, The University of Oklahoma	
12. SPONSORING AGENCY NAME AND ADDRESS Oklahoma Department of Transportation Materials and Research Division 200 N.E. 21st Street, Room 3A7 Oklahoma City, OK 73105		10. WORK UNIT NO.	
		11. CONTRACT OR GRANT NO. ODOT SP&R Item Number 2240	
15. SUPPLEMENTARY NOTES		13. TYPE OF REPORT AND PERIOD COVERED Final Report Oct 2011 - Oct 2014	
		14. SPONSORING AGENCY CODE	
16. ABSTRACT <p>Keeping Oklahoma's roadways, highways, and bridges in good condition is necessary to our state's safety and to avoid expenditures in billions of dollars each year for road repairs and replacement. According to a study done by state of Oregon in 2009, heavy vehicles account for 79% (or \$60 million) of annual expenditures required for roadway repaving. Likewise, they were also responsible for 66.8% (or \$27 million) of pavement and shoulder reconstruction; 65.1% (or \$145 million) of pavement and shoulder rehabilitations; and 61.5% (or \$140 million) of pavement maintenance. To weigh traveling trucks, the state of Oklahoma has installed 20 permanent Weigh-in-Motion (WIM) sites. Expanding site coverage to include additional roadways and highways improves data accuracy; however, it requires significant roadside construction and costly infrastructure support. This report presents deployment results of a novel portable WIM system and compares captured data with that collected at a nearby permanent WIM system. Design, development, and road-installation details of the heavy-vehicle centric, portable WIM system are also provided. Outcomes demonstrate that the portable system maintains data quality but for short intervals and provides a viable alternative to permanent systems at merely 10 percent of the cost. The portable WIM system uses off-the-shelf components and commercially available WIM controllers. The WIM controller used was IRD iSINC Lite. The fabricated portable system could be promoted as an alternative WIM monitoring solution to permanent WIM systems and/or static scale stations, both of which are extremely expensive to install on highways. The portable WIM uses RoadTrax BL piezoelectric class-1 sensors, galvanized metal fixtures equipped with pocket tapes to house the sensors, and a trailer with cabinet to house WIM electronics, batteries, and REECE device for real-time monitoring. The system is solar powered with three 100-Watt panels, and it costs roughly \$20,000.</p>			
17. KEY WORDS Weigh in Motion, WIM, Portable, Permanent, Piezoelectric Detectors		18. DISTRIBUTION STATEMENT No restrictions. This publication is available from the Materials and Research Div., Oklahoma DOT.	
19. SECURITY CLASSIF. (OF THIS REPORT) Unclassified	20. SECURITY CLASSIF. (OF THIS PAGE) Unclassified	21. NO. OF PAGES 93	22. PRICE N/A

SI* (MODERN METRIC) CONVERSION FACTORS

APPROXIMATE CONVERSIONS TO SI UNITS				
SYMBOL	WHEN YOU KNOW	MULTIPLY BY	TO FIND	SYMBOL
LENGTH				
in	inches	25.4	millimeters	mm
ft	feet	0.305	meters	m
yd	yards	0.914	meters	m
mi	miles	1.61	kilometers	km
AREA				
in²	square inches	645.2	square millimeters	mm ²
ft²	square feet	0.093	square meters	m ²
yd²	square yard	0.836	square meters	m ²
ac	acres	0.405	hectares	ha
mi²	square miles	2.59	square kilometers	km ²
VOLUME				
fl oz	fluid ounces	29.57	milliliters	mL
gal	gallons	3.785	liters	L
ft³	cubic feet	0.028	cubic meters	m ³
yd³	cubic yards	0.765	cubic meters	m ³
NOTE: volumes greater than 1000 L shall be shown in m ³				
MASS				
oz	ounces	28.35	grams	g
lb	pounds	0.454	kilograms	kg
T	short tons (2000 lb)	0.907	megagrams (or "metric ton")	Mg (or "t")
TEMPERATURE (exact degrees)				
°F	Fahrenheit	5 (F-32)/9 or (F-32)/1.8	Celsius	°C
ILLUMINATION				
fc	foot-candles	10.76	lux	lx
fl	foot-Lamberts	3.426	candela/m ²	cd/m ²
FORCE and PRESSURE or STRESS				
lbf	poundforce	4.45	newtons	N
lbf/in²	poundforce per square inch	6.89	kilopascals	kPa

APPROXIMATE CONVERSIONS FROM SI UNITS				
SYMBOL	WHEN YOU KNOW	MULTIPLY BY	TO FIND	SYMBOL
LENGTH				
mm	millimeters	0.039	inches	in
m	meters	3.28	feet	ft
m	meters	1.09	yards	yd
km	kilometers	0.621	miles	mi
AREA				
mm²	square millimeters	0.0016	square inches	in ²
m²	square meters	10.764	square feet	ft ²
m²	square meters	1.195	square yards	yd ²
ha	hectares	2.47	acres	ac
km²	square kilometers	0.386	square miles	mi ²
VOLUME				
mL	milliliters	0.034	fluid ounces	fl oz
L	liters	0.264	gallons	gal
m³	cubic meters	35.314	cubic feet	ft ³
m³	cubic meters	1.307	cubic yards	yd ³
MASS				
g	grams	0.035	ounces	oz
kg	kilograms	2.202	pounds	lb
Mg (or "t")	megagrams (or "metric ton")	1.103	short tons (2000 lb)	T
TEMPERATURE (exact degrees)				
°C	Celsius	1.8C+32	Fahrenheit	°F
ILLUMINATION				
lx	lux	0.0929	foot-candles	fc
cd/m²	candela/m ²	0.2919	foot-Lamberts	fl
FORCE and PRESSURE or STRESS				
N	newtons	0.225	poundforce	lbf
kPa	kilopascals	0.145	poundforce per square inch	lbf/in ²

*SI is the symbol for the International System of Units. Appropriate rounding should be made to comply with Section 4 of ASTM E380.

ACKNOWLEDGMENTS

PI Dr. Refai and his research team recognize Daryl Johnson, Jon Mitchell, Aaron Fridrich, and Brian Thompson at the Oklahoma Department of Transportation for their support in coordinating highway deployments, testing the developed system, and engaging in insightful discussions throughout this project. In addition, the authors acknowledge International Road Dynamics (IRD) for the technical support provided to aid in configuring the iSINC Lite WIM controller.

TABLE OF CONTENTS

ACKNOWLEDGMENTS	vi
TABLE OF CONTENTS	vii
LIST OF FIGURES	x
Executive Summary	1
1 Introduction and Background	3
1.1 Introduction.....	3
1.2 Existing knowledge.....	4
1.3 WIM sensors	5
1.4 Current portable WIM systems	6
1.5 Report organization	7
2 Portable WIM System	8
2.1 Introduction.....	8
2.2 Portable WIM system design	8
2.2.1 Sensors and sensors housing.....	8
2.2.2 Housing trailer.....	9
2.2.3 REECE and embedded software development	9
2.2.4 WIM controller.....	10
3 Sensor Installation and Highway Deployments	12
3.1 Introduction.....	12
3.2 Single lane deployment	12
3.2.1 Initial sensor layout	12
3.2.2 Sensors fixture affixing methods	13
3.2.3 Site selection	14
3.2.4 Site installation steps	14
3.3 Two-Lane deployments	16
3.4 Portable-specific configuration and calibration factors	16
3.5 Deployment durability	17
4 Calibration and Field-Testing	18
4.1 Introduction.....	18
4.2 Portable WIM configuration.....	18

4.2.1	Sensors thresholds and bounce adjustments.....	18
4.2.2	Calibration method and special adjustments.....	18
4.3	Field testing using test-trucks.....	19
4.3.1	Data analysis for the weight recorded by portable WIM system.....	20
5	Temperature Effect on Portable WIM Measurement.....	24
5.1	Introduction.....	24
5.2	Experiment setup.....	24
5.3	Portable WIM measurement analysis for campus deployment:.....	25
5.4	Portable WIM measurement analysis for highway deployment:.....	26
5.5	Conclusion.....	27
6	Vehicle Signature Development Using WIM Data.....	28
6.1	Introduction.....	28
6.2	Large-scale vehicle signature study and data mining.....	28
6.3	Vehicle detection at multiple WIM sites.....	29
6.4	Conclusion.....	30
7	Portable WIM Aggregate Data Analysis.....	32
7.1	Introduction.....	32
7.2	Vehicle count statistical distribution analysis.....	32
7.2.1	Class 9 First Axle Weight (FXW) distribution.....	32
7.2.2	Class 9- Gross Vehicle Weight (GVW) distribution.....	33
7.2.3	Vehicle classification.....	34
7.2.4	Class 9 vehicle speed distribution.....	34
7.2.5	Class 9 First Axle Spacing (FXS) distribution.....	35
7.3	Aggregate linear regression analysis.....	36
8	Portable WIM Per-Vehicle Analysis.....	40
8.1	Introduction.....	40
8.2	Time shift and alignment algorithm.....	40
8.3	Advance alignment algorithm (AALA) development.....	41
8.3.1	Anchors extraction.....	41
8.3.2	ALAA performance analysis.....	44
8.4	Per-vehicle analysis:.....	45
8.5	Probability of error.....	50
8.5.1	GVW deference histogram:.....	50
8.5.2	FXW difference histogram.....	50
8.6	WIM data analysis day-by-day.....	50

9	WIM Error Modeling and Site Calibration Monitoring	57
9.1	Introduction.....	57
9.2	Related work	58
9.3	Outliers (Anomaly) detection.....	59
9.3.1	Introduction	59
9.3.2	Algorithm formulation	59
9.3.3	Detecting outliers in WIM16 data	62
9.3.4	Detecting outliers in portable WIM data.....	70
9.4	WIM data quality monitoring software	72
9.4.1	Software architecture	72
9.4.2	Software Implementation	73
10	Conclusion	77
	References	79

LIST OF FIGURES

Figure 2.1 Portable WIM system architecture.....	8
Figure 2.2 Measurement Specialties Roadtrax BL piezoelectric sensor	8
Figure 2.3 Portable WIM trailer before the installation of the power system, WIM controller and the REECE	9
Figure 2.4 REECE device, courtesy of Diamond Systems	9
Figure 2.5 Main steps for configuring the iSINC Lite as portable WIM station	11
Figure 3.1 Sensors layout in early deployments.....	12
Figure 3.2 Revised sensor layout.....	13
Figure 3.3 Two-lane portable WIM system deployment, near WIM16.....	14
Figure 3.4 Pocket tape insertion using fishing wire and lubricant	15
Figure 3.5 The fixture affixing	15
Figure 3.6 Two lanes schematic.....	16
Figure 3.7 Deployment durability sensors after 20-day deployment and then after 40 days.	17
Figure 4.1 Calibration Methodology.....	19
Figure 4.2 iSINC calibration steps for one sensor in the first lane	20
Figure 5.1 Temperature probe schematics.....	24
Figure 5.2 REECE data acquisition I/O connector.....	25
Figure 5.3 Weight measurements with temperature variations	26
Figure 5.4 Regression plot to detect temperature trends in portable WIM systems	27
Figure 7.1 First axle weight class 9 vehicles for phase I, II, and III respectively.....	33
Figure 7.2 GVW comparison study, first, second and third phases respectively	34
Figure 7.3 Vehicle classes comparison study first, second and third phases respectively	35
Figure 7.4 Speed comparison study, Phases I, II, and III respectively.....	36
Figure 7.6 GVW regression for the first 4 days of deployment.....	38
Figure 7.5 GVW regression for days 5 to 19.	38
Figure 7.7 FXW regression analyses for the first 4 days (left) and days 5-19 (right).....	39
Figure 7.8 Speed regression analyses for the first 4 days (left) and days 5-19 (right)	39
Figure 8.1 Alignment using anchors algorithm (ALAA) flow graph.....	42
Figure 8.2 ALAA anchor-based relative-detection-time computation	43
Figure 8.3 Histogram of recorded classes of both sites on two different days.	44
Figure 8.4 The extraction of anchors and test records.....	45
Figure 8.5 Anchors' List	45
Figure 8.6 Changes of under-matched records percentage.....	46
Figure 8.7 Linear regression for permanent to portable GVW comparison	49
Figure 8.8 Linear regression for permanent to portable FXW comparison.....	49
Figure 8.9 Linear regression of speed measurements obtained from permanent and portable systems.....	50
Figure 8.10 GVW error histogram	51
Figure 8.11 FXW error histogram.....	51
Figure 8.12 The relative classification error of portable WIM.....	52
Figure 8.13 Daily relative error in axles' weight	53
Figure 8.14 Daily relative speed error.	53
Figure 8.15 Daily relative GVW error.....	54
Figure 8.16 The distribution of class 9 GVW in days 4 and 32	55
Figure 8.17 Daily changes of mean GVW	55
Figure 8.18 The relationship between GVW error and true GVW	56

Figure 9.1 Changes in WIM16 traffic volume and number of class 0 during 2013.	57
Figure 9.2 Exponential growth in number of class 0 vehicles prior to re-calibration.	58
Figure 9.3 Feature 2 vs. Feature 1 scatter plot.	60
Figure 9.4 Distributions of Features 1 and 2.	61
Figure 9.5 Bivariate distribution of Feature 1 and 2 and corresponding contour.	61
Figure 9.6 Scatter of test observations on training contour plot.	62
Figure 9.7 Classification and speed accuracy of WIM16.	63
Figure 9.8 Percentage of class 9 vehicles detected following calibration.	64
Figure 9.9 Linear regression of GVW and fourth-axle weight for days 1 and 52.	64
Figure 9.10 Relationship between GVW and first- and fourth-axle weights.	65
Figure 9.11 Distribution of class 9 GVW in permanent and portable WIM.	66
Figure 9.12 Results of Applying EM on WIM16 class 9 GVW data.	67
Figure 9.13 Histograms and PDFs of speed and weight ratio for unloaded trucks.	67
Figure 9.14 Bivariate model of unloaded trucks.	68
Figure 9.15 Histograms and PDFs of speed and weight ratio for loaded trucks.	68
Figure 9.16 Bivariate model of loaded trucks.	69
Figure 9.17 Anomaly detection flow diagram.	69
Figure 9.18 Relative number of outliers in WIM16 data.	70
Figure 9.19 Histograms of GVW vs. class for days 1 and 41.	71
Figure 9.20 Percentage of outliers in portable WIM.	71
Figure 9.21 The relationship between system performance and time.	72
Figure 9.22 WIM quality software architectures.	74
Figure 9.23 Sub-database diagram of the monitoring.	76
Figure 9.24 Email addresses GUI.	76

Executive Summary

The Federal Highway Administration issues the Mechanistic Empirical Pavement Design Guide to aid engineers in improving paved road design. Precise truck weight input data is necessary to calculate optimal pavement thickness. To comply, many states have installed permanent Weigh-in-Motion (WIM) sites to gather such information. Expanding site coverage to include additional roadways and highways would improve data accuracy; however, doing so requires significant roadside construction and costly infrastructure support. This report presents deployment results of a novel portable WIM system and compares captured data with that collected at a nearby permanent WIM system. Design, development, and road-installation details of the heavy-vehicle centric, portable WIM system are also provided. Outcomes demonstrate that the portable system maintains data quality but for short intervals and provides a viable alternative to permanent systems at merely 10 percent of the cost.

This report presents results of a newly developed portable WIM system that uses off-the-shelf components and commercially available WIM controllers. The commercial WIM controller used in this project was IRD iSINC Lite. The fabricated portable system could be promoted as an alternative WIM monitoring solution to permanent WIM systems and/or static scale stations, both of which are extremely expensive to install on highways. The portable WIM uses RoadTrax BL piezoelectric class-1 sensors, galvanized metal fixtures equipped with pocket tapes to house the sensors, and a trailer with cabinet to house WIM electronics, batteries, and REECE device for real-time monitoring. The system is solar powered with three 100-Watt panels. Total cost of system is roughly \$20,000.

The developed portable WIM system was deployed at various locations for the duration of the project. However, the majority of the deployments occurred on ODOT WIM16 located on US412 with concrete roadway. An optimal installation and on-road sensor concrete affixing processes were developed to allow extended deployment periods of the portable WIM system. System performance showed acceptable WIM measurement results with little variations within the first 15 days following the sensor road installation. Portable WIM data was compared to data collected at nearby permanent WIM sites. Error and regression analyses were performed. Root mean square errors and correlation coefficient were calculated on a record-by-record and aggregate basis for GVW, speed, classification, and FXW. 98% of successful vehicle classification by the portable WIM was achieved. 62% of detected class 9 vehicles had a GVW within 30% of that measured at the permanent WIM site.

This Page Is Intentionally Blank

Chapter I

1 Introduction and Background

1.1 Introduction

Keeping the public's roadways, highways, and bridges in good condition is not only vital to our nation's safety, it is necessary to avoid expenditures in the billions of dollars each year for road repair and replacement. In 2009, a study of highway cost allocation conducted in the state of Oregon showed that heavy vehicles account for 79% (or \$60 million) of annual expenditures required for new roadway repaving. Likewise, heavy vehicles were responsible for 66.8% (or \$27 million) for pavement and shoulder reconstruction; 65.1% (or \$145 million) for pavement and shoulder rehabilitations; and 61.5% (or \$140 million) for pavement maintenance [1]. Road deterioration is the result of many factors, including: road characteristics (pavement materials and thickness); weather conditions (temperature cycles and precipitation); and dynamic interaction between vehicle and road (speed, suspension characteristics, and surface roughness), in addition to loads distinguished by axle spacing, tire pressure, and weight per axle [2]. Of these, vehicle axle weight proves to be the most significant factor for accelerating road wear. "Reducing the average weight of truck axles would substantially reduce the rate of pavement wear. Reducing the load on an axle by half, for example from 30,000 to 15,000lbs, would reduce wear by a factor of roughly 16"[2]. A study of the American Association of State Highway Transportation Officials, (AASHTO) [3] found that removing a single, significantly overweight truck (e.g., 20,000lbs above the weight limit) would have the same positive impact on roadway conditions as eliminating 44,500 passenger vehicles [4]. Given this information, one can see that it is imperative to engineer a solution to reduce the rate of road deterioration resulting from heavy vehicle wear.

Both appropriately weighted and overweight trucks are chiefly responsible for rapid road deterioration. Collecting accurate weight data to aid in pavement design, and then enforcing weight limit on highways could mitigate unnecessary wear. Accordingly, the life expectancy of roads and bridges would increase while maintenance costs would decrease.

To slow the rate of road deterioration, weight-monitoring systems should be deployed across interstate and intrastate roadways and highways. The State of Oklahoma currently employs permanent weigh-in-motion (WIM) and/or static weight stations. However, high installation costs limit system implementation to interstate highways and state port of entries. Permanent WIM installation could exceed \$200k per site, and static weight station installation could surpass \$800k per site. The project reported herein presents research critical to implementing an inexpensive portable WIM system to monitor and enforce heavy vehicle weight limits. The system uses piezoelectric technology to detect and weigh traveling vehicles by measuring applied force. The system integrates a commercially-available WIM sensor and controller with a roadside embedded extensible computing equipment (REECE) unit.

1.2 Existing knowledge

For over 40 years WIM technology has been considered an effective means of collecting data for highway planners, pavement designers, and weight enforcement. The American Society for Testing and Materials (ASTM) defines WIM as “the process of measuring the dynamic tire forces of a moving vehicle and estimating the corresponding tire loads of the static vehicle” [5]. Modern technologies enable WIM devices to collect dynamic information that can be compared to a static scale—defined in 1998 by the National Institute of Standards and Technology—for accurate measurement. With its dynamic capability, a WIM device can perform weight measurement for vehicles traveling at high speeds and minimize unnecessary stops and delays inherent with a more invasive type of regulation enforcement.

WIM devices are commonly divided into three categories: permanent, semi-permanent, and portable systems. Each is comprised of two elements—a sensor and a controller—for data collection and analysis. Categories are differentiated based on equipment portability. Permanent devices collect and analyze data inclusively at a single, fixed location. Although semi-permanent systems have sensors built into the pavement, the system controller can be relocated from one site to another. Portable device equipment, as inferred by the name, can be moved as a total system from site to site.

Accurately measuring vehicle weight using a WIM proves challenging dependent upon various conditions, requirements, and factors (e.g. quality of the deployment site [6]; WIM sensor installation and road placement [7]; system calibration; vehicle dynamics at the time the WIM sensor is impacted; and accurate vehicle classification).

WIM site selection criteria include grade, curvature, cross-slope, width, speed, surface smoothness, pavement rutting, visibility, and effects from dirt or leftover sand administered during winter conditions. A level grade is required to prevent the effects of weight shifting between front and back axles of a loaded truck. WIM site performance is best when traffic is traveling at a constant speed. A straight and visible section of the road should be selected to prevent drivers from changing lanes or speed. Also, sites should be located away from highway entry and exit ramps.

Vehicle speed, acceleration, and deceleration dynamics impact weight measurement accuracy as vehicles travel over the WIM sensor [8]. Likewise, vehicle air pressure and travel direction (e.g., lane changing) are also factors that impact measurement accuracy. Unlike site selection, such dynamics are beyond the control of WIM site selection.

Improving the accuracy and increasing the life span of WIM devices has been investigated extensively in the literature. Generally, researchers have discussed two approaches. The first is improving calibration techniques, which can be established by either taking advantage of statistical analysis of road pavements and vehicle data [9]-[10] or by applying signal processing techniques [11]-[12] on the originated signal by the sensor, thus increasing the system’s immunity to noise. The second approach is

applying new sensor technologies, such as acoustic wave WIM [13], multisensory WIM [14], fiber optics WIM [15][16], or bridge WIM [17][18], to the system. Although new solutions have been presented, WIM systems remain inadequate and suffer from high installation and maintenance costs.

1.3 WIM sensors

Durability, accuracy, ease of handling, on-road installation and maintenance, calibration needs and frequency, and cost are among varying factors that distinguish sensors. Although a completely reliable sensor is not yet commercially available, the following provides a list of current sensor types along with their published advantages and disadvantages [19].

1. Bending plate:
 - Advantages:
 - Designed for traffic data collection and weigh estimation use
 - High accuracy (more so than piezoelectric systems) and low cost (less than load cell systems)
 - Minimal maintenance with required refurbishing after four to five years
 - Disadvantages:
 - Less accurate than load cells
 - More expensive than piezoceramic
2. Piezoceramic
 - Advantages:
 - High speed (e.g., 10 to 70 miles per hour) tolerance
 - Monitors up to four lanes
 - One piezoceramic
 - Least expensive
 - Disadvantages:
 - Less accurate than load cells and bending plate
 - Sensitive to temperature and speed variations
 - Replacement required within three years of deployment
3. BL (Brass Linguni) Piezoceramic
 - Advantages:
 - In addition to those listed above for piezoceramic, BL piezoceramic sensors are extremely flexible, which proves to be significantly beneficial during installation
 - Disadvantages:
 - In addition to those listed above for piezoceramic, high output voltages (e.g., up to 35V) are generated
4. Piezoquartz (partially piezoelectric but with newer technology)
 - Advantages:
 - Negligible temperature effect enables immunity to age or fatigue
 - Accuracy and cost within load cells range
 - Disadvantages:
 - Inoperative for portable WIM application
 - More expensive than other piezoceramic technologies

5. Hydraulic Load cell
 - Advantages:
 - Most accurate
 - Inoperative for traffic data collection and weight estimation
 - Disadvantages
 - Inoperative for portable WIM applications
 - Most expensive
 - Highest maintenance cost
 - Replacement required five years after deployment
6. Capacitive Mat
 - Advantages:
 - Functional for portable WIM applications
 - Monitors up to four lanes
 - Disadvantages
 - Less accurate than load cells, bending plates, or piezoquartz WIM devices
 - Trucks easily avoid driving on the mats
 - Trucks easily damage mats when breaks are applied to the mat surface
 - High equipment and installation cost are similar to those for load cell
7. Fiber-optic based
 - Advantages:
 - Light-weight
 - Immune to electromagnetic interference
 - Hostile environment insertion
 - High bandwidth capability
 - Lower cost
 - Time-saving installation
 - Low power requirements
 - Disadvantages
 - Inaccurate weight measurements when using long fibers
 - Fragile
 - Limited availability—only one known device is available in the marketplace
 - Underdeveloped technology

1.4 Current portable WIM systems

Several commercial, low-speed portable WIM systems, including DAW300 PC from IRD [20], are currently available. This particular system uses portable bending plates that weigh vehicles up to 40,000lbs per axle at speeds up to 40 mph. The manufacturer claims $\pm 3\%$ accuracy for vehicles traveling < 8 mph, and $\pm 4\%$ for travel speeds between 8 and 15 mph. From this information one can easily surmise that accuracy is inversely proportional to the speed of the vehicle.

A more precise, low-speed portable WIM system for vehicle speeds of 5kph (i.e., approximately 3mph) is also commercially available. CAPTELS CET 10-4 SLIM [21]

weighs vehicles up to 60,000lbs per axle with a declared accuracy of $\pm 2\%$ for vehicles traveling at the recommended speed. This portable WIM system employs metal weight pads fashioned from strengthened aluminum and covered with a special coating.

A highly accurate, slow-speed portable WIM developed by Oak Ridge National Laboratory (ORNL) [22] was originally designed for military use to control air force cargo loads. Advanced software features enable tracking and military vehicle location services, as well as calculating vehicle center-of-balance [23]. According to army specifications, two generations were developed. First generation (WIM Gen I) accuracy was $\pm 3\%$, and second generation (WIM Gen II) was less than $\pm 1\%$ [24].

Dr. Taek Kwon from the University of Minnesota, Duluth has developed a weigh pad-based portable WIM system with easy-to-install road sensors. Similar to our design, this particular WIM uses a RoadTrax BL piezoelectric sensor. The sensor is placed between two convey belts for rapid road installations. Notably, this configuration will not support deployment beyond one or two days. Software algorithms must be developed to calculate weight from piezoelectric sensors signals [25]. Unlike Kwon's design, ours uses a commercially available WIM controller that does not require software development for weigh calculations.

1.5 Report organization

This report is organized as follows; Chapter I provides an extensive background presenting various sensors used in current WIM system developments. It further presents related research and/or development in portable WIM systems. Chapter II details the portable WIM system design including hardware and software components. Chapter III illustrates the sensor road installation and layout. It presents various layout configurations for one or two lane installations. Chapter IV explains the process of portable WIM equipment calibration necessary for accurate WIM measurements. It also presents results of the field-testing with a test-truck with a known load weight. Chapter V briefly examines the effect of temperature on the WIM measurements made with the developed portable system. Chapter VI attempts to explore the potential of identifying class 9 vehicles as they travel across the state of Oklahoma passing by various permanent WIM sites. Chapter VI and VII extensively analyzes the accuracy of the portable WIM measurements by comparing them with their counterpart measurements collected at the associated permanent site. WIM measurements including among others gross vehicle weight (GVW), front axle weight (FXW), vehicle classification, and misdetection have been examined record-by-record and in aggregate fashion. Chapter IX details a multivariable statistical tool to detect when permanent or portable WIM measurements are becoming inaccurate and a site recalibration is required to improve the system performance. Chapter X concludes this report.

Chapter II

2 Portable WIM System

2.1 Introduction

This short chapter details the design of the portable WIM system. The system was developed to self-powered using solar panels and was equipped with broadband wireless telemetry system to allow for remote site communication.

2.2 Portable WIM system design

This section describes the portable WIM system components, namely sensors and trailer components, including cabinet, batteries, wiring, solar panel controllers, REECE, and WIM electronic controller, among others. The overall portable WIM system logical architecture is shown in Figure 2.1.

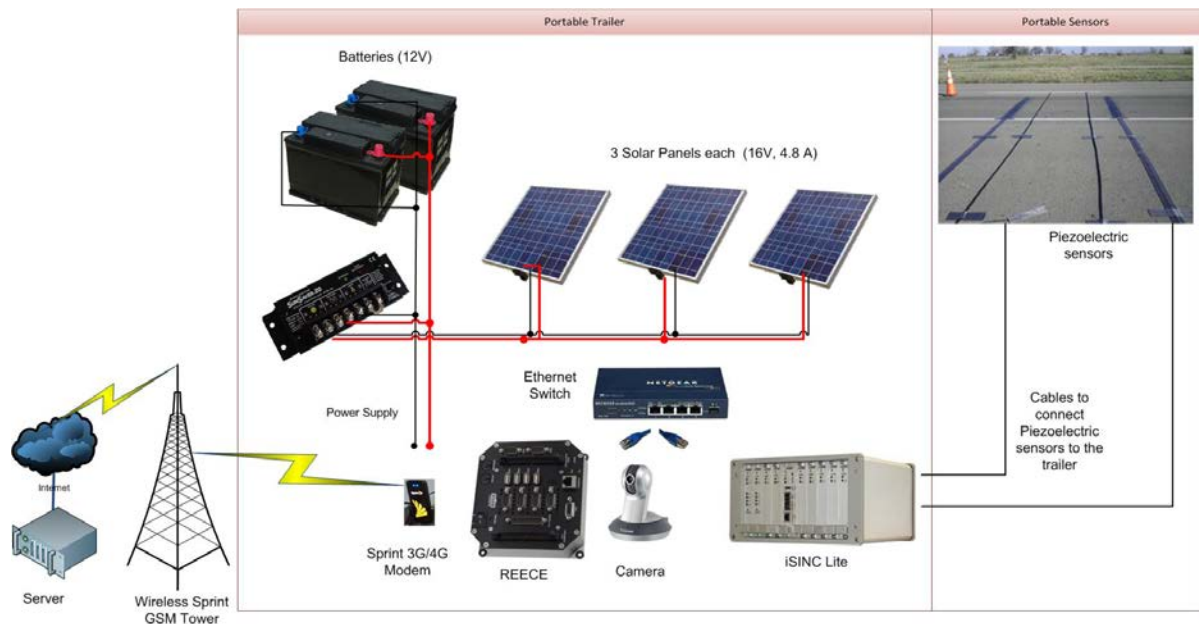


Figure 2.1 Portable WIM system architecture

2.2.1 Sensors and sensors housing

Two 12ft, class 1 piezoelectric Roadtrax BL sensors were employed in the portable WIM system, as shown in Figure 2.2. This technology has proven highly effective for traffic applications and weight measurements. The sensors are manufactured by Measurement Specialties and designed to withstand a substantial amount of weight. The sensors deliver bell-



Figure 2.2 Measurement Specialties Roadtrax BL piezoelectric sensor

shaped pulses when activated by passing vehicle axle loads. Although the sensor Roadtrax sensor is relatively expensive, the special road surface deployment of the proposed system requires a highly dependable and reliable sensor of this type.

2.2.2 Housing trailer

ODOT supplied a trailer with cabinet for our research project. Figure 2.3 shows the trailer and cabinet prior to installing the power system, WIM controller, and REECE device.



Figure 2.3 Portable WIM trailer before the installation of the power system, WIM controller and the REECE

The trailer power system was fabricated by wiring three 100 W/M2 Pro 4 JF solar panels manufactured by Siemens® Solar Industries. Maximum generated power is 75 watts at over 4.4amps. Solar panels were interfaced with a Morningstar® SunSaver-20 voltage regulator to adjust and control battery current up to 20amps with 16volts for both solar and load current. Solar panels charge two 100 amp/hour deep cycle batteries, which were placed inside the trailer along with the selected WIM controller and REECE device.

2.2.3 REECE and embedded software development

The REECE device is an embedded computer system with a Linux core operating system. REECE was first developed in 2005 by the PI and his research team with funds from the Oklahoma Transportation Center (OTC). The 2005 project objective was to enable remote wireless access to ODOT traffic automatic vehicle classifying (AVC) sites. Diamond Systems Prometheus was used for the



Figure 2.4 REECE device, courtesy of Diamond Systems

embedded computing system.

A new generation Diamond Systems Helios unit was designed for improved functionality. The Helios 800 vortex86DX CPU processor is equipped with four USB ports, six serial RS-232 ports, PS/2 mouse and keyboard ports, 10/100 Ethernet port, and ports, PS/2 mouse and keyboard ports, 10/100 Ethernet port, and a VGA port. In addition to four analog outputs, the system has 40 digital manageable Input/Output (I/O) lines connected to a built-in Data Acquisition (DAQ) board.

2.2.4 WIM controller

Portable WIM deployment utilizes an IRD iSINC Lite WIM electronic controller connected to the REECE through a crossover PC-PC Ethernet cable. This section explains the special configuration of the WIM system controller. The portable WIM deploys iSINC Lite to interface only with piezoelectric sensors. The following iSINC configuration is essential for appropriate portable WIM implementation:

- 1- Disable loops
- 2- Set a zero distance between axle sensors and loops
- 3- Interface sensors with accurate module

Subsequent mandatory configuration steps include creating a new site, configuring site parameters, and loading the classification scheme, as shown in Figure 2.5. Note that chosen settings and various menu factors, including values for each menu and submenu in the settings, are illustrated below.

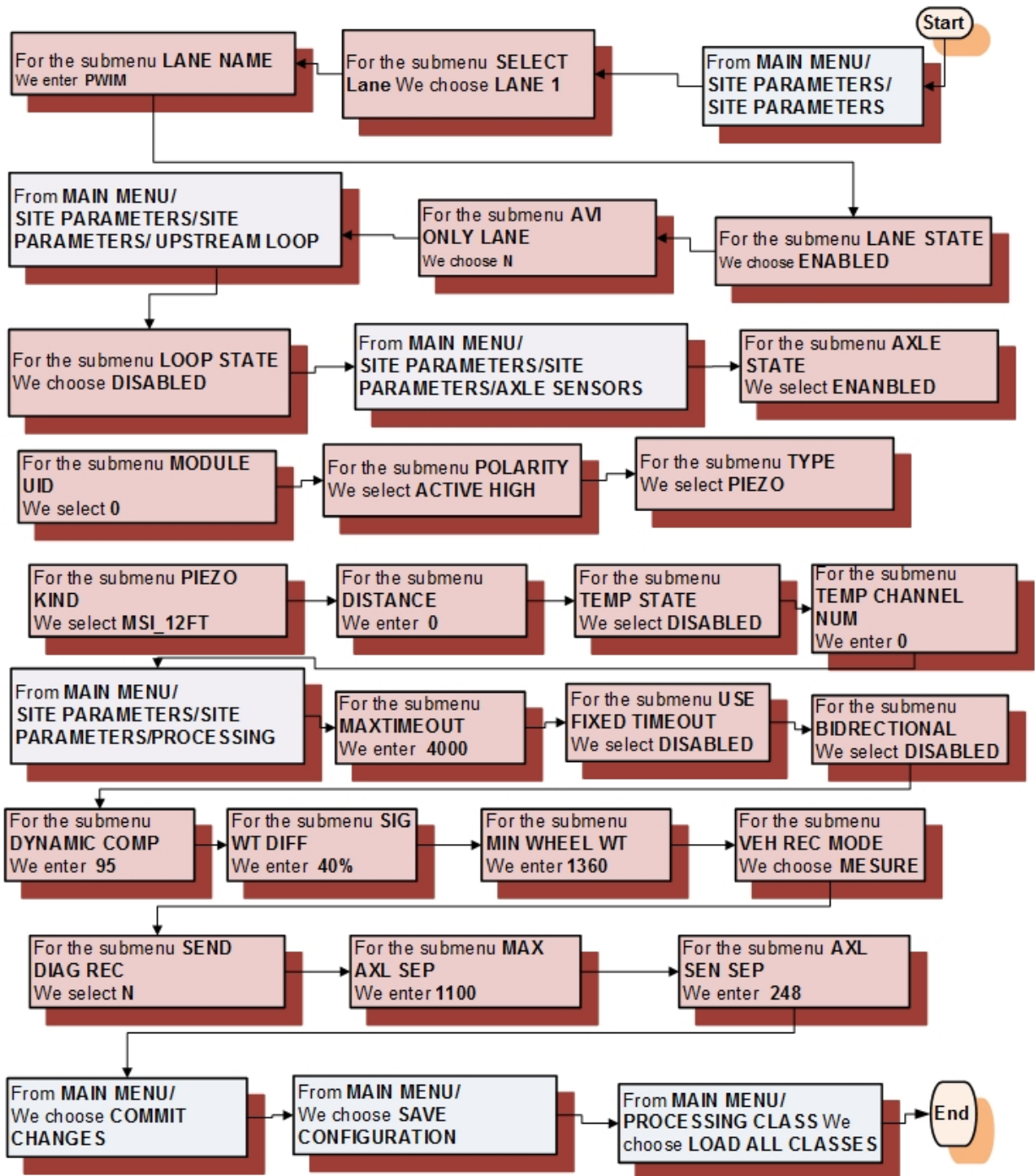


Figure 2.5 Main steps for configuring the iSINC Lite as portable WIM station

Chapter III

3 Sensor Installation and Highway Deployments

3.1 Introduction

This chapter reports single- and two-lane installation, including sensor layout and an affixing method developed after several portable WIM deployments. The research team implemented lessons learned to ensure acceptable road installation. By recording a lower level of sensor vibration, the number of detected signal ticks resulting from vehicle impact on the sensor is reduced, as is the number of undetected vehicles. Results obtained from deployments are presented in the succeeding chapters.

3.2 Single lane deployment

3.2.1 Initial sensor layout

Two 8ft metal steel fixtures were used to protect the sensors. Four inches of highly adhesive Bituthane tape with a 1in pocket were attached to the metal plates to encase and protect the sensor from direct exposure to vehicles tires. Materials were chosen to ensure rapid installation on a road surface and avoid prolonged traffic interruption.

After analyzing system performance during deployment one and two, the team revised the layout. An early deployment layout is illustrated in Figure 3.1.

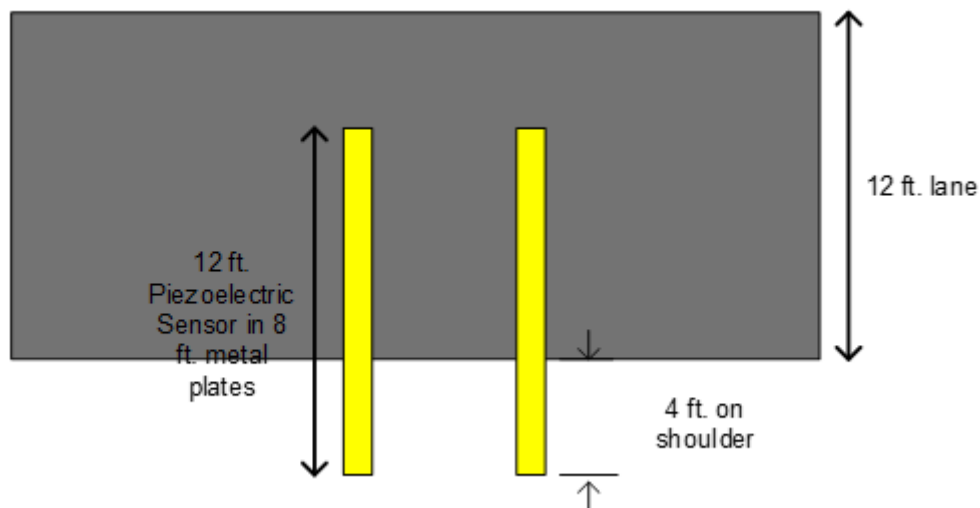


Figure 3.1 Sensors layout in early deployments.

To improve performance, the ground surface sensory area was reduced to a minimum. For this configuration, BL sensor length was reduced to 6ft. Sensor signal quality from overpassing vehicles increased significantly. The revised sensor layout is illustrated in Figure 3.2.

Performance improvement resulted from minimizing propagated vibration caused by vehicle impact with either the sensors or the fixture on which the sensors are held.

Twelve-foot sensors were shortened to a more effective 6ft length. Errant vehicle detection and classification were directly influenced by sensor vibration and number of ticks recognized by the WIM controller. A tick threshold is configured in the WIM controller to filter out noise from actual vehicles.

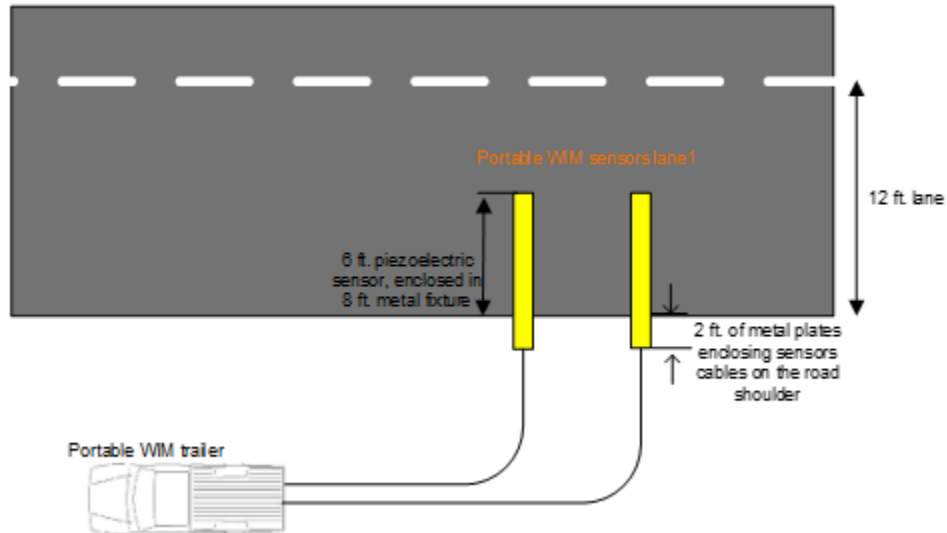


Figure 3.2 Revised sensor layout.

3.2.2 Sensors fixture affixing methods

As indicated earlier, sensor vibration increases errant vehicle detection. Hence, it is important that the fixture used to hold the sensors on the roadways is designed to limit vibration. The fixtures used for deployment were made of a 22 gauge, 8ft sheet of steel metal cut in specific dimensions to accommodate a piece of Mar Mac tape to house the sensor. Fixture width was 1ft, and 1in on each side edge was folded. Nail/screw holes in the leading edge facing traffic were drilled every 6in. Holes were drilled every 1ft in the back edge. The center of the sheet was sanded to a rough surface, and then heated to 90 degrees Celsius for tape attachment. Mar Mac tape was placed on the opposite of roadside of the sheet and served as a cushion between the fixture and the road. The fixture was outfitted with tape and sensor before road installation to facilitate rapid road installation with nails or screws.

The main portable WIM system field-testing and deployments were on concrete. The research team employed 3in concert screws instead of PK nails used on pavement. Concrete surface holes were drilled to a depth of 3in; concrete screws were inserted through the top of the fixtures. Sensor vibration was limited significantly, which reduced the number of undetected and misclassified vehicles. Of note is that each installation required 1-1/2 hours for expert installers.

3.2.3 Site selection

ODOT permanent WIM016 site is located on a concrete highway section of US-412 near Chateau, OK. Its proximity to the OU-Tulsa campus made it a good choice for the majority of the study. The portable WIM was positioned 75ft downstream from the permanent site. This section of highway is characterized by heavy traffic. However, far fewer class 9 trucks and significantly more passenger vehicles travel past previous deployment at WIM005 site located on US69 highway. The two lanes sensor deployment is shown in Figure 3.3.



Figure 3.3 Two-lane portable WIM system deployment, near WIM16.

3.2.4 Site installation steps

Best practices learned from the second deployment informed that the pocket tape should not be enlarged for sensor insertion. An enlarged pocket allows increased sensor vibrations and detection errors. Subsequent deployments used fishing wire and lubricant to ease sensor insertion into the pocket tape. See Figure 3.4.

Three-inch concrete screws were used to attach metal fixtures to the road surface. Two portable Milwaukee battery-powered hammering drills were initially used to drill 3in deep holes into the concrete prior to inserting and firmly tightening the screws. Spare drill batteries and extra drill bits were carried on site for installation purposes. Single-lane deployment lasted approximately 3hrs and required two persons. One drilled the hole

while another placed and fastened the fixture onto the roadway. Figure 3.5 shows the concrete installation of the fixture.



Figure 3.4 Pocket tape insertion using fishing wire and lubricant

Three-inch concrete screws were used to attach metal fixtures to the road surface. Two portable Milwaukee battery-powered hammering drills were initially used to drill 3in deep holes into the concrete prior to inserting and firmly tightening the screws. Spare drill batteries and extra drill bits were carried on site for installation purposes. Single-lane deployment lasted approximately 3hrs and required two persons. One drilled the hole while another placed and fastened the fixture onto the roadway. Figure 3.5. shows the concrete installation of the fixture.



Figure 3.5 The fixture affixing

3.3 Two-Lane deployments

After proven effective, the sensor layout shown in Figure 3.6 was employed for all subsequent deployments. The configuration requires that all sensors be connected to a single WIM controller, thus minimizing the cost of the two-lane deployment. Coax cables connected to sensors on the far end of the trailer were protected by road tape, as shown in Figure 3.6. The research team discovered that the road tape did not provide adequate protection for the sensor. On the fourth day of deployment, the far end sensors were disconnected from the controller. This drastically shortened fields testing. After this, the PI determined that metal plates would suffice to protect far end sensor cables against the heavy traffic.

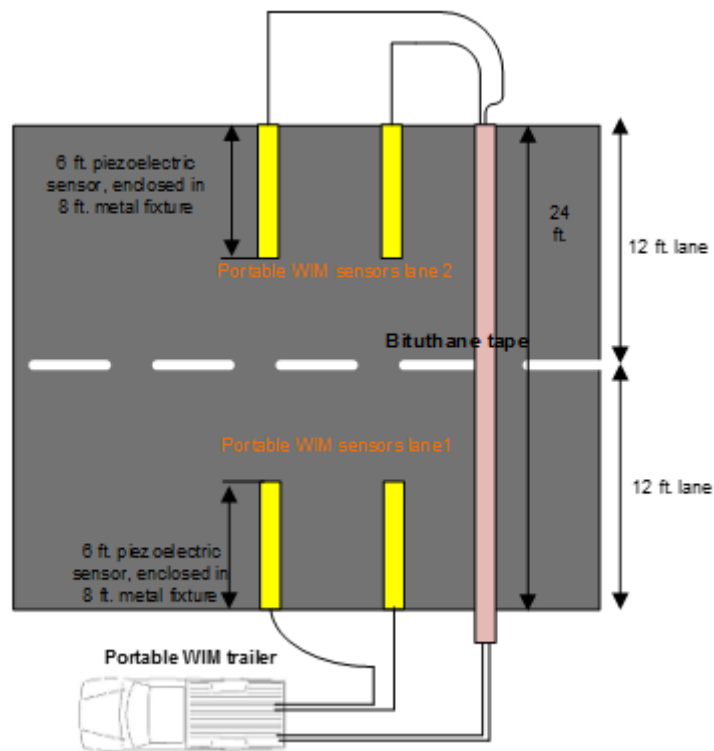


Figure 3.6 Two lanes schematic

3.4 Portable-specific configuration and calibration factors

Default iSINC calibration settings and thresholds of permanent WIM sties cannot be ported or utilized for portable WIM configurations. Since portable WIM sensor installation is above ground, sensor vibration from high-speed traffic is significantly more than sensor vibration at a permanent permanent site. Therefore, sensor threshold-value settings at portable WIM sites were applied differently to default iSINC settings. Vehicle detection is highly correlated to tick threshold value. If set too high, the system fails to count axles; if set too low, the system falsely registers electronic noise as axle counts. Threshold range could be between 0 and 1,023. Portable WIM site threshold values proved to be significantly different from those at permanent sites. Although a threshold default value of 40 was set at permanent sites, values up to 150 were determined applicable for sensors experiencing a high number of ticks at portable sites. Sensors

embedded and flush on highway surfaces typically experienced between 20 and 30 ticks. Tick number in the portable WIM system exceeded 100 in some instances. In spite of this, the enhanced sensor layout and improved affixing method, resulted in the system reporting tick values within the range reported by the permanent WIM system. The team conducted calibration practices similar to those proposed by IRD Inc. technical support engineers. After calibration, a setting of 1,660 was used for all speed bins for concrete deployments and a setting of 1,800 for all speed bins for pavement deployments.

Performance improvement was based on minimizing propagated vibration caused by vehicle impact with either the sensors or the fixture housing the sensor. Twelve-foot sensors were shortened to a more effective 6ft length. Errant vehicle detection and classification were directly influenced by sensor vibration and number of ticks recognized by the WIM controller. A tick threshold was configured in the WIM controller to filter out noise from actual.

3.5 Deployment durability

Procedures for affixing the sensors to the roadway rendered the deployed system operable for several weeks. Regardless if PK nails or concrete screws were used, the team projected that roadway installation would provide quality data for more than two weeks. To the team's consternation, some PK nails loosened their tight grip on the metal fixture after only one week. Figure 3.7 shows expected pocket-tape wear.



Figure 3.7 Deployment durability sensors after 20-day deployment and then after 40 days.

Chapter IV

4 Calibration and Field-Testing

4.1 Introduction

This chapter describes iSINC portable WIM controller configuration and calibration procedures. Calibration factors and configuration were implemented to achieve accurate WIM measurements. This chapter also presents results of WIM accuracy analyses conducted under a controlled environment in which a truck (hereafter known as test-truck) with known axle weight and dimension was used to evaluate system performance. Test-truck axle weight and spacing, speed, and classification performance parameters are reported in this chapter.

4.2 Portable WIM configuration

4.2.1 Sensors thresholds and bounce adjustments

During the first two deployments, the WIM IRD iSINC Lite controller required special configuration to overcome a significant amount of sensor vibration caused by high-speed traffic. A different sensor tick threshold-value settings was applied to the default iSINC settings that are typically configured at the permanent WIM sites.

4.2.2 Calibration method and special adjustments

Calibration is imperative for each deployment at every site. Results from deployment one proved that calibration factors at permanent sites should not be employed at portable sites, as erroneous WIM measurements result. New calibration factors must be discovered using test-trucks. The portable WIM controller was successfully calibrated immediately after highway deployment (i.e., weight measurements were accurate within acceptable error). Results were consistent and repeatable. More details are provided in the following sections.

An ODOT truckload of sand with known weight and length was used for testing. Test-truck speed at time of sensor overpass is an important factor for calculating truck weight. Hence, the WIM controller must accurately measure truck weight prior to the start of the calibration process. Minor sensor separation (i.e., distance between the two installed sensors on one lane) adjustments were performed until an acceptable speed measurement was achieved. WIM speed should match driver-reported test-truck speed. This method considers human factor error. Notably, radar technology was used when available as an alternative method for obtaining more accurate vehicle speed measurements.

Front axle weight (FXW) and gross vehicle weight (GVW) were calibrated by driving the test-truck multiple times over the sensors, and then inputting average WIM readings into the following calibration factor equation:

$$New\ CF = \frac{Actual\ GVW}{Average\ WIM\ GVW} * Current\ CF \quad (Eq. 4.1)$$

During weight calibration, both FXW and GVW parameters can be adjusted. A tradeoff between these two exists, as FXW may adversely impact overall GVW, and GVW may adversely influence FXW. Accordingly, balance between these two parameters was achieved by adaptively adjusting parameters during calibration. Calibration factors were determined for each speed bin (e.g., 10mph) to obtain improved WIM measurements. Although the same factors could be used for all speed bins, it is important to know that WIM measurements will deviate from their true actual values.

The equation used to calibrate GVW can also be used to calibrate FXW. This procedure is required to obtain accurate overall weight measurements. The diagram in Figure 4.1 depicts calibration methodology.

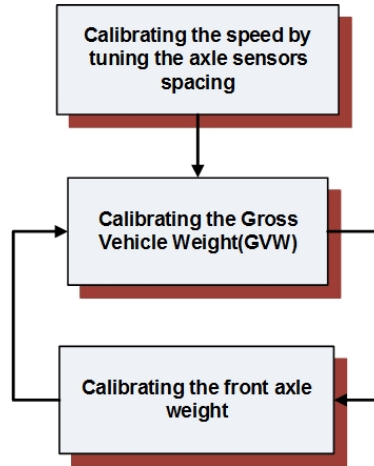


Figure 4.1 Calibration Methodology

Steps to navigate iSINC menus and perform WIM calibration are described in Figure 4.2. Portable WIM calibration factors are significantly different from default values at permanent sites. IRD ships iSINC with default calibration factors of 4,000 for the first three speed bins. ODOT configured the permanent sites for calibration factors of 10,500. After completing a third calibration, settings of 1,800 and 1,660, respectively, were used for pavement and concrete deployments to obtain acceptable GVW for all speed bins.

4.3 Field testing using test-trucks

This section describes deployment results and observations for drive tests conducted with an ODOT class 6 sand truck. Results were used to evaluate the developed portable WIM system and its ability to accurately and consistently measure test-truck weight. An evaluation of the accuracy and inconsistency of weight measurements follows.

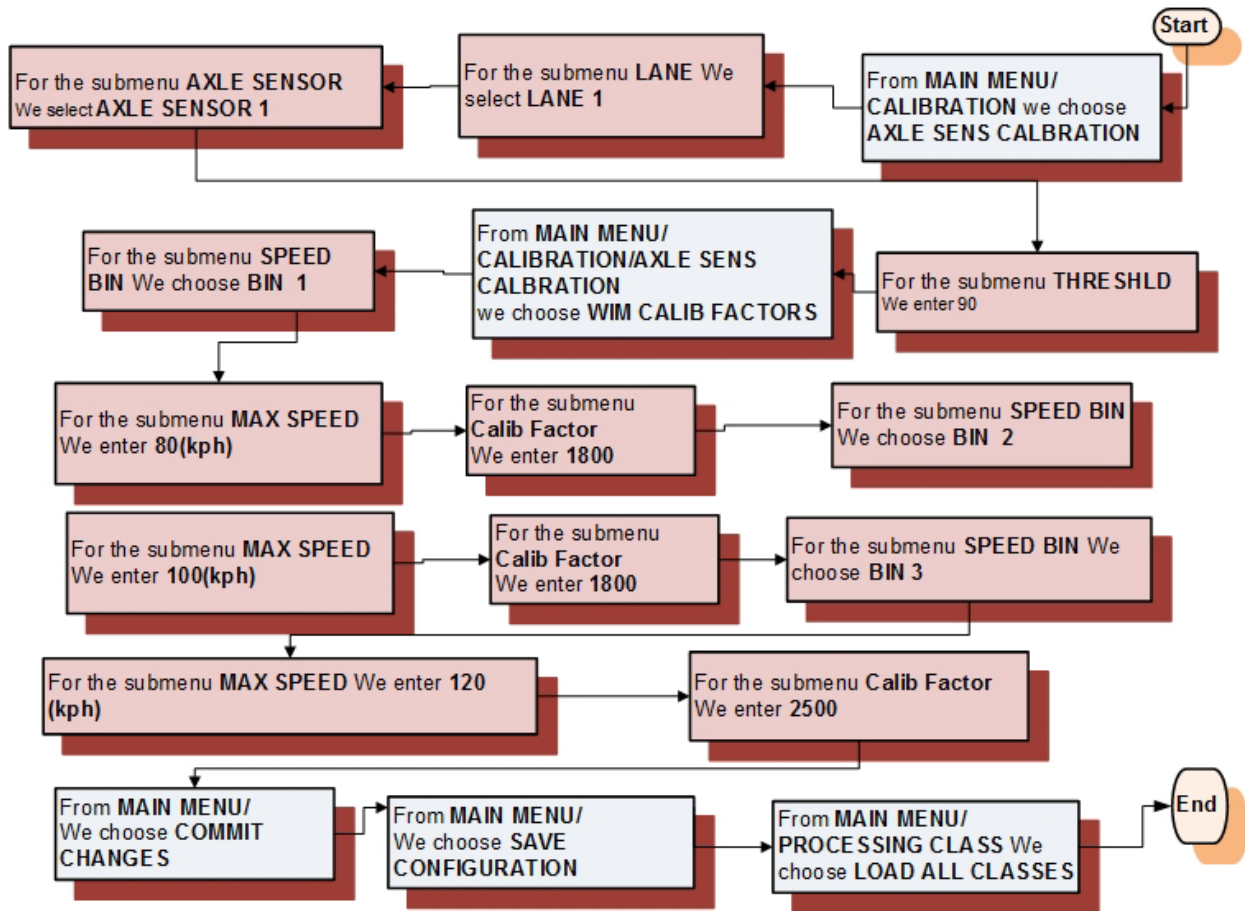


Figure 4.2 iSINC calibration steps for one sensor in the first lane

4.3.1 Data analysis for the weight recorded by portable WIM system

The research team conducted a series of 20 test drives using a 1996 ODOT class 6, International-4900 series dt466, 10-wheel sand truck filled with sand (i.e., non-shifting cargo). Four of the drive tests were erroneous (i.e., not detected by the portable WIM system, as indicated in the table below). Calibration was conducted, and system calibration factors were tuned two days prior to testing. No adjustments or further configuration changes were made during this round of field-testing. The average GVW error was limited to less than 7%, while FXW was limited to less than 1.5%. Portable reported weight measurements, axle spacing and weights, and calculated mean and standard deviation, as well as average errors, are listed in Table 4.1.

Careful assessment of earlier deployments was vital for setting adjustments to the WIM controller, optimizing sensors layout, and determining the method for attaching the fixture to the roadway. These refinements enhanced the results obtained during the fourth set of test drives.

In order to compare the portable WIM measurements to those measured by the permanent system during deployment three, the PI and his research team also recorded

test-truck WIM measurements obtained from the permanent WIM system, which was located in close proximity to the portable WIM site. Notably, the permanent site was calibrated two weeks prior to portable WIM deployment. Table 4.2 shows permanent WIM site measurements. The permanent site was able to achieve zero percent error in front axle weight measurements.

Table 4-1 Accuracy of portable WIM drive test results.

Run	FAS (inches)	SAS (inches)	Speed (mph)	FAW (lbs)	SAW (lbs)	TAW (lbs)	GVW (lbs)	Length (ft)
1	170	56	55	14,178	14,760	15,805	44,743	18
2	170	56	55	13,825	15,532	16,701	46,058	18
3	170	56	55	14,090	15,708	17,768	47,566	18
4	171	56	55	16,074	15,342	17,314	48,730	18
5	172	56	55	14,747	15,404	15,051	45,202	18
6	171	57	57	14,438	14,981	16,551	45,970	18
7	173	56	55	12,758	14,844	16,440	44,042	19
8	171	55	56	15,382	15,170	17,649	48,201	18
9	Error	Vehicle	Too	Slow				
10	170	54	54	14,888	15,267	16,992	47,147	18
11	171	56	57	13,693	14,028	16,361	44,082	18
12	173	56	57	13,402	14,280	14,385	42,067	18
13	Error	Vehicle	Too	Slow				
14	171	56	55	13,905	14,994	16,586	45,485	18
15	171	55	55	13,151	14,862	15,744	43,757	18
16	170	55	55	14,090	14,130	16,679	44,899	18
17	170	55	55	13,984	14,862	14,235	43,081	18
18	173	56	55	13,111	15,029	14,562	42,702	19
19	Error	Vehicle	Too	Slow				
20	Error	Vehicle	Too	Slow				
Mean	171	56	55	14,107	14,950	16,176	45,233	18
SD	1	1	1	810	451	1,051	1,843	0
Actual	166	54	-	14,320	34,260	0	48,580	18
Average Error	3.0%	3.1%	-	1.5%	9.1%	-	6.9%	1.0%

Table 4-2 Accuracy of Permanent WIM drive-test results.

Run	FAS (inches)	SAS (inches)	Speed (mph)	FAW (lbs)	2nd AW (lbs)	3rd AW (lbs)	GVW (lbs)	Length (ft)
1	176	56	57	14,284	14,747	15,801	44,832	27

Final project report

Run	FAS (inches)	SAS (inches)	Speed (mph)	FAW (lbs)	2nd AW (lbs)	3rd AW (lbs)	GVW (lbs)	Length (ft)
2	176	56	57	12,723	14,019	14,050	40,792	26
3	175	56	57	14,593	15,607	14,509	44,709	27
4	175	56	55	12,013	12,529	11,814	36,356	26
5	176	56	57	15,029	17,115	15,510	47,654	26
6	175	56	58	15,620	16,044	15,761	47,425	26
7	176	56	57	15,691	16,048	15,938	47,677	26
8	176	56	57	14,249	14,725	14,187	43,161	27
9	175	56	57	14,174	13,376	15,095	42,645	27
10	176	57	57	15,501	17,243	16,414	49,158	27
11	176	56	58	12476	14628	14094	41,198	27
12	176	56	58	12,965	14,937	13,971	41,873	26
13	176	56	57	15,338	15,528	15,043	45,909	27
14	175	56	57	15,250	14,619	14,945	44,814	27
15	175	56	56	14,654	16,105	17,018	47,777	26
16	176	57	57	15,334	16,445	15,461	47,240	27
17	176	56	57	14,249	15,078	13,587	42,914	26
18	176	56	55	13,852	14,350	14,443	42,645	26
19	175	56	57	14,606	14,760	15,316	44,682	26
20	175	55	56	13,803	16,158	14,063	44,024	26
Mean	176	56	57	14,320	15,203	14,851	44,374	26
SD	0.47	0.37	0.77	1,030	1,129	1,098	2,926	0
Actual	166	54	-	14,320	34,260	0	48,580	18
Average Error	5.8%	3.8%	-	0%	12.3%	-	8.7%	44.3%

Table 4.3 summarizes results obtained from permanent and portable WIM systems during drive testing. The set of experiments indicated lower average error in GVW measurements, as reported by the developed portable WIM system. Aside from first axle weight measurements, test results illustrate that the portable WIM outperformed permanent WIM for both consistency (i.e., lower standard deviation) and average error.

The portable WIM system reported consistent measurements, as did the permanent WIM system. GVW measurement errors were limited to 6.9% for the portable WIM, compared to 8.7% for the permanent WIM system. Portable WIM front and second axle spacing measurements were superior to permanent site measurements, as well. Only front axle weight reported by the permanent WIM was more accurate than the portable WIM.

Table 4-3 Portable vs. Permanent WIM comparison summary

	GVW (lbs)	FXW (lbs)	FAS (inches)	SAS (inches)
Actual	48,580	14,320	166	54
Portable Mean	45,233	14,107	171	55
Permanent Mean	44,375	14,321	176	56
Portable Standard Deviation	1,146	810	1	1
Permanent Standard Deviation	2,926	1,030	0.24	0.15
Portable System Error	6.9%	1.5%	3.0%	3.1%
Permanent System Error	8.7%	0%	5.8%	3.8%

Chapter V

5 Temperature Effect on Portable WIM Measurement

5.1 Introduction

This short chapter reports the efforts performed to examine the effect of temperature on the weight measurements. The design of the portable WIM system lacks the temperature sensor required to compensate for WIM measurement variation. The objective of these efforts to quantify the effect and determine if the design should include a temperature sensor.

5.2 Experiment setup

A temperature probe 108-L from Campbell Scientific and a Vantage Pro2 weather station from Davis were used to collect road surface temperature and weather conditions during the experiment. A data acquisition system collected and stored temperature measurements.

The temperature probe has four connections: clear for shield ground; purple for signal ground; red for temperature signal; and black for voltage excitation. The connection is shown in the schematic of Figure 5.1.

A temperature probe was used to interface with the data acquisition I/O board on the REECE system. The probe requires an excitation +5 volt, which was supplied by the I/O REECE board.

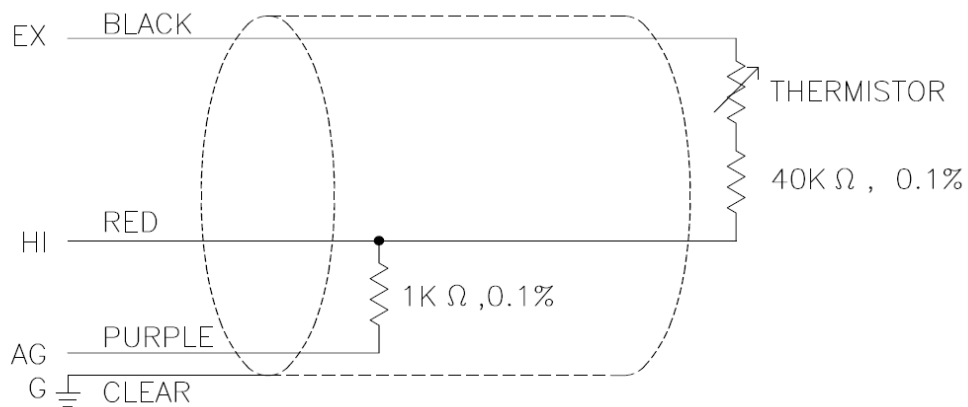


Figure 5.1 Temperature probe schematics

The REECE I/O port 27 was connected to the black on lead of the probe. The temperature signal lead was connected on port 39. Both purple and clear connectors were connected to port 34 (ground) on the REECE I/O connector, as shown in Figure 5.2.

Final project report

DIO A0	1	2	DIO A1
DIO A2	3	4	DIO A3
DIO A4	5	6	DIO A5
DIO A6	7	8	DIO A7
DIO B0	9	10	DIO B1
DIO B2	11	12	DIO B3
DIO B4	13	14	DIO B5
DIO B6	15	16	DIO B7
DIO C0	17	18	DIO C1
DIO C2	19	20	DIO C3
DIO C4 / Gate 0	21	22	DIO C5 / Gate 1
DIO C6 / Clk 1	23	24	DIO C7 / Out 0
Ext Trig	25	26	Tout 1
+5V Out	27	28	Dground
Vout 0	29	30	Vout 1
Vout 2	31	32	Vout 3
Aground (Vout)	33	34	Aground (Vin)
Vin 0	35	36	Vin 8
Vin 1	37	38	Vin 9
Vin 2	39	40	Vin 10
Vin 3	41	42	Vin 11
Vin 4	43	44	Vin 12
Vin 5	45	46	Vin 13
Vin 6	47	48	Vin 14
Vin 7	49	50	Vin 15

Figure 5.2 REECE data acquisition I/O connector

Probe voltage measurements were converted into calibrated temperature values using a Steinhart-Hart equation. The equation interpreted the voltage reading based on thermistor resistance (R_s). The ratio of measured voltage (V_s) to the excitation voltage (V_x) is linearly related to (R_s), and the 41,000 ohm-fixed resistor, as shown below:

$$R_s = 1000 * (V_x / V_s) - 41,000$$

The software calculates R_s from the voltage ratio and converts R_s to temperature using the Steinhart-Hart equation:

$$T_c(\text{Celsius}) = 1 / (A + B(\ln R_s) + C(\ln R_s)^3) - 273.15$$

whereas the coefficient: $A = 8.271111e-4$, $B = 2.088020e-4$, and $C = 8.059200e-8$

To convert temperature from Celsius to Fahrenheit degrees, the following equation was used:

$$T_{\text{Feh}} = T_{\text{Cel}} * (9/5) + 32;$$

5.3 Portable WIM measurement analysis for campus deployment:

A Ford club wagon (henceforth “van”) with known-weight was driven 57 times over WIM sensors at predetermined speeds and at various surface temperatures to determine weight measurement value consistency during similar temperature readings and to

determine whether or not weight measurements obtained from the piezoelectric sensors vary with surface temperature. Analyzed data showed weight information obtained during testing changed as temperature varied. Data analysis obtained during drive tests indicated that vehicle weight decreases as temperature increases, as shown in Figure 5.3. Note that these results are not conclusive.

Weight measurements were not consistent. The WIM controller measured the van at varying weights even when road surface temperature was constant.

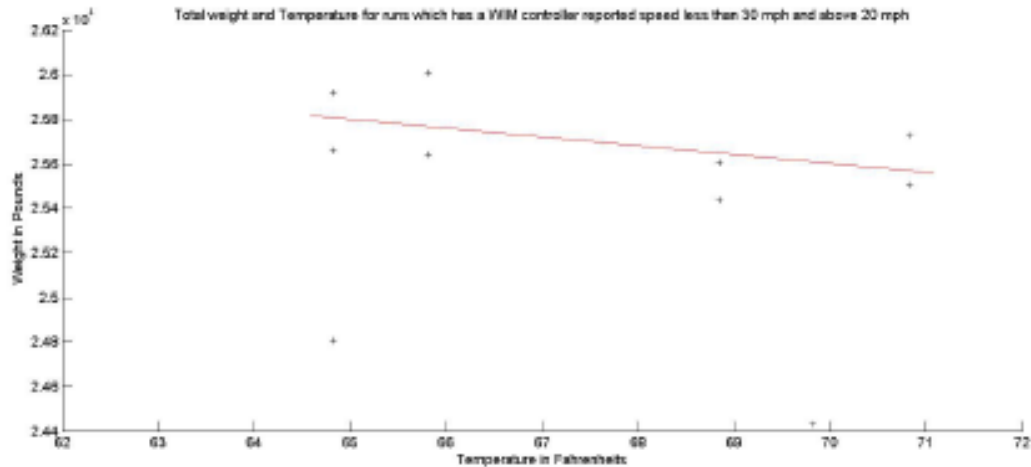


Figure 5.3 Weight measurements with temperature variations

5.4 Portable WIM measurement analysis for highway deployment:

The PI and his research team investigated the effect of temperature on portable WIM system performance during a highway deployment. IRD iSINC WIM controller used in the portable system can be configured to apply correction factors to compensate for temperature variations. A temperature probe was connected to the WIM controller to provide temperature measurements for adjusting WIM calculations. However, the temperature factors and compensation were disabled in the portable WIM system to eliminate the need to incorporate a temperature probe into the design.

During highway deployment, recorded air temperature varied from 67° F to 103° F. Class 9 GVW measurements collected from the portable WIM system were compared to those collected by the permanent system. Unlike the portable system, the permanent system uses a probe to compensate for variations in road subsurface temperature. The comparison manifested in the regression graphs, shown in Figure 5.4, and confirmed that the portable system performance during the PM periods at lower temperatures is better than AM periods. In fact, the “goodness fit” factor improved by 37% during PM periods.

5.5 Conclusion

A temperature effect on the portable WIM measurements was confirmed. Although air temperature values varied little between AM and PM evaluation periods, WIM measurements demonstrated pronounced variation. To limit the effect of temperature on WIM measurements, a temperature probe should be included in portable WIM system design.

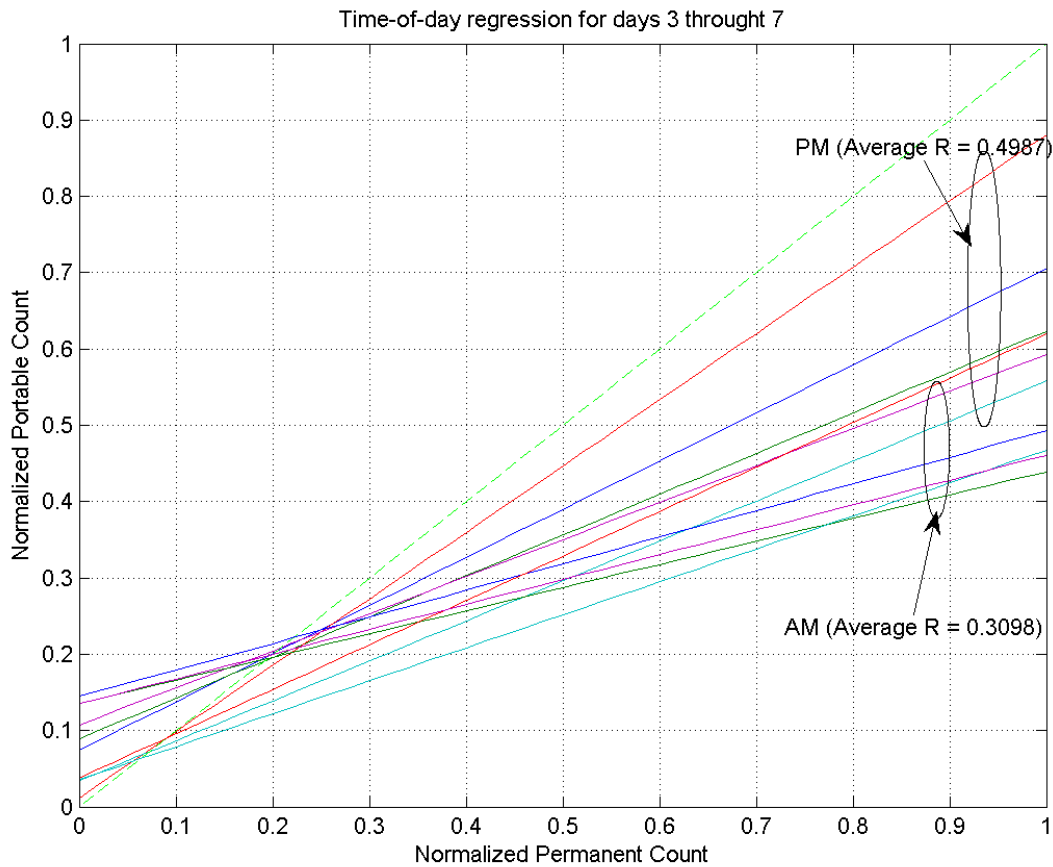


Figure 5.4 Regression plot to detect temperature trends in portable WIM systems

Chapter VI

6 Vehicle Signature Development Using WIM Data

6.1 Introduction

This chapter explains research activities conducted to develop signatures of heavy vehicles and to examine signatures uniqueness toward identifying heavy vehicles as they travel from one WIM site to another within the state of Oklahoma. Signatures are based on vehicle axle separation, length, weight, and class—all of which are parameters measured and provided by a WIM controller. Results of the signature development and algorithms are given in this chapter.

6.2 Large-scale vehicle signature study and data mining

A vehicle signature was developed to include parameters measured by the WIM controller, including GVW, axle weight, number of axles, and axle spacing. Speed measurements cannot be included in the vehicle signature, as values are variable. However, prior to vehicle signature development, it is important to confirm that measurements made by two WIM controllers installed at two different locations will yield the same measurements for the same vehicle, meaning that the WIM measurements are repeatable and accurate.

Class 9 vehicles were chosen for signature development. A full year of WIM class 9 truck data was analyzed to investigate nominal (or average) values of FXW and axle spacing. Figure 6.1 shows the histogram of class 9 FXW. Average value is 9,448 lbs, and standard deviation is 2,515 lbs. Average value proved to be consistent with typical class 9 FXW. However, standard deviation is larger than would be expected. This could be attributed to WIM calibration accuracy during data collection.

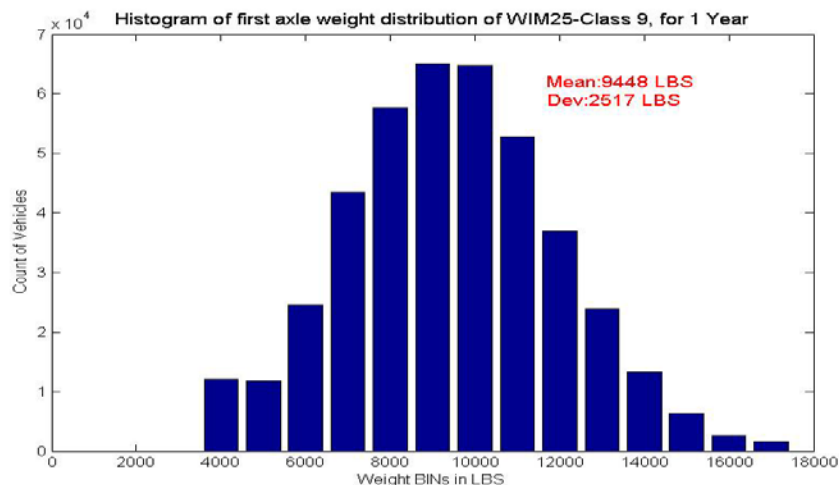


Figure 6.1. Histogram distribution of class 9 FXW.

The first, second, and third axle spacing distribution is given in Figure 6.2. Notably, some class 9 trucks have a longer fourth axle spacing, which indicates longer trailer beds, as shown in the bottom right illustration of Figure 6.2.

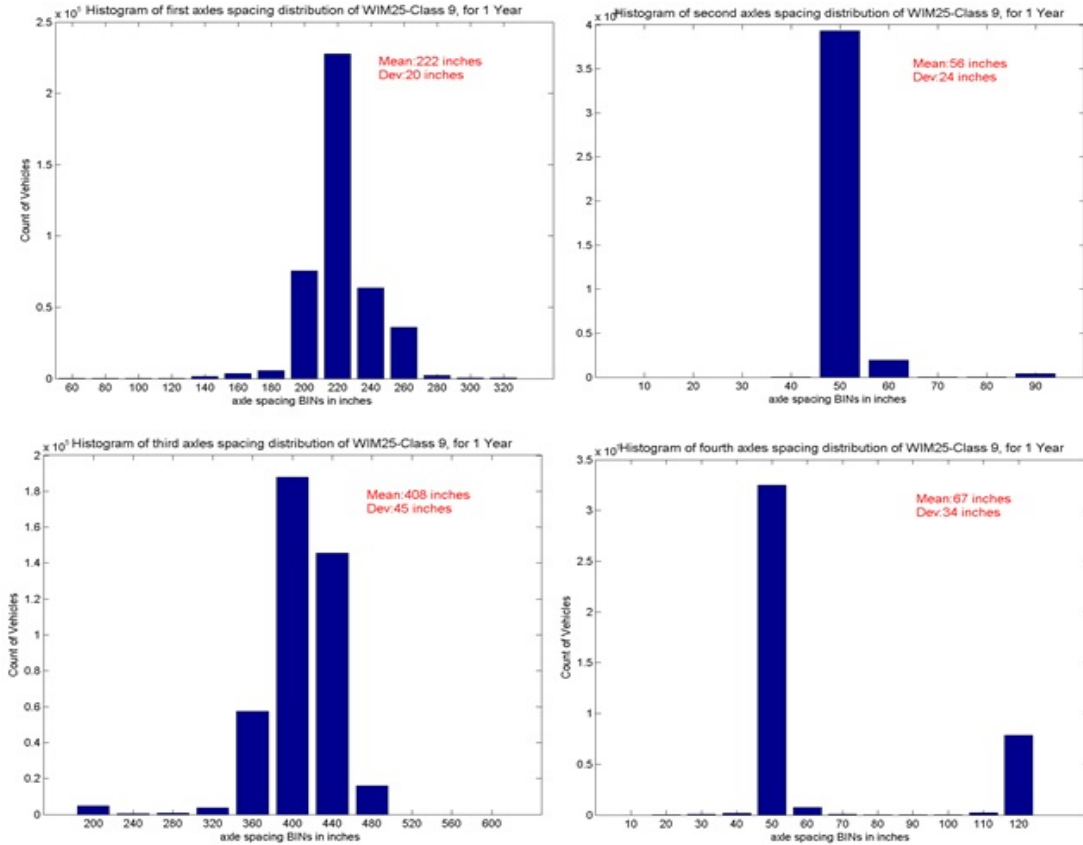


Figure 6.2. Histogram distribution of first, second, third and fourth axles spacing

Preliminary WIM data analysis shown above in the last two figures indicates a large deviation in class 9 FXW. This result contributes to the inaccuracy of unique vehicle signature development. However, though limited, some variations in axle spacing can be used to identify various traveling vehicles.

6.3 Vehicle detection at multiple WIM sites

Although the initial analysis didn't provide encouraging results, the research team developed a WIM data mining algorithm to identify vehicles that travel multiple WIM sites across Oklahoma roadways. When a vehicle passes a WIM site, its GVW, FXW, and FXS parameters are measured and stored in a database for future detection of the vehicle as it travels various sites. The algorithm attempts to identify the vehicle at a second WIM site station farther along the highway. Depending on distance between two sites, the algorithm is designed to examine data after a period of time calculated as equal to vehicle travel time to a second site, as estimated by Google traffic flow model.

The data mining algorithm was performed on vehicles traveling on I-35 between WIM 02 and WIM104, as shown in Figure 6.3.

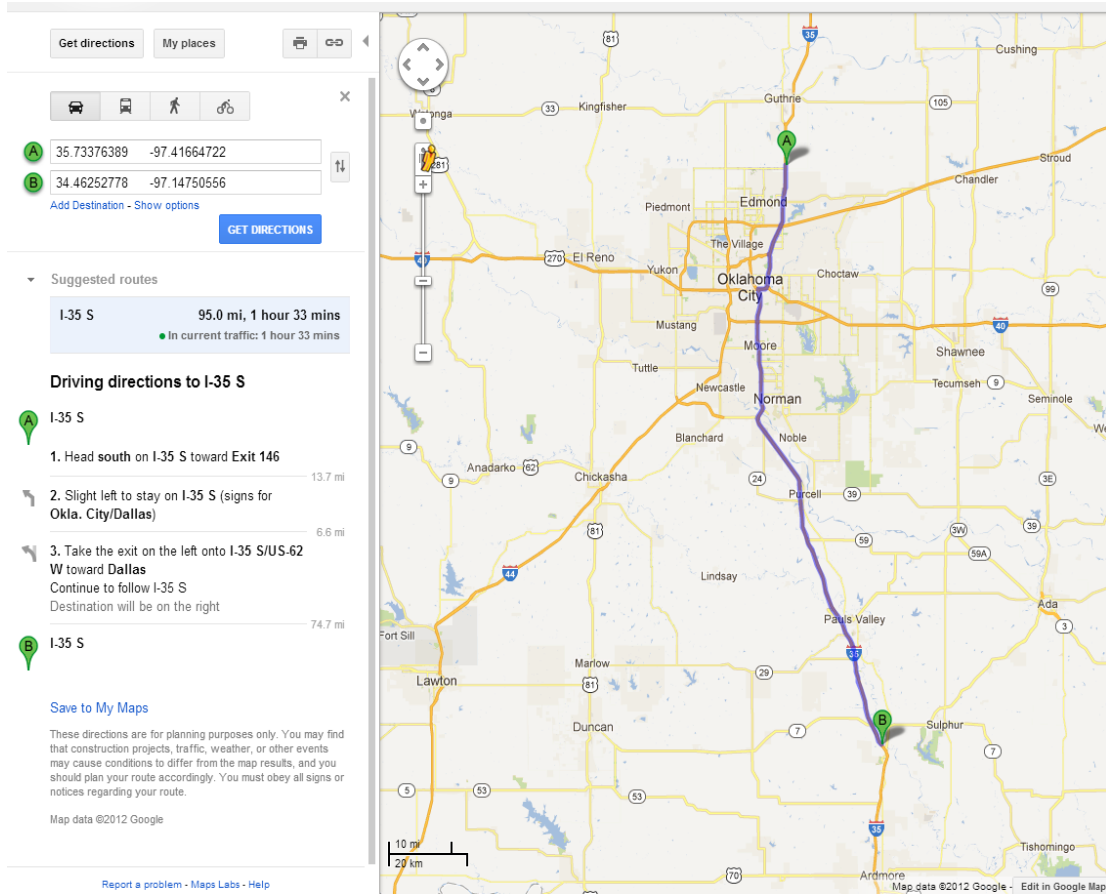


Figure 6.3. Locations of WIM02 and WIM104 on I-35

Distance between these two sites is 95m. An additional 15min window beyond estimated arrival time was added to allow for slow traffic flow. A vehicle's GVW, FXW, and FXS are searched throughout data for a match. Results of the algorithm are depicted in Figure 6.4. Only seven vehicles were matched when GVW deviation tolerance was limited to $\pm 5\%$ from the GVW registered at the first site. Fifty eight vehicles were matched when tolerance was increased to $\pm 10\%$, and 100 were matched when tolerance was increased to $\pm 15\%$. FXW mean error was 496 lbs and 782 lbs, respectively.

6.4 Conclusion

The number of vehicles that travel these two sites daily is in the order of thousands. Matching only 100 vehicles from such a large number of vehicles is not effective. Hence, the team concluded that GVW, FXW, and FAS parameters might not be ample to identify unique signatures of vehicles traveling past multiple WIM sites.

Final project report

The 100 matched vehicles were not validated using other technology, including visual- or laser-based systems. Vehicles were validated using only WIM measurements.

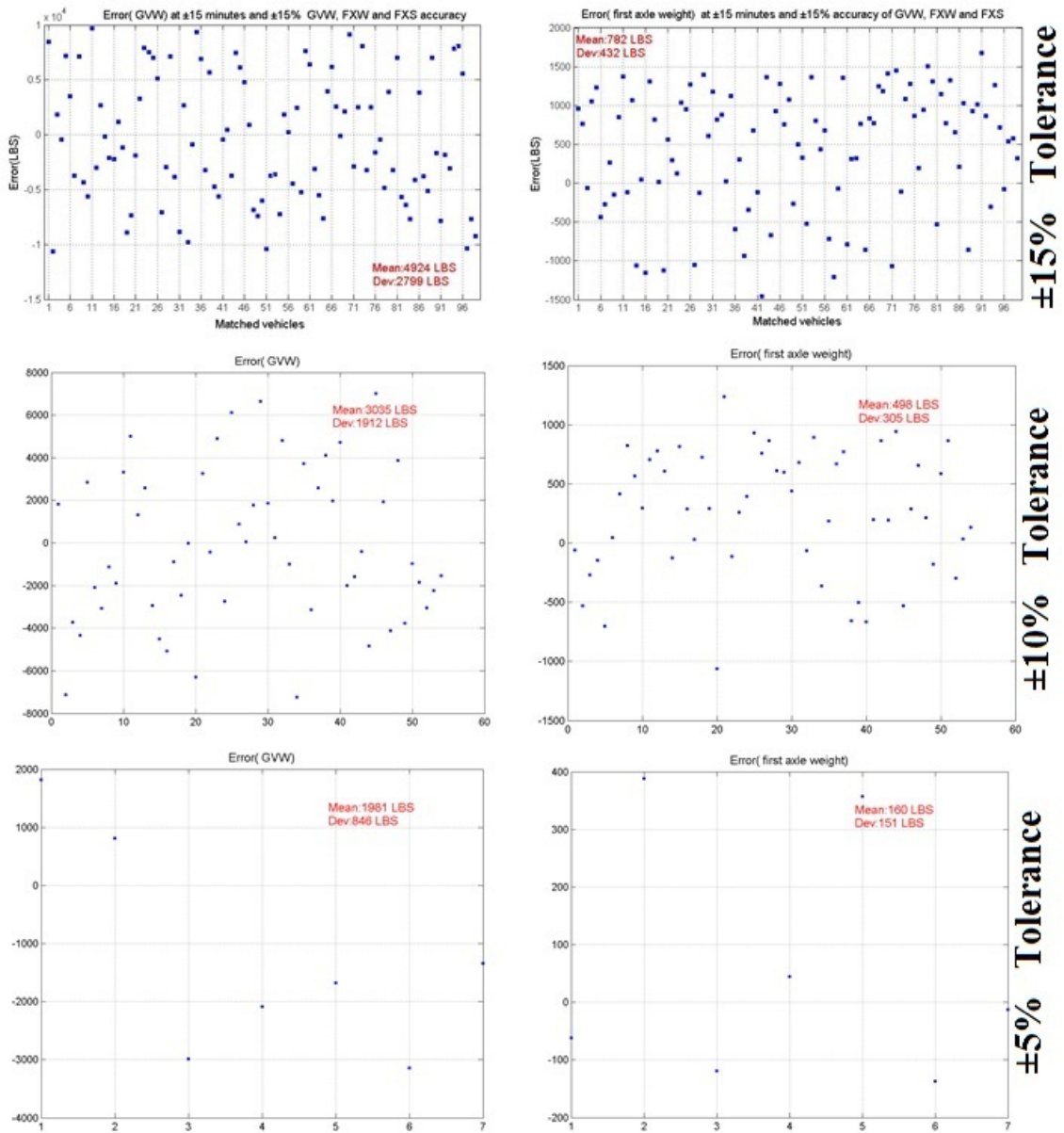


Figure 6.4. Data mining algorithm results

Chapter VII

7 Portable WIM Aggregate Data Analysis

7.1 Introduction

This chapter presents results obtained by processing aggregated WIM data (i.e., data without per vehicle matching). Chapter IV presented a comparison study of portable and permanent WIM systems using test-trucks with known weights following a site calibration. Test-truck field-testings typically lasted three to four hours. This chapter analyzes and compares aggregated WIM data collected at portable and permanent sites during a typical deployment. Deployment data is divided into three phases, each of which consists of roughly 15 days worth of data. Portable WIM system performance was highest during phase I. Portable WIM data severely deviated from permanent WIM data in phase III.

Vehicle statistical distributions of FXW, GVW, vehicle classification, speed, and FAS (i.e., distance between the first and the second axles) are presented in this chapter. It is important to note that the permanent WIM site is assumed to provide accurate weight measurements, although this assumption may not hold or apply if the permanent site is out of calibration. However, this is not the case. The research team collected portable WIM data from ODOT WIM16 two weeks after ODOT performed site calibration there, and permanent WIM data was confirmed accurate.

7.2 Vehicle count statistical distribution analysis

This section presents detected vehicle distributions calculated for FXW, GVW, classification, speed, and FAS. Since the focus of this project was to track overweight trucks, the distributions presented in this chapter focus on class 9 vehicles—trucks with five axles and a single trailer. This work is important because FXW is typically used for automatic calibration of weight measurements. Most electronic WIM controllers ship with specific software procedures to perform automatic calibration based on class 9 vehicle first axle weight of 10,000lbs.

7.2.1 Class 9 First Axle Weight (FXW) distribution

Prior to data presentation, WIM data was conditioned by removing all records in which an error occurred during vehicle detection. Vehicle count distributions of class 9 FXW during all three phases are shown in Figure 7.1. Class 9 FXW is roughly standardized at a weight equal to 10,000lbs. The figure confirms that the percentage of undetected vehicles during the last two deployment phases was extremely high, unlike phase one. The reason for the elevated errant vehicle detection was due to depreciation of piezoelectric sensor affixing.

The mean FXW value of the portable WIM system was close to 10,000lbs in all three phases, while standard deviation was wider than that of the permanent system, as shown in the Figure 7.1.

Table 7.1 presents the calculated mean and standard deviation of the FXW measurements obtained by the portable and permanent WIM systems. On average, the portable WIM system provided a good estimate of first axle weight; however, its standard deviation proved wider than its permanent counterpart. Data quality of the portable WIM system during phase I outperformed data recorded during later phases.

Final project report

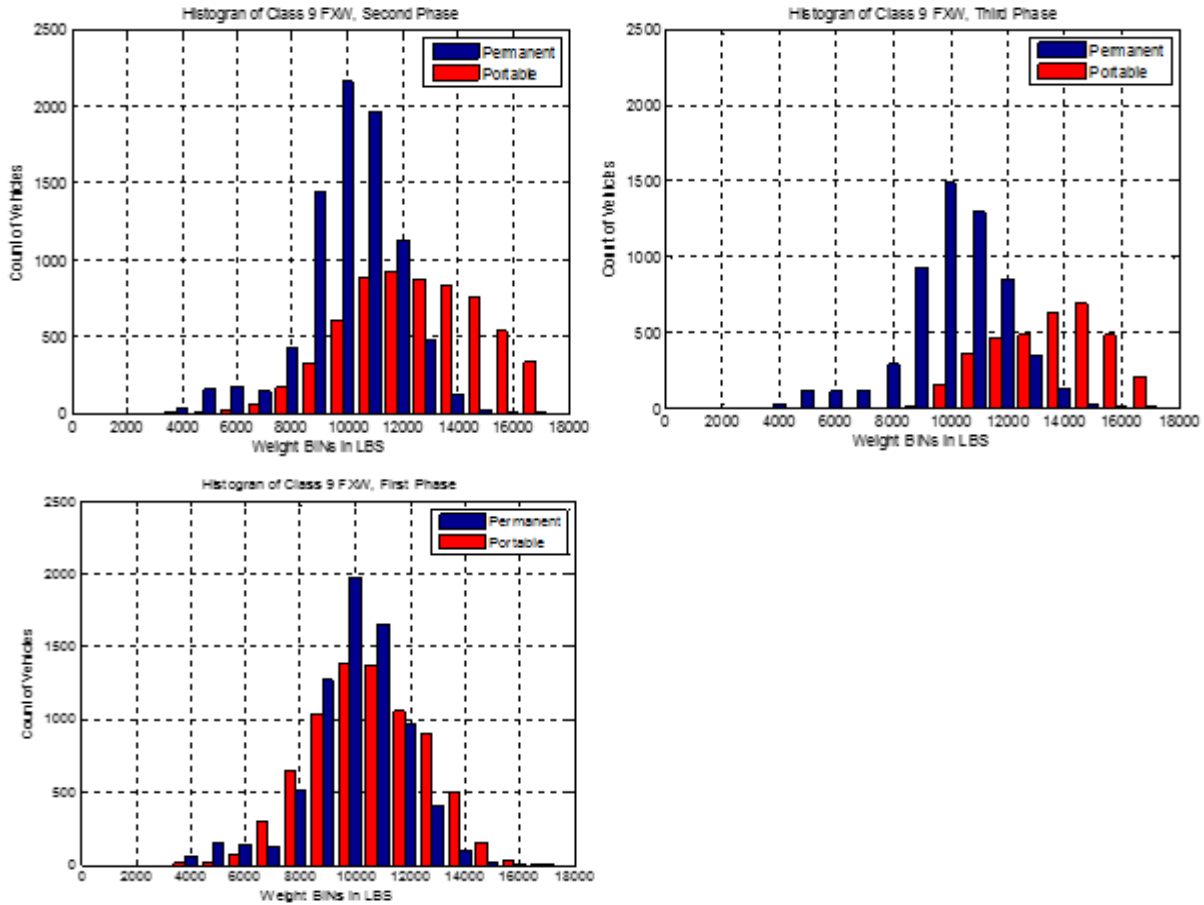


Figure 7.1 First axle weight class 9 vehicles for phase I, II, and III respectively.

Table 7-1 Class 9 FXW mean and standard deviation measured during phase I, II, and III

	Phase I	Phase II	Phase III
Portable Mean (lbs)	10,742	12,716	13,737
Portable SD (lbs)	1,988	2,444	1,988
Permanent Mean (lbs)	10,143	10,233	10,306
Permanent SD (lbs)	1,791	1,758.5	1,900.6

7.2.2 Class 9- Gross Vehicle Weight (GVW) distribution

GVW measurement accuracy is an important WIM system performance factor. GVW as related to vehicle count distribution for a calibrated WIM site should exhibit two or possibly three bell shaped curves. The first bell shaped curve (shown far left below) represents trucks carrying no loads, while the second (shown far right below) represents trucks carrying a full load. Figure 7.2 shows GVW distributions for class 9 vehicles detected by the portable and permanent systems. Vehicle count distribution obtained from the permanent site clearly exhibits two bell shaped curves. On the other hand, portable WIM GVW distribution exhibited such distribution to a lesser degree (i.e., its two peaks are less pronounced than those produced by the permanent site).

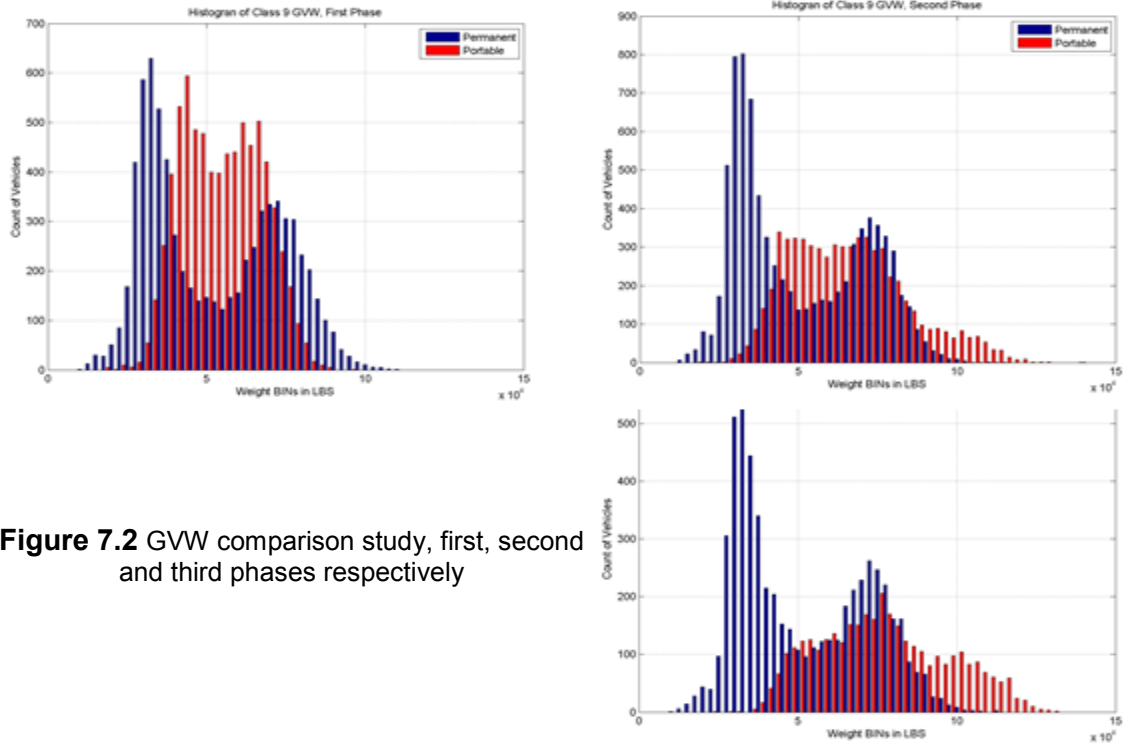


Figure 7.2 GVW comparison study, first, second and third phases respectively

7.2.3 Vehicle classification

Vehicle classification distributions are presented in Figure 7.3. The classes investigated were large vehicles, including those in classes 6 to 13. These classes were the focus since this project was aimed at developing a portable WIM to monitor overweight trucks. As shown, the number of misclassified vehicles increased in phase II and III.

7.2.4 Class 9 vehicle speed distribution

Detecting accurate speed is important for calculating axle weight. Since different calibration factors are assigned to different speed bins, accurate speed determination is closely related to accurate vehicle weight calculation. The calculation of speed depends on accurate configuration of the distance separating road installation of the two sensors. During calibration and field-testing, the research team adjusted separation distance to match the speed reported by the driver of the test truck. In hindsight, data could have been more accurate if the research team had used radar technology to acquire a more precise measurement of speed.

Figure 7.4 illustrates speed distributions during phase I, II, and III. Again, speed measurements during phase I more accurately matched permanent site reported speeds.

Table 7.2 presents calculated mean and standard deviation of speed measurements for class 9 vehicles obtained by the portable and permanent WIM systems.

Standard deviation stability is a clear indicator that the permanent WIM system is more consistent. Increase of standard deviation in the portable WIM system reflects the depreciation of its collected data with time.

Final project report

Table 7-2 Speed mean and standard deviation for class 9 vehicles in phases I, II, and III

	Phase I	Phase II	Phase III
Portable Mean (mph)	67.8319	65.9809	62.2681
Portable SD (mph)	3.9487	6.6254	7.52
Permanent Mean (mph)	70.44	70.6338	70.2224
Permanent SD (mph)	4.2323	4.2638	4.2381

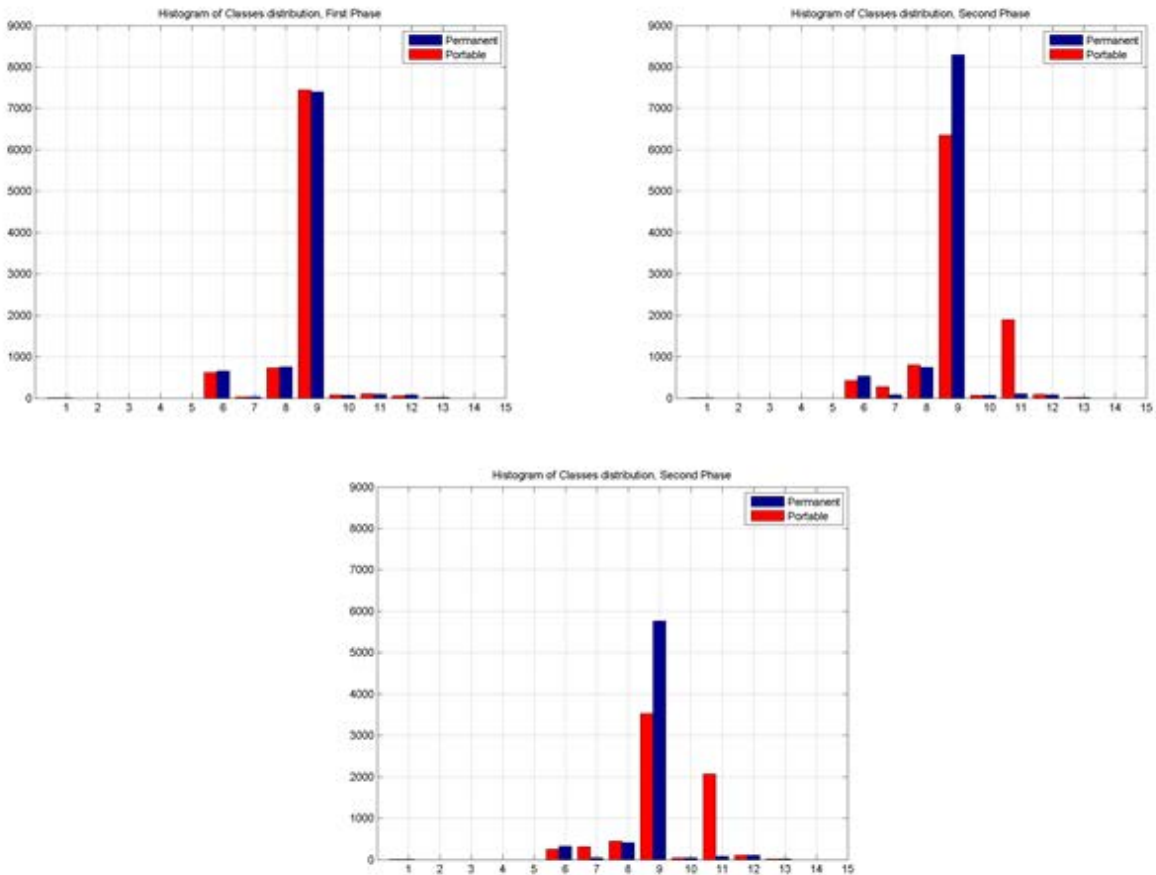


Figure 7.3 Vehicle classes comparison study first, second and third phases respectively

7.2.5 Class 9 First Axle Spacing (FXS) distribution

First Axle spacing in class 9 vehicles is standardized and fixed. Hence, it becomes another performance parameter that could be monitored, collected, and analyzed. As expected, accurate spacing calculations were achieved by the portable WIM system during phase I. Table 7.3 presents the calculated mean and standard deviation of FXS measurements obtained by the portable and permanent WIM systems for class 9 vehicles.

Final project report

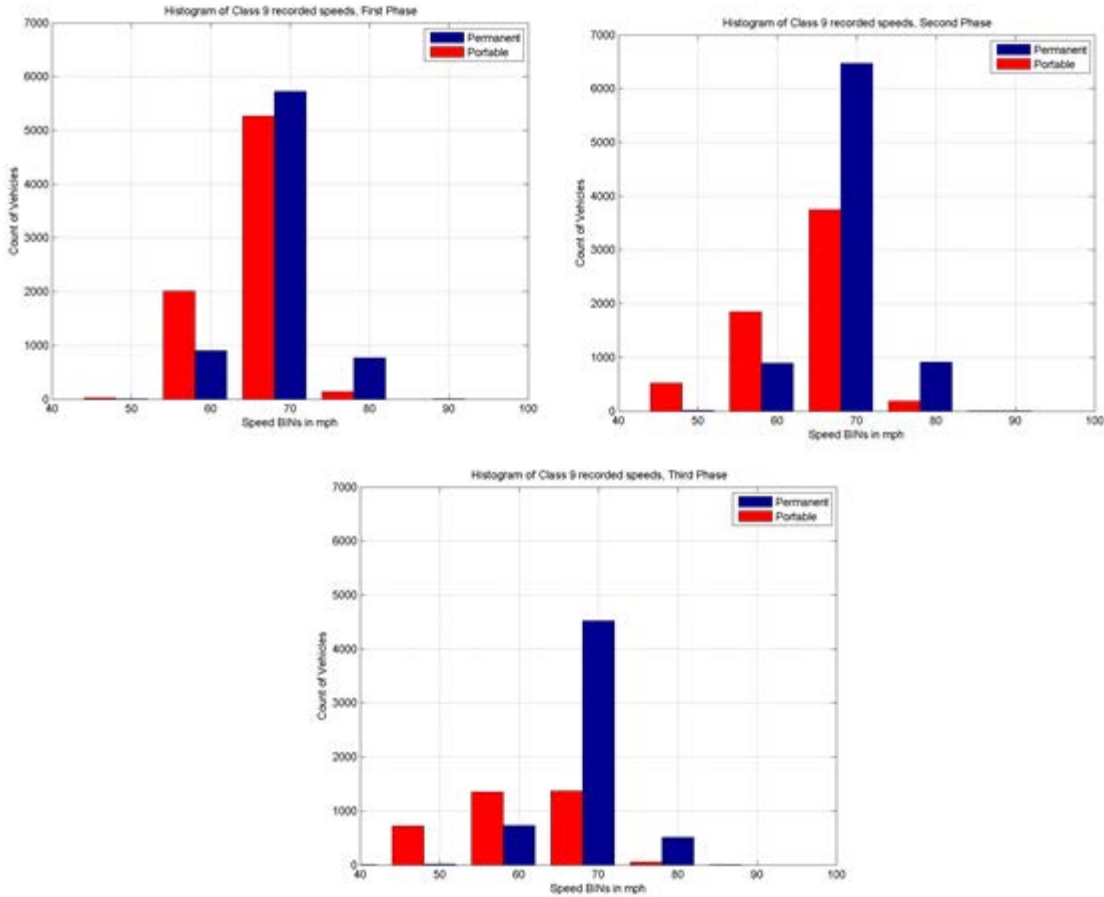


Figure 7.4 Speed comparison study, Phases I, II, and III respectively

Table 7-3 FXS mean and standard deviation for class 9 vehicles in phases I, II, and III

	Phase I	Phase II	Phase III
Portable Mean (inches)	202.1581	203.5154	198.7089
Portable SD (inches)	28.9671	34.4405	36.7099
Permanent Mean (inches)	209.3846	211.1689	209.4766
Permanent SD (inches)	30.4166	30.3968	30.2555

7.3 Aggregate linear regression analysis

This section presents linear regression analysis on portable WIM data and compares GVW for class 9 vehicles collected from the portable WIM data against data collected from the permanent WIM site. The fact that both systems were deployed within close proximity implies that the relationship between measurements of the two should be linear, $y = x$ ideally, where y represents the portable WIM data and x represents the permanent WIM data. The research team applied a simple binning scheme. GVW data was binned into 52 different weight bins. The

chosen range of weights was between 5,000 and 130,000lbs with a step size of 2,500lbs for each successive bin.

Consequently, a simple linear regression model was built based on Eq. (7.1) to approximate a day-by-day relationship between the two sets of portable and permanent binned GVW data. Accuracy of the newly developed system was determined based on how close the linear model was to the ideal case ($y = x$).

$$\hat{y}_i = b_0x_i + b_1 \quad (\text{Eq. 7.1})$$

where: b_0 is the y-intercept of the relationship.

b_1 is the slope of the relationship.

Coefficients b_0 and b_1 are determined using the Ordinary Least Squares method.

Coefficient R is a statistical measure of how well the regression line approximates real data points; it is calculated using the formula in Eq. (7.2). A high R value indicates that the portable and permanent site data are highly correlated.

$$R = \sqrt{1 - \frac{\sum (y_i - \hat{y}_i)^2}{\sum (y_i - \bar{y})^2}} \quad \text{where} \quad 0 < R < 1 \quad (\text{Eq. 7.2})$$

\bar{y} is the mean value of the measured output variable y

Results of applying linear regression analysis on the aggregate data collected throughout the 18-day deployment are shown in Figures 7.5 and 7.6. Each circle indicates a GVW measurement recorded at portable WIM and the corresponding measurement recorded at permanent WIM. A circle on the diagonal $y = x$ line means that the same GVW measurement was recorded at both systems. As the circles depart from the diagonal line, an error due to unequal GVW measurements is indicated.

The quality the GVW was monitored daily to detect signs of any system performance degradation during the first four days of the deployment, as shown in Figure 7.5. Results showed that system performance was improved during the few days following sensor road installation. It was expected that as more vehicles traveled the portable site, the performance of the system would deteriorate.

Similar results of linear regression analysis for speed and FXW are shown in Figure 7.7 and 7.8, respectively. Results obtained for speed show exceptional performance by portable WIM during the first four days; after which in the following 15 days, system performance degrades significantly. First Axle Weight performance was slightly better in the first phase, although performance was relatively very poor in both phases.

Final project report

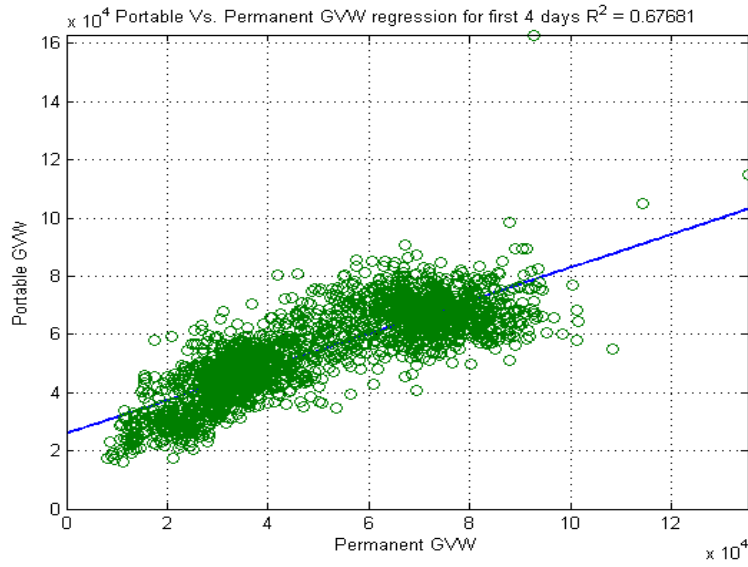


Figure 7.6 GVW regression for the first 4 days of deployment

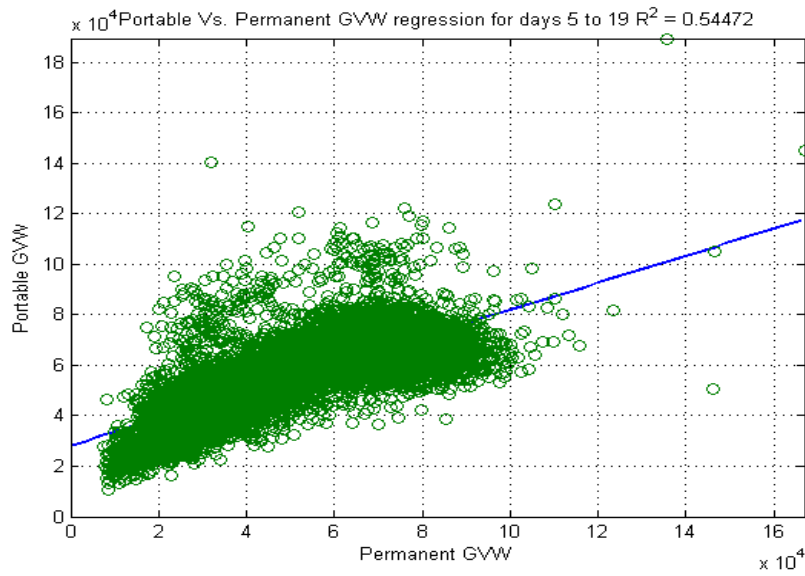


Figure 7.5 GVW regression for days 5 to 19.

Final project report

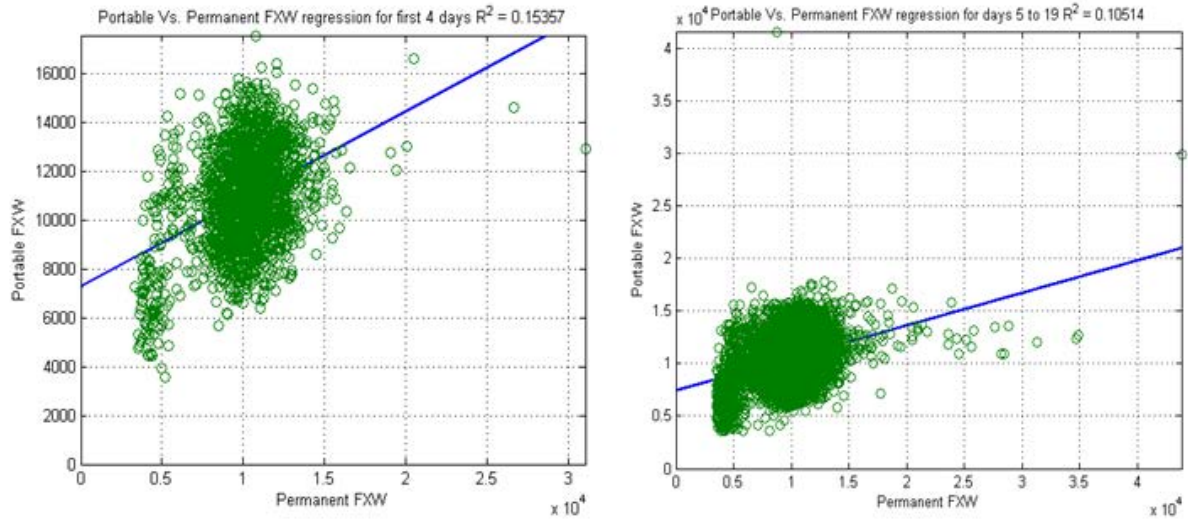


Figure 7.7 FXW regression analyses for the first 4 days (left) and days 5-19 (right)

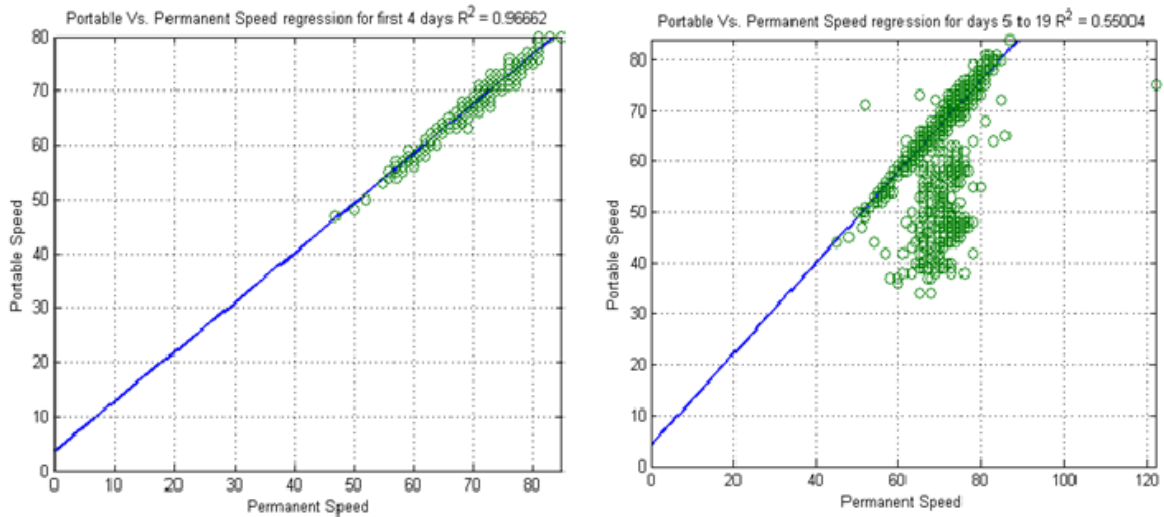


Figure 7.8 Speed regression analyses for the first 4 days (left) and days 5-19 (right)

Chapter VIII

8 Portable WIM Per-Vehicle Analysis

8.1 Introduction

This chapter focuses on per-vehicle comparison of portable and permanent WIM site data to analyze accuracy of the collected data. This analysis was conducted immediately after permanent site WIM16 was calibrated with the intent to provide accurate WIM measurements. Hence, it was assumed that permanent WIM data is highly accurate.

Per-vehicle comparison of vehicle records between the permanent and portable WIM systems was very challenging. Vehicle splitting occurred more frequently in portable WIM deployments, which caused an unequal number of vehicles detected by both systems. A greater number of vehicles were detected by the portable WIM than by the permanent WIM system. Furthermore, vehicle-processing times between both systems were unequal, primarily due to the fact that portable WIM systems are deployed on one or two lanes while permanent WIM are installed to monitor all lanes. The difference in the processing time ranged from a few milliseconds to a few seconds in worst-case scenarios. These included when the number of running WIM background tasks (i.e., processes) was high. Hence, an algorithm was developed to align vehicle records to perform a per-vehicle accuracy study.

8.2 Time shift and alignment algorithm

This section details the advance alignment algorithm (AALA) developed to align and match time-shifted per-vehicle records between the portable and permanent WIM data records.

To align vehicle records, the research team extensively (and often manually) examined data collected by both systems to identify factors that skewed the time between them. The factors are explained in the following cases.

1. *Unequal number of vehicle detection or persistent misdetection of vehicles from either WIM systems:* This scenario is the result of differences in on-surface sensor deployment at portable sites and in-pavement sensor deployment at permanent WIM sites. Unlike portable sites, permanent sites utilize an inductive loop to sense vehicle presence, and then trigger (i.e., prepare) piezosensors to measure oncoming vehicles.
2. *Different system processing times between the two measuring WIM devices:* This scenario is mainly the result of monitoring an unequal number of lanes. Portable WIM is deployed to monitor one or two lanes while the permanent WIM monitors all lanes of the roadway.
3. *Deployment site:* The two WIM systems are deployed at a distance from one another, thus, a vehicle detected at the first site will not be sensed at the same at the second. Additional time is required for the vehicle to travel to the other site.

Because vehicles travel at various speeds, interim time between various vehicle travel time will be different for each system. This phenomenon causes excessive misalignment during high volume traffic, which in turn adversely affects vehicle detection time, making it difficult for per-vehicle record comparison.

4. *Clock implemented in the WIM electronic controller continuously drifts:* According to the WIM controller Operating Manual, each machine has two clocks. A detection clock adjusts to the system clock only when drifting exceeds 5 seconds. Thus, uncertainty is inevitable, even if the main system clock remains synchronized with Internet timeservers using Network Time Protocol (NTP).

8.3 Advance alignment algorithm (AALA) development

To eliminate the need to manually examine thousands of vehicle records during each deployment, the research team developed an algorithm to minimize time spent manually processing record-by-record WIM data. Instead, WIM data was analyzed by using a newly developed algorithm that utilizes vehicle relative-detection-time.

Initially, a quick scan of vehicle records was performed to identify records that belonged to the same vehicle and were accurately detected by both portable and permanent WIM controllers. Such vehicles typically arrived at WIM site with no vehicles arriving at the sites closely behind. Visually spotting these vehicles was relatively easy. Class, detection time, GVW, and length are vehicle parameters used to match vehicles between the portable and permanent WIM sites. The list of matched records was divided into two sets. The first set, namely “anchor”, was used to adjust for time discrepancies between the two WIM sites. The second list, namely “validate”, was used to evaluate algorithm performance and accuracy. The algorithm is assumed to be 100% accurate if it matches all vehicle records in validate list.

The AALA flow graph is illustrated in Figure 8.1. The algorithm for computing relative-detection-time is explained using the flow graph in Figure 8.2.

Special algorithm adjustments:

- The initial version of AALA incorporates milliseconds in its calculation, primarily because this number was found to be a determining factor in ensuring that timing error does not rapidly accumulate and cause an increased rate of under-alignment. Such a phenomenon would impose the need for more data anchors.
- We suggest that researchers manually identify 2% of the records—1% as anchors and 1% as testing records.
- The revised AALA incorporates vehicle speed or travel time in the equation.
- A detection window of 1.1 seconds is configured to compensate for margins and errors resulting from approximation in the analysis.

8.3.1 Anchors extraction

As aforementioned, implementation of ALAA requires manually extracting several data points visually identified as matching records (i.e., anchors), and then repeating the process daily.

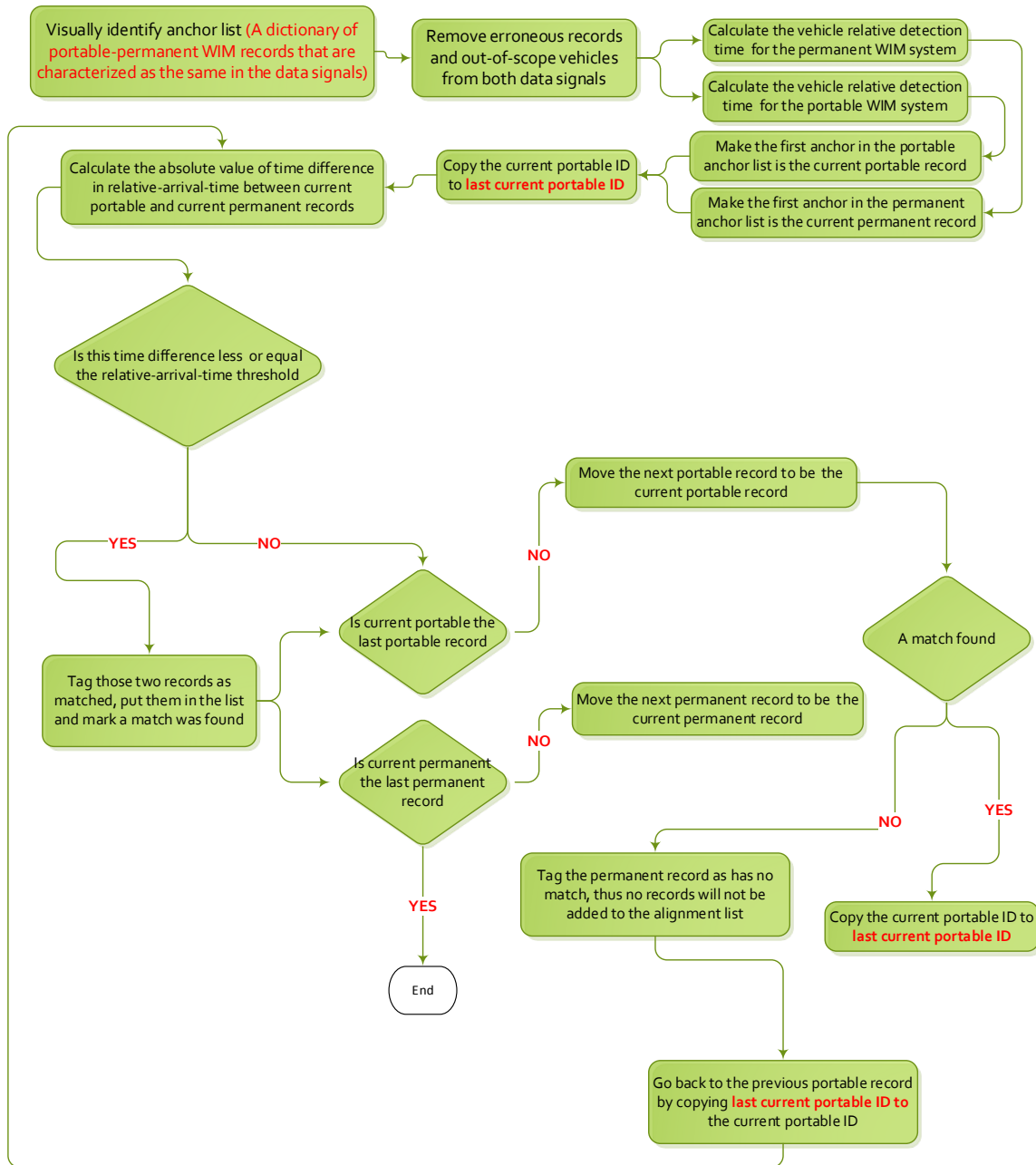


Figure 8.1 Alignment using anchors algorithm (ALAA) flow graph

A careful study of data from both sites suggested that using class 9 vehicles would be the most efficient and accurate method to identify the anchors. This is true due to the abundance of vehicles in this class at the chosen site, as well as significant similarity and relative stability with respect to time between system performance at both sites for this class. Figure 8.3 illustrates similarity by comparing vehicle number in each class reported by the portable WIM with their counterparts in the permanent site on two dates. It can be clearly inferred that although the overall vehicle detection and classification

capabilities of the portable WIM degraded with time, it remained superior for class 9 vehicles.

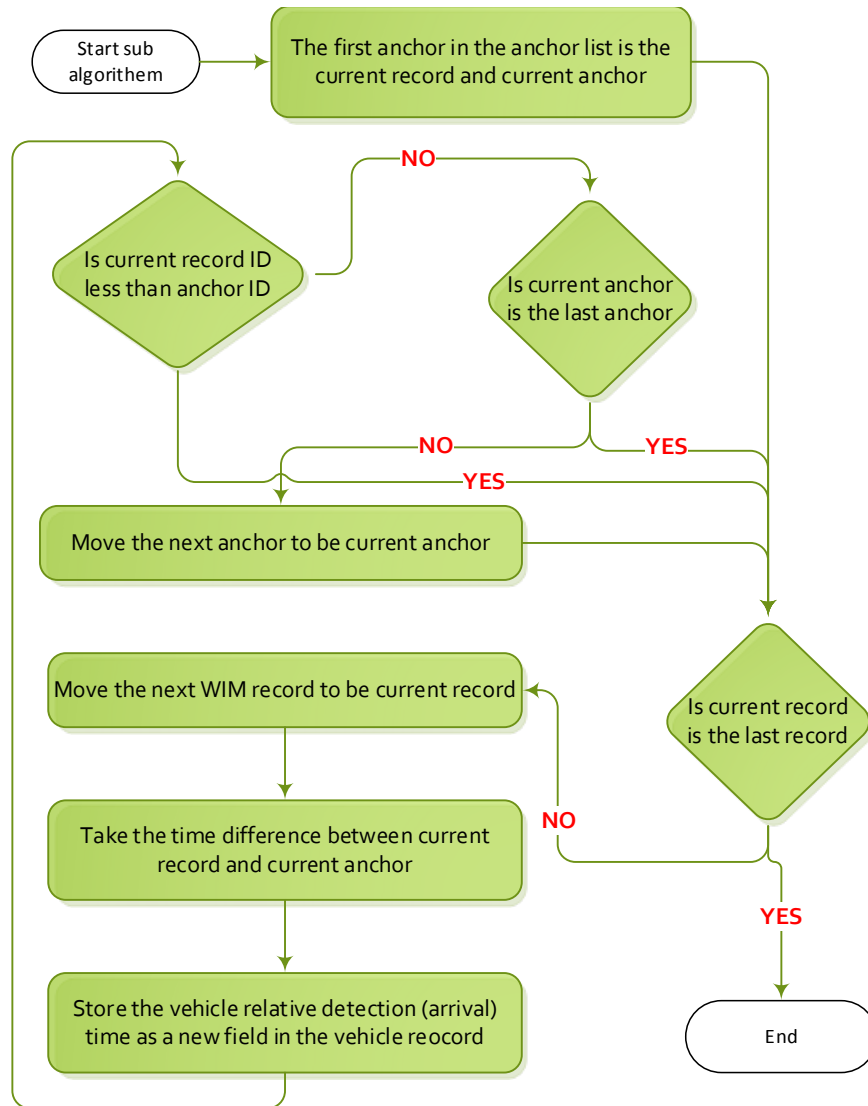


Figure 8.2 ALAA anchor-based relative-detection-time computation

The procedure for extracting anchors included:

- a- Class 9 vehicles in both sites were separated.
- b- Times of occurrence for a certain number of records reported at both sites were compared to approximate constant delay between sites.
- c- Based on information from step (b), a matching record was manually identified and marked every two hours, as shown in Figure 8.4.
- d- The Sequence IDs of the anchors were saved in a table like the one shown in Figure 8.5.
- e- Steps b to d were repeated to extract test records for verifying ALAA accuracy.

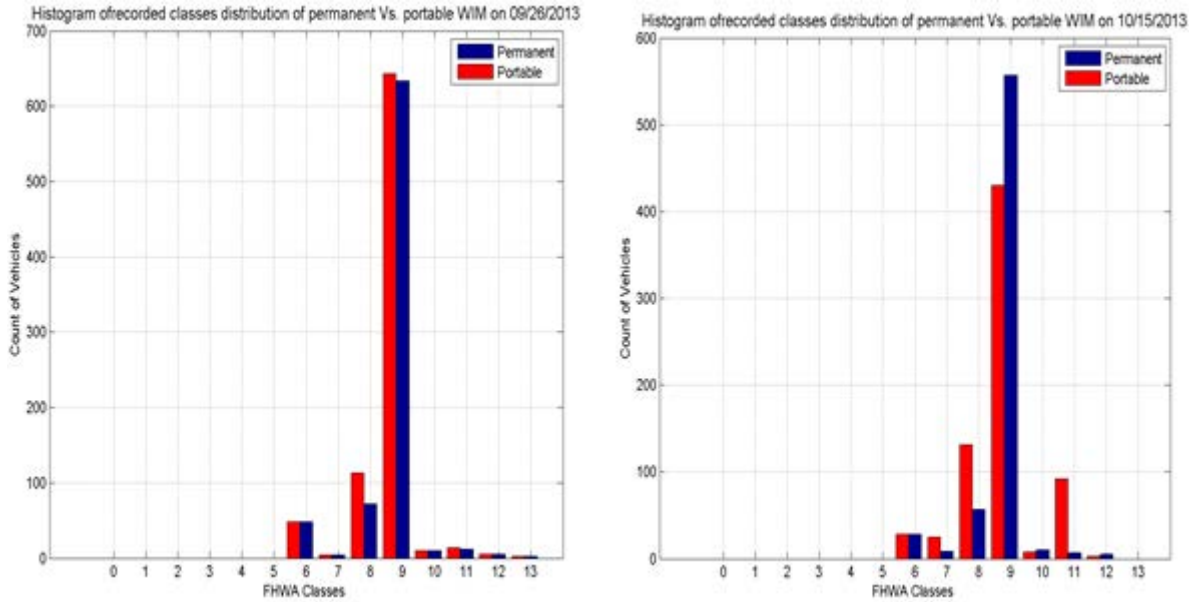


Figure 8.3 Histogram of recorded classes of both sites on two different days.

8.3.2 ALAA performance analysis

While processing record-to-record alignment using ALAA several observations were made:

- a- Algorithm performance was relatively poor on weekends compared to workdays. Figure 8.6 shows day-by-day percent variations of under-matched vehicles. Furthermore, increasing the number of anchors on weekends did not improve performance.

The under-matched rate was calculated using the following equation:

$$missRate = \frac{\text{no. of records reported by permanent} - \text{no. of records aligned}}{\text{no. of records reported by permanent}} * 100 \%$$

- b- The portable WIM experienced sudden drifts in time, possibly due to power failures that trigger a watchdog timer on the iSINC. These drifts terminated synchronization with the permanent site. As a result, more errors were added to the alignment procedure and consequently increased the difficulty of data alignment. The moment at which the portable WIM goes out of synchronization should be identified and registered as an anchor to calculate new time delays caused by such drifts. Fortunately, synchronization was automatically restored after both devices updated their times using NTP servers.

We, further, define two parameters used to measure performance of the developed algorithm. *Matching rate* is the percentage of the number of algorithm-matched records to the total number of records in the validate list. *Alignment rate* is the percentage of the number of successful algorithm-matched records to the total vehicle records.

Final project report

20131009.xls

	A	B	E	F	G	H	I
375	374	10/9/2013 1:25:03 PM:100	9	62	863	0	32486 80
377	376	10/9/2013 1:25:28 PM:310	9	67	797	0	68481 80
380	379	10/9/2013 1:26:52 PM:980	9	70	917	0	31064 80
386	885	10/9/2013 1:29:18 PM:150	9	65	896	0	39194 80
390	389	10/9/2013 1:30:49 PM:290	9	75	596	0	85203 80
394	393	10/9/2013 1:31:08 PM:940	9	79	764	0	30180 80
396	395	10/9/2013 1:33:02 PM:780	9	75	693	0	78767 80
398	397	10/9/2013 1:33:11 PM:140	9	73	804	0	33267 80
400	399	10/9/2013 1:34:29 PM:730	9	81	645	0	85863 80

port20131009.xls

	A	B	E	F	G	H	I
1	SequenceID	DateTime	Class	Speed	Length	18-K ESAL	GV
1398	1397	10/9/2013 1:19:58 PM:320	9	59	541	0	81523
1442	1441	10/9/2013 1:24:18 PM:770	9	47	376	0	1E+05
1496	1495	10/9/2013 1:29:18 PM:340	9	50	520	0	89629
1511	1510	10/9/2013 1:31:08 PM:870	9	60	482	0	72915
1527	1526	10/9/2013 1:33:11 PM:180	9	48	406	0	88299
1548	1547	10/9/2013 1:35:09 PM:320	9	55	499	0	90559
1686	1685	10/9/2013 1:50:14 PM:500	9	57	491	0	78941

Anchor
 Test Sample

Figure 8.4 The extraction of anchors and test records.

	A	B	C	D
1	Perm Anchor	Port Anchor	Perm Test	Port Test
2	13	14	2415	7324
3	153	505	1830	4710
4	269	1039	1762	4477
5	393	1510	1539	3983
6	552	2002	1273	3495
7	765	2510	1010	2995
8	1050	3068	2482	2482
9	1277	3506	546	1980
10	1558	4012	385	1495
11	1786	4525	246	922
12	2185	6408	146	462

Figure 8.5 Anchors' List

Algorithm performance was evaluated using vehicle records collected during a four-day deployment, as shown in Table 8.1. Seven vehicle records were visually identified and matched in the validate list. These records were then used to evaluate the algorithm's matching rate. The algorithm correctly matched all records in the validate list. The alignment rate achieved using the algorithm was $753/779 = 97\%$ accounting for 3% of records unmatched or misaligned. Table 8.1 indicates algorithm performance measures, as reported.

8.4 Per-vehicle analysis:

This section presents a vehicle-by-vehicle comparison between permanent and portable WIM site data. The analysis presumes permanent WIM data is completely accurate and serves as a reference. This assumption, in fact, is not true because errors might and

most likely will occur at the permanent WIM site even when the site is newly calibrated. The only accurate method to examine portable WIM system accuracy is the use of static scales, this was not possible for the purposes of this project due to the excessive amount of time required to implement the method.

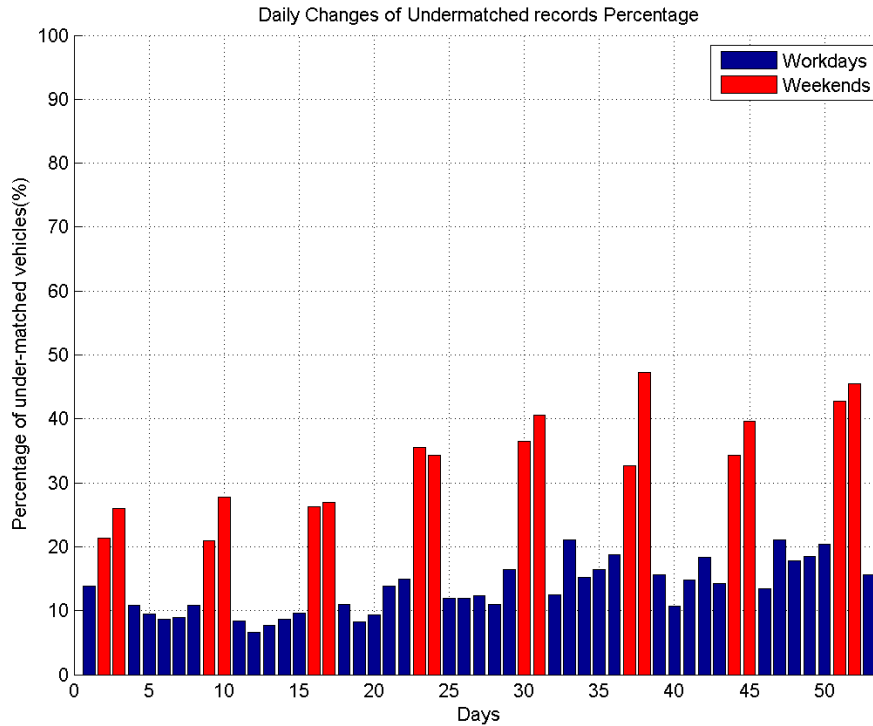


Figure 8.6 Changes of under-matched records percentage.

To measure deviation of portable WIM data from those collected by the permanent site, several statistical tools were employed: Root Mean Square Error (RMSE) given in Eq. 8.1; Normalized RMSE or NRMSE given in Eq. 8.2; and correlation coefficient given in Eq. 8.3, along with its R^2 . The RMSE calculates the absolute deviation or error between the portable and permanent WIM measurements per vehicle record. The NRMSE calculates the percent error. These tools were used to characterize deviation as well as correlation in classification, GVW, FXW, FAS (defined as the distance between the first and second axles), and speed.

Table 8-1 Accuracy and optimality of ALAA for permanent-portable record aligning

Day	Records Mismatching	In-sample under-matching	Out-of-sample alignment-rate
09/13/2013	0/5 (0%) 100% Accurate	0/5 (0%) 100% Optimal	731/787 = 93% 93% Optimal
09/14/2013	0/7 (0%) 100% Accurate	0/7 (0%) 100% Optimal	328/343 = 96% 96% Optimal
09/15/2013	0/7 (0%) 100% Accurate	0/7 (0%) 100% Optimal	237/253 = 94% 94% Optimal

Final project report

Day	Records Mismatching	In-sample under-matching	Out-of-sample alignment-rate
09/16/2013	0/7 (0%) 100% Accurate	0/7 (0%) 100% Optimal	753/779 = 97% 97% Optimal
09/17/2013	0/10 (0%) 100% Accurate	0/10 (0%) 100% Accurate	707/736 = 96% 96% Optimal
09/18/2013	0/13 (0%) 100% Accurate	0/13 (0%) 100% Accurate	753/760 = 96% 96% Optimal
09/19/2013	0/10 (0%) 100% Accurate	0/10 (0%) 100% Accurate	714/786=96% 96% Optimal
09/20/2013	0/10 (0%) 100% Accurate	0/10 (0%) 100% Accurate	595/614=97% 97% Optimal
09/21/2013	0/10 (0%) 100% Accurate	0/10 (0%) 100% Accurate	236/256 = 92% 92% Optimal
09/22/2013	0/10 (0%) 100% Accurate	0/10 (0%) 100% Accurate	253/286 = 88% 88% Optimal
09/23/2013	0/10 (0%) 100% Accurate	0/10 (0%) 100% Accurate	797/833 = 96% 96% Optimal
09/24/2013	0/10 (0%) 100% Accurate	0/10 (0%) 100% Accurate	826/859=93% 93% Optimal
09/25/2013	0/10 (0%) 100% Accurate	0/10 (0%) 100% Accurate	724 /758 = 96% 96% Optimal
09/26/2013	0/10 (0%) 100% Accurate	0/10 (0%) 100% Accurate	759 /786 = 97% 97% Optimal
09/27/2013	0/10 (0%) 100% Accurate	0/10 (0%) 100% Accurate	680 /715 = 95% 95% Optimal
09/28/2013	0/10 (0%) 100% Accurate	0/10 (0%) 100% Accurate	270 /277 = 97% 97% Optimal
09/29/2013	0/10 (0%) 100% Accurate	0/10 (0%) 100% Accurate	223/239=93% 93% Optimal
09/30/2013	0/10 (0%) 100% Accurate	0/10 (0%) 100% Accurate	706/792=89% 89% Optimal
10/1/2013	0/8 (0%) 100% Accurate	0/8 (0%) 100% Accurate	701/768=91% 91%

$$RMSE = \sqrt{\frac{\sum_{i=1}^n (y_i - x_i)^2}{n}} \quad (\text{Eq. 8.1})$$

$$NRMSE = \frac{RMSE}{\text{average}(y)} \quad NRMSE = \frac{RMSE}{\text{average}(y)} \quad (\text{Eq. 8.2})$$

where y_i represents the portable WIM data and x_i represents the permanent WIM data

$$\text{Correlation}(x, y) = \frac{\text{cov}(x, y)}{\sigma_x \sigma_y} \quad (\text{Eq. 8.3})$$

where $\text{cov}(x, y)$ is the covariance between the portable and permanent measurements; σ_x is standard deviation of x , namely the permanent WIM data; and σ_y is the standard deviation of y , namely the portable WIM data.

Correlation coefficient varies between [0,1], where 1 indicates strong correlation and 0 indicates no correlation. Correlation coefficient values of 90% or higher indicate high

linear correlation between portable and permanent WIM data. The coefficient R^2 , is calculated to present a statistical measure of how well the regression line approximates the scattered data points.

Table 8.2 summarizes the calculated NRMSE and correlation. The correlation coefficient is strong between portable and permanent WIM data. Correlated WIM information is first axle weight followed by GVW data. The best correlated WIM information is speed, followed by vehicle type classification. Notably, a 26% error (the highest) was calculated for GVW.

Table 8-2 NRMSE, Correlation between portable and permanent WIM systems.

Parameter	NRMSE	Correlation Coefficient
Classification	0.0340 (3.4%)	0.9475
GVW	0.2905 (29%)	0.8030
FXW	0.2681 (26.8%)	0.3200
FAX	0.0558 (5.6%)	0.9611
Speed	0.0407 (4%)	0.9669

Regression results and R^2 values of GVW, FXW, and speed are respectively presented in Figures 8.7 through 8.9. The FXW measurements obtained from the portable system were the least correlated to those collected by the permanent site. Table 8.3 indicates that 98% of detected vehicles classification matched between systems. Only 2% of vehicle classifications were incorrectly matched.

Table 8-3 Classification matching results between portable and permanent WIM system

Status	Number of Occurrences	Percentage of Occurrences
Total number of aligned records	9099	
Vehicle classification matching	8939	98.24%

Final project report

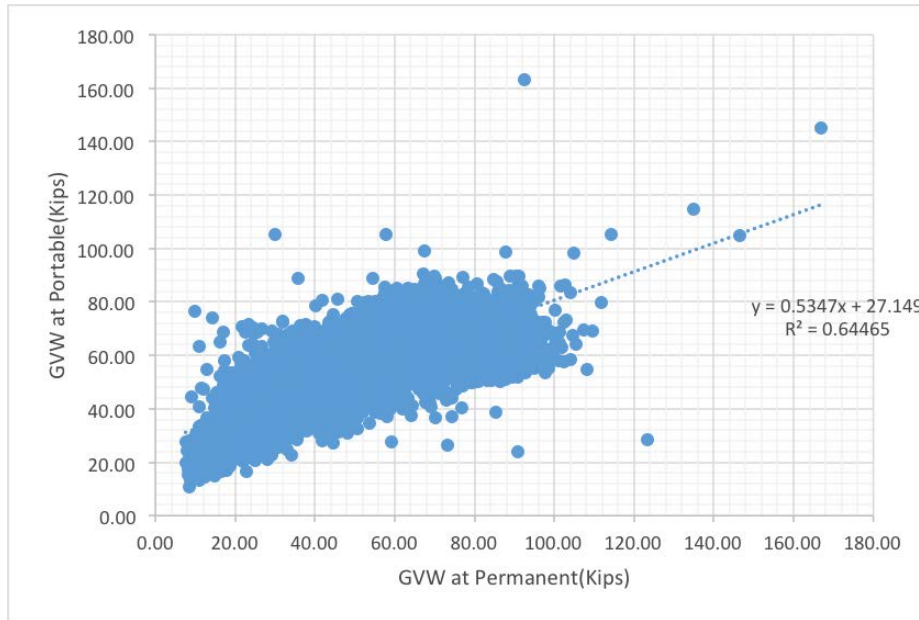


Figure 8.7 Linear regression for permanent to portable GWW comparison

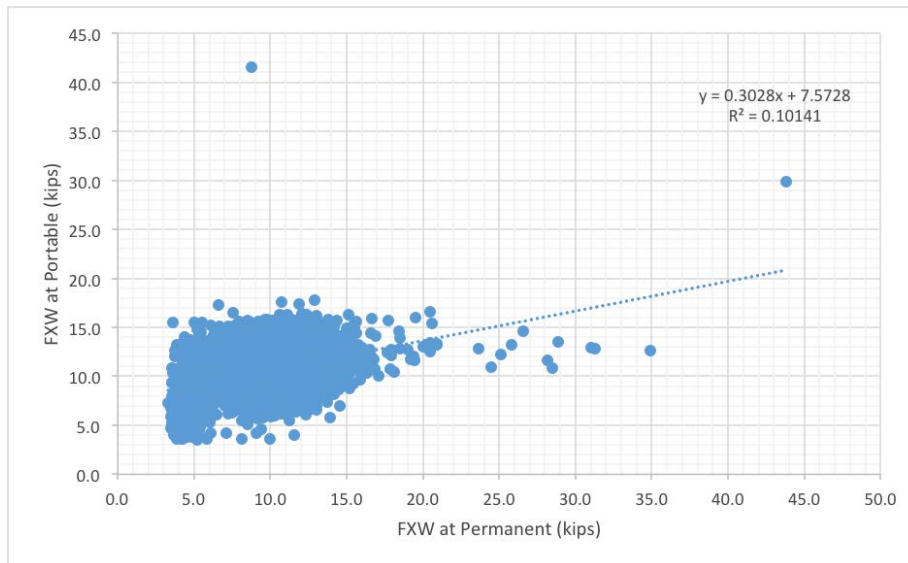


Figure 8.8 Linear regression for permanent to portable FXW comparison

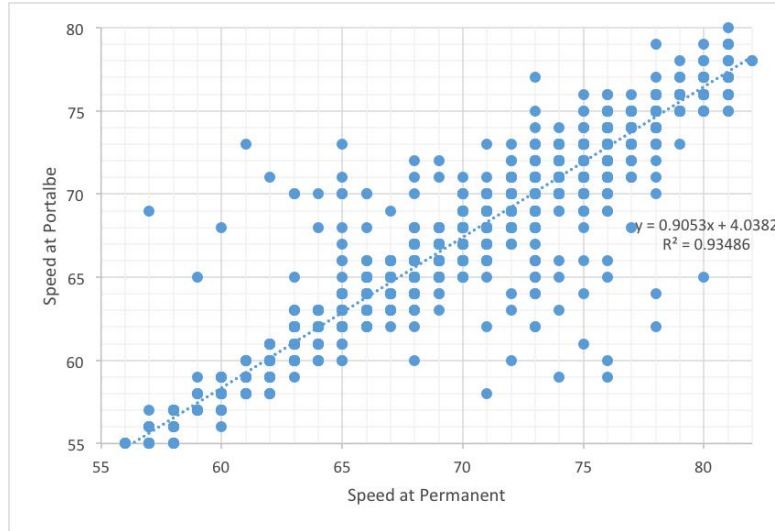


Figure 8.9 Linear regression of speed measurements obtained from permanent and portable systems.

8.5 Probability of error

8.5.1 GVW deference histogram:

Overall error in GVW was 29% on average during phase I of deployment. It increases to 53% during phase II. If GVW data was further examined to provide details of percentage of vehicles with a specific error during phase I, we found that 32% of vehicles had GVW error of equal or less than 10%; 49% of vehicles had GVW error of equal or less than 20%; and 62% of vehicles had GVW error of equal or less than 30%. Complete analysis results are presented in Figure 8.10.

8.5.2 FXW difference histogram

Overall error in FXW was 23% on average during the phase I of deployment. FXW data was further inspected to obtain details about the percentage of vehicles with a specific error. We found that 39% of vehicles had FXW error of less than 10%; 60% of vehicles had FXW error of less than 20%; and 74% of vehicles had FXW error of less than 30%. The comprehensive analysis is illustrated in Figure 8.11.

8.6 WIM data analysis day-by-day

This section presents results of daily WIM data analysis of the last successful portable WIM deployment, which lasted a continuous 50 days. Portable and permanent WIM data was logged and analyzed to monitor portable WIM system performance, including WIM data accuracy and validity. Analyzed parameters included vehicle classification, gross vehicle weight, axle weight, and speed.

Post deployment data processing and record-to-record alignment procedures were completed for the first 50 days. Several analysis techniques were applied to arrive at performance errors and accuracy of the developed portable WIM system.

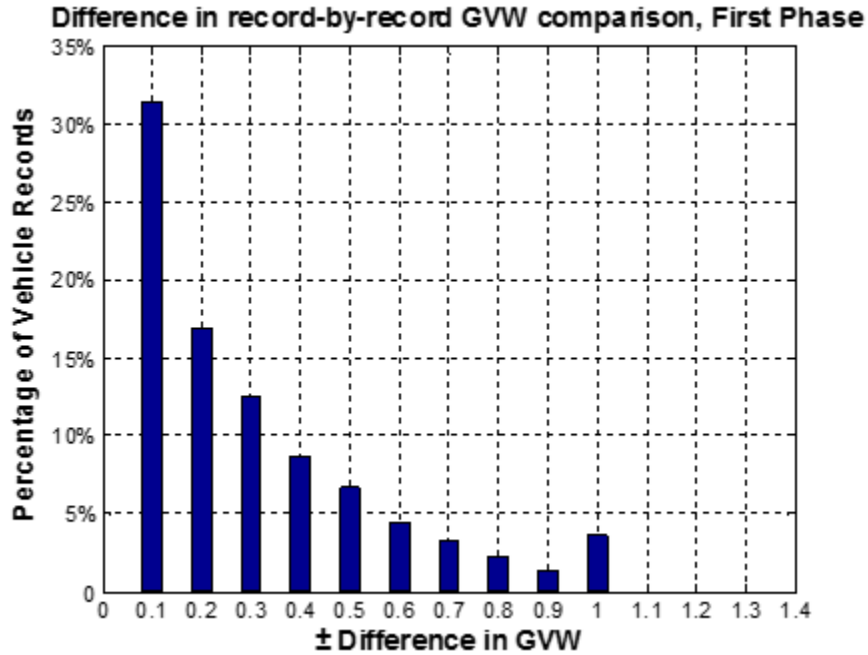


Figure 8.10 GVW error histogram

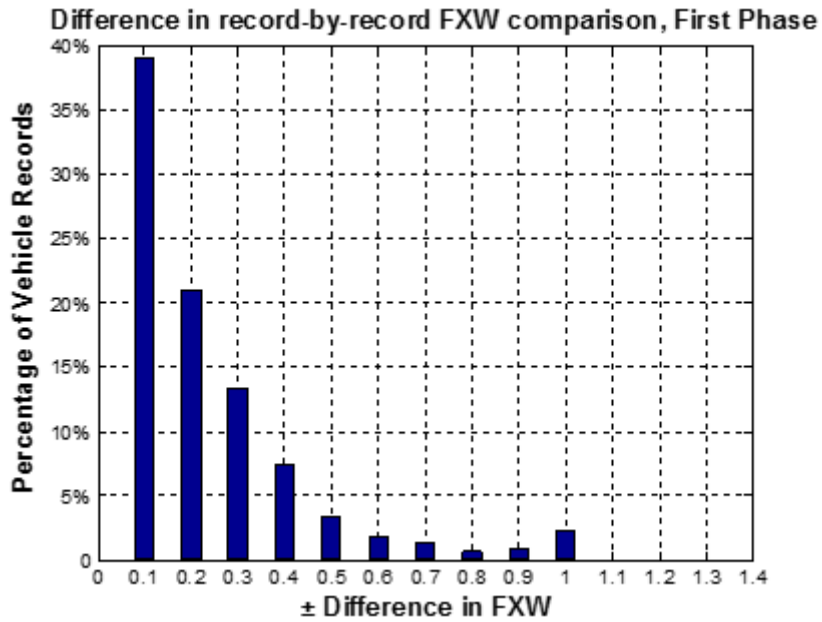


Figure 8.11 FXW error histogram

System accuracy was evaluated by comparing all vehicle parameters, including class, speed, GVW, FXW, and others reported by the portable WIM with their corresponding records in the permanent site. It was assumed that the permanent site provided sufficient measuring accuracy to serve as a truth system.

Figure 8.12 shows day-by-day relative error in classification. It's obvious, given a classification error as low as 3% that classification accuracy was excellent during the first 16 days of deployment, and degradation gradually increased as the number of deployment days grew.

Classification error for each day was calculated using the following formula:

$$\text{Daily Classification Error} = \frac{\text{Number of misclassified vehicles in portable WIM for day } n}{\text{No. of vehicles in day } n} * 100\% \quad (\text{Eq. 8.4})$$

Figure 8.13 shows daily changes in relative error for first, second, third, fourth, and fifth axle weight for class 9 vehicles. The error can be calculated using the following formula:

$$\text{Relative Axle Weight Error} = \frac{|\text{Axle Weight in permanent} - \text{Axle Weight in Portable}|}{\text{Axle Weight in Permanent}} * 100\% \quad (\text{Eq. 8.5})$$

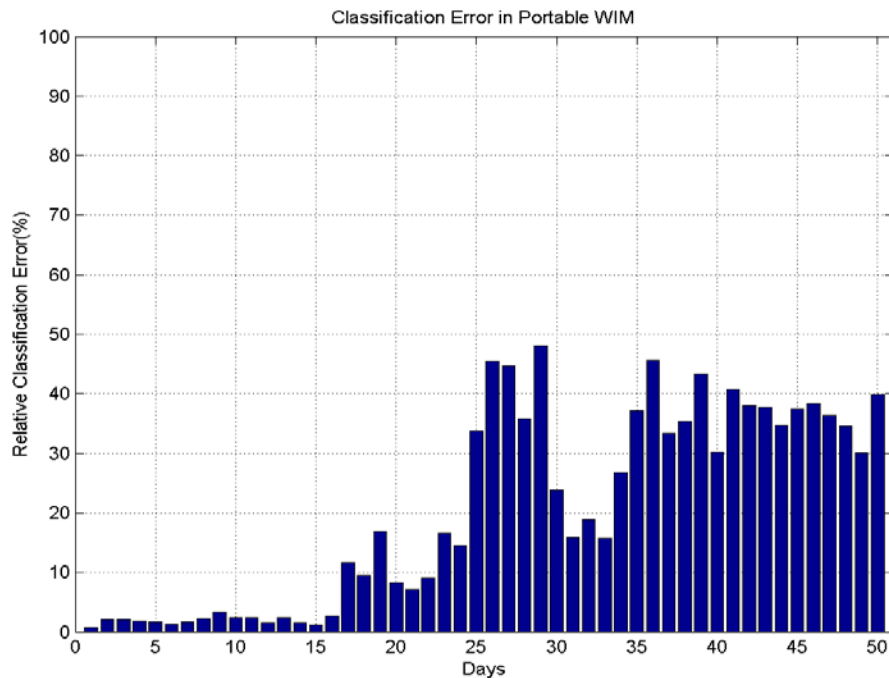


Figure 8.12 The relative classification error of portable WIM

It can be inferred from the figure that the fourth axle weight measurement is highly inaccurate compared to other axle measurements. More investigation should be performed to determine the cause.

Figures 8.14 and 8.15 depict error in measured speed and GVW, respectively. From these figures we conclude that the portable WIM system exhibits a stable performance in all measures for the first 16 days of deployment. Sudden spikes in error rates occur afterwards, requiring system re-calibrated or sensors replacement.

Final project report

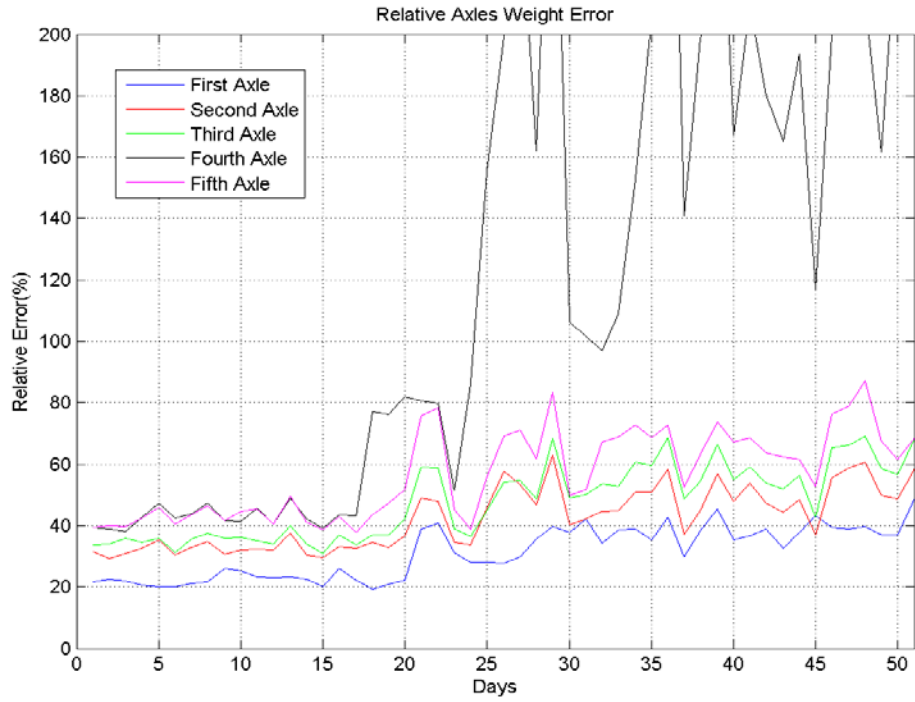


Figure 8.13 Daily relative error in axles' weight

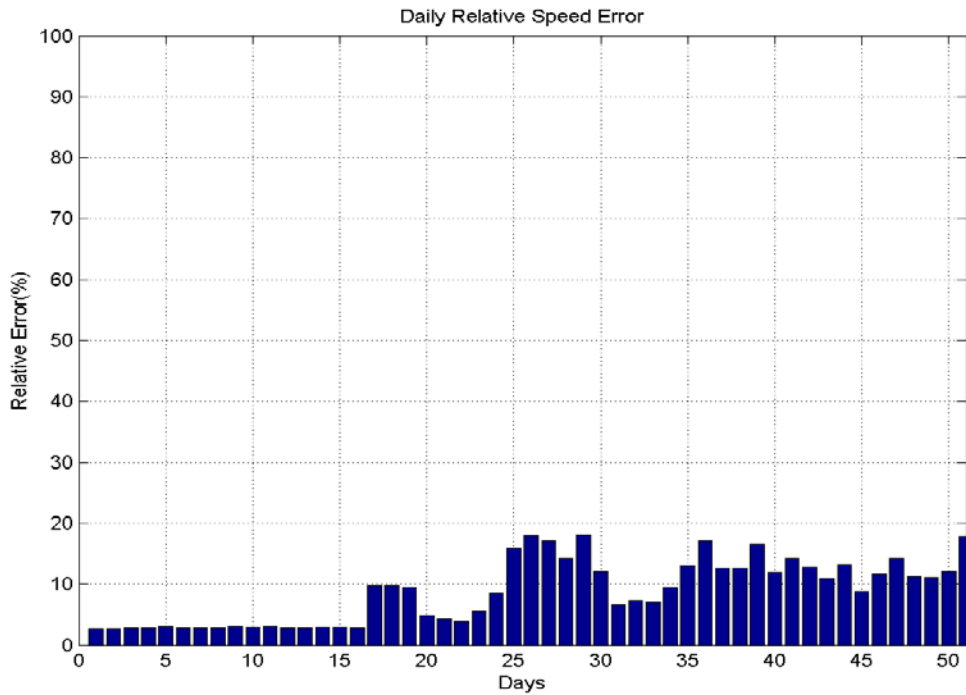


Figure 8.14 Daily relative speed error.

For approximate simple model of systems performance, several statistical and graphical analysis techniques were used to explore the relationship between measurement error and various vehicle parameters, including weight and speed. Of interest was determining how relationships changed over time.

Figure 8.16 shows distribution of GVW for class 9 vehicles for deployment days 4 and 32.

Clearly the permanent site remained approximately a fixed distribution, while distribution of the portable WIM drifted to a higher mean value, as illustrated in Figure 8.17. Also, the number of vehicles detected at the portable site dropped significantly when compared to the permanent site.

To determine parameters most affecting measurement accuracy, relationships between error, speed, and true weight were investigated by means of simple linear regression and curve fitting.

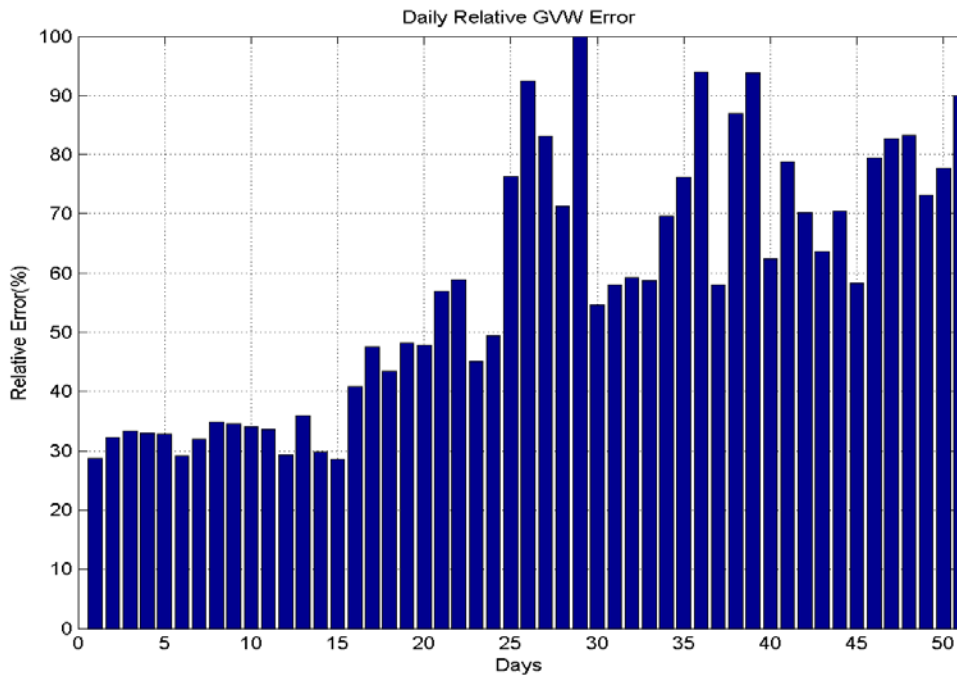


Figure 8.15 Daily relative GVW error.

Figure 8.18 depicts the relationship between relative GVW error and true weight of vehicles, assuming permanent GVW is sufficiently accurate during different days of deployment. Several curve fitting algorithms (e.g., polynomial, Gaussian, and rational fitting) were tested; however, the following rational fitting equation produced the highest “goodness of fit” factor (R2) when compared to others:

$$y = a * \frac{1}{x} + c \tag{Eq. 8.7}$$

where y is the relative GVW error and x is the true weight of the vehicle.

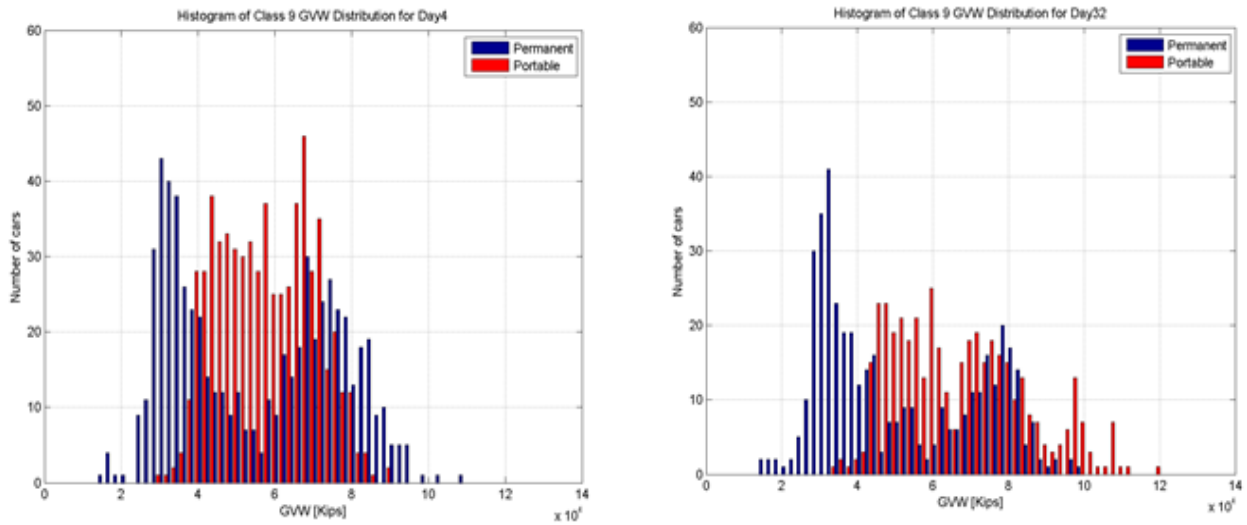


Figure 8.16 The distribution of class 9 GVW in days 4 and 32

From this relationship we can deduce that the error in GVW measurement will be significantly higher for lighter vehicles than heavier ones. One possible explanation is that lighter vehicles experience more vibration and oscillation. As such, they add more noise to the piezoelectric sensors signal.

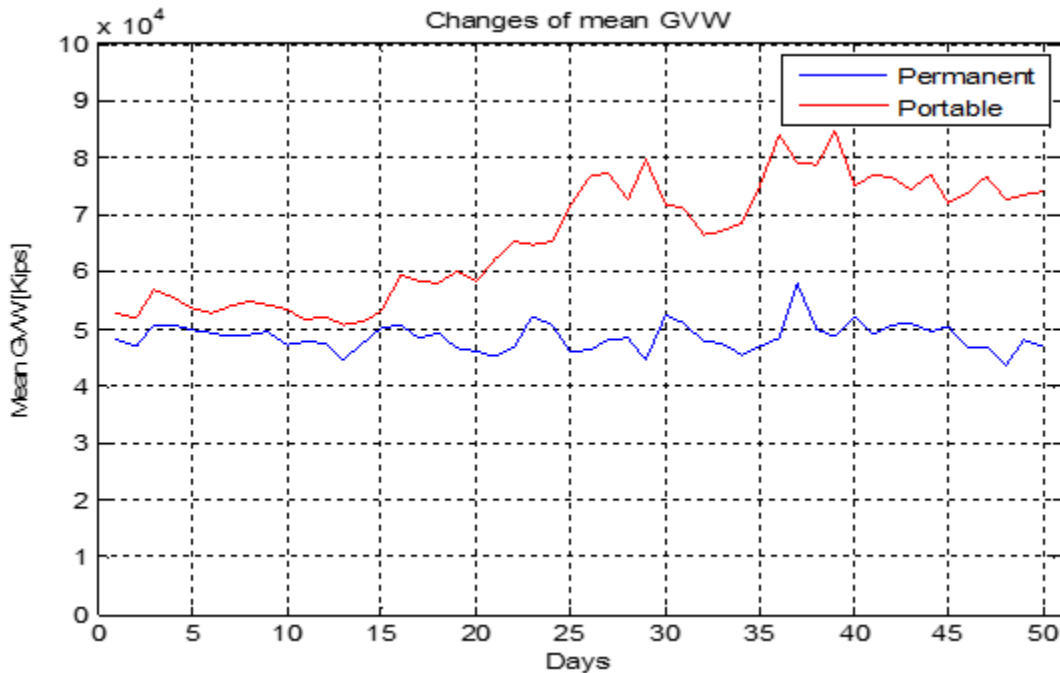


Figure 8.17 Daily changes of mean GVW

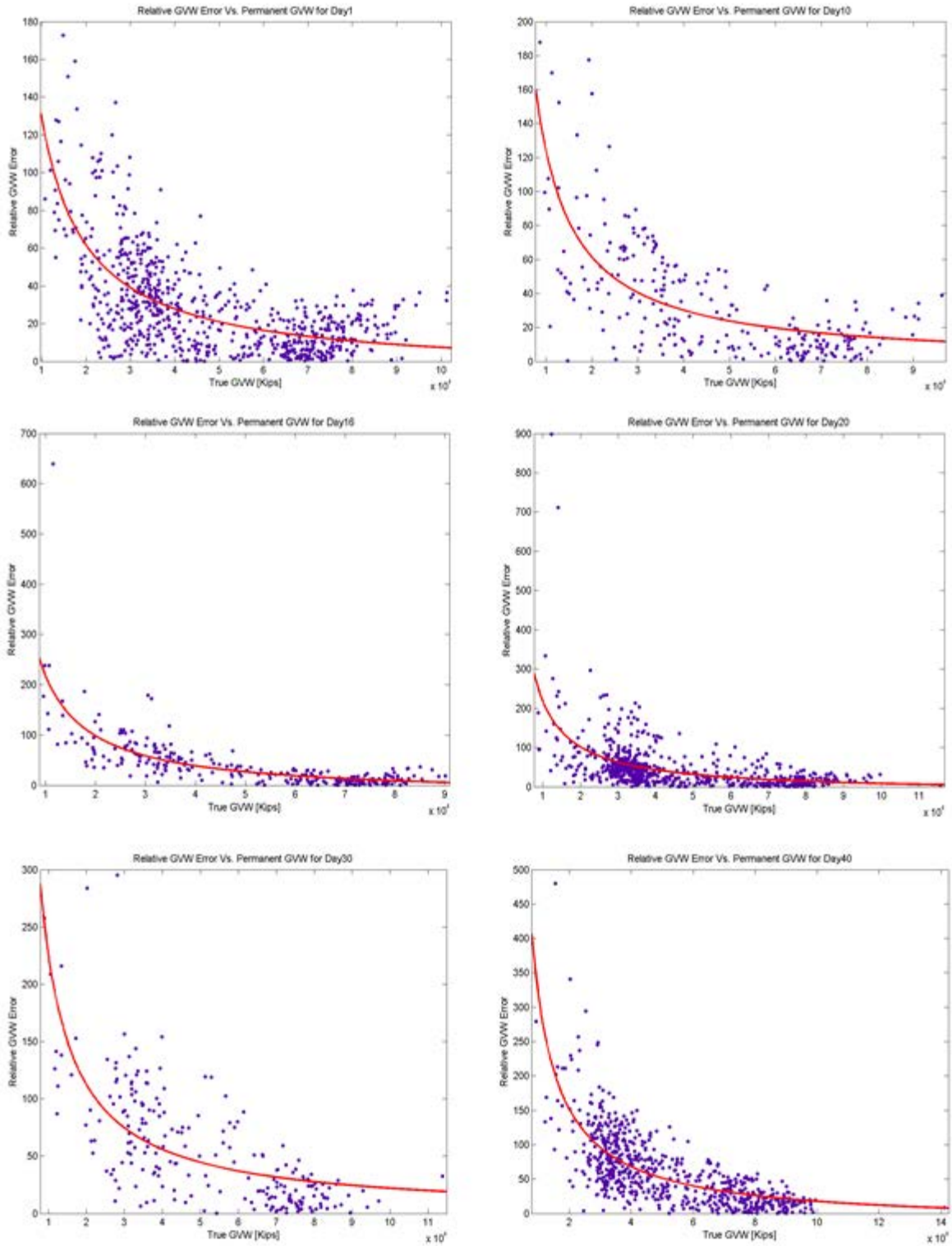


Figure 8.18 The relationship between GWV error and true GWV

Chapter IX

9 WIM Error Modeling and Site Calibration Monitoring

9.1 Introduction

In previous chapters several methods for analyzing portable WIM system performance were introduced. Most methods were based on statistical tests and comparisons assuming the following:

- a- Permanent WIM sites provide highly accurate measurements of class, speed, GVW, FXW, and other factors, rendering it applicable as a ground truth system.
- b- Accuracy is maintained during deployment.

Although such assumptions are acceptable within certain boundaries, a 2013 study of classification and detection accuracy variations of ODOT's WIM16 site confirmed that WIM classification inaccuracy grows exponentially over time.

Figure 9.1 shows changes in number of vehicles detected and class 0 records (i.e., records not classified) for site WIM16 throughout 2013. A significant improvement in performance following site re-calibration is evident.

Figure 9.2 depicts exponential growth in classification inaccuracy prior to site re-calibration.

Previous assumptions might lead to increasing performance analysis error. A new approach will leverage highly accurate WIM16 measurements following recalibration that can be used for developing an optimal statistical model for portable WIM measurements and for evaluating the system's accuracy by studying temporal performance changes with respect to an optimal model.

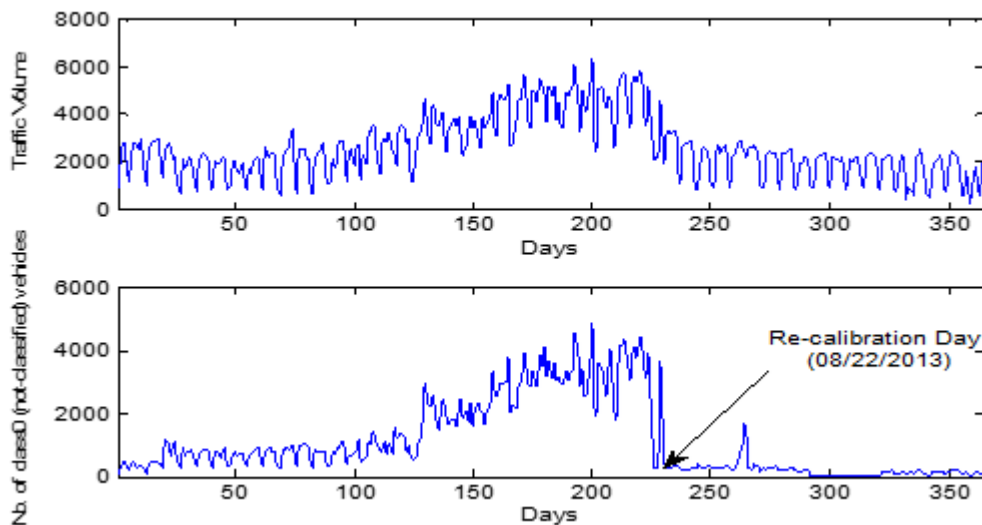


Figure 9.1 Changes in WIM16 traffic volume and number of class 0 during 2013.

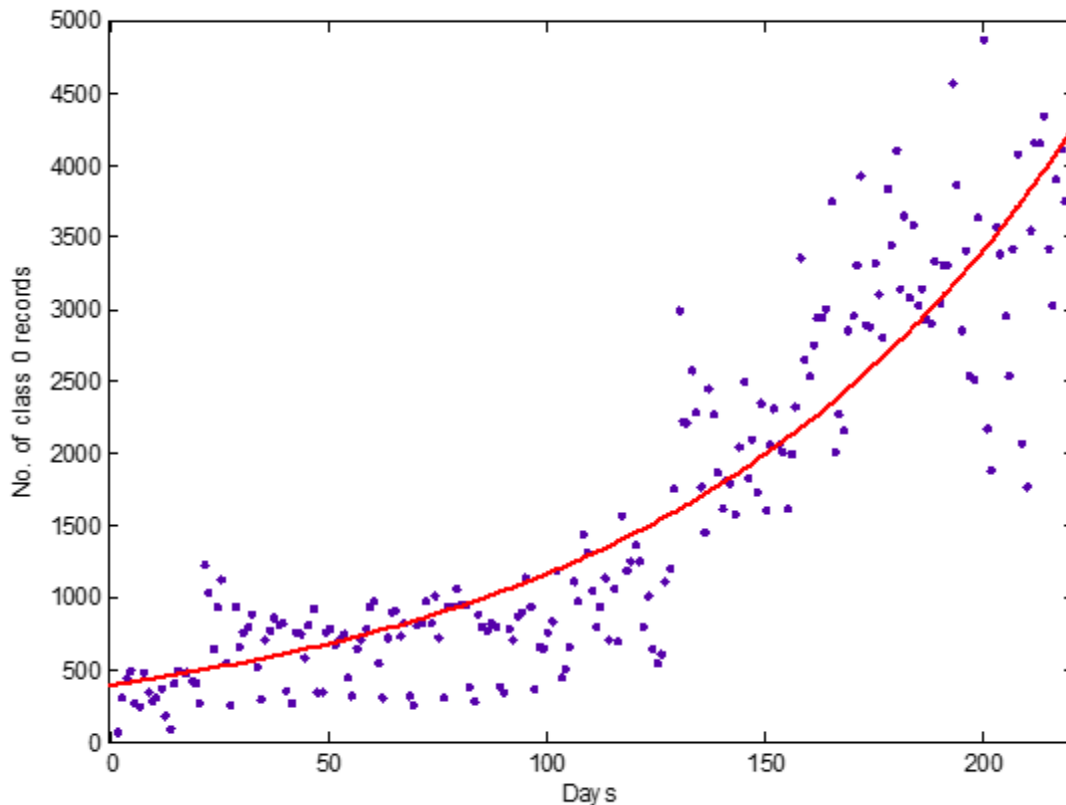


Figure 9.2 Exponential growth in number of class 0 vehicles prior to re-calibration.

In this chapter several machine-learning algorithms are utilized to build a multivariate statistical model for describing optimal WIM station performance using data obtained after WIM16 calibration. Portable WIM performance can then be evaluated by measuring the correlation between newly collected data and the obtained optimal model. ODOT can incorporate this algorithm to examine WIM data quality collected at the sites, and then monitoring calibration state of permanent or portable WIM sites. The algorithm can also be implemented for processing real-time data. A proposed calibration software is presented at the end of this chapter.

9.2 Related work

Transportation research centers around the nation have utilized various methods for evaluating WIM systems accuracy. Most have been based on comparison with a ground truth system (e.g., static scale stations) or statistical quality assurance charts (e.g., CUSUM) to maintain statistical properties of the system within a predefined acceptable range.

In [29] Virginia WIM site performance was evaluated by calculating relative error in GVW measurements and comparing results with a nearby static scale. Researchers in [28] proposed using GVW CUSUM charts to detect WIM sensor drift.

Outlier (i.e., anomaly) detection algorithms have been widely used to evaluate sensor systems. A simple estimating approach in [30] detected anomalies using histograms to evaluate wireless sensor network performance in real-time. Authors in [31] blended three techniques (namely multivariate Gaussian model, principal component analysis (PCA), and a kernel functions based model) to detect anomalies in acoustic sensor networks.

Anomaly detection algorithms haven't typically been used for traffic data analysis and evaluation. A research team at Carnegie Mellon University studied the viability of using various anomaly-detection techniques for analyzing WIM data. Their investigation focused on applying Rectmix, Percentile, and Daikon techniques for evaluating WIM station performance in Minnesota [32]. Researchers' algorithms used human intervention to define outliers among a training set.

The next chapter investigates the application of a multivariate Gaussian anomaly detection technique for analyzing permanent and portable WIM systems.

9.3 Outliers (Anomaly) detection

9.3.1 Introduction

Because WIM data accuracy deteriorates over time, a suitable statistical tool must be used to monitor changes in data characteristics. Control charts (e.g., CUSUM and Shewhart's) are commonly used tools for this purpose. Although charts are powerful tools for quality control, they cannot be used to analyze and identify features of individual records with low probability of occurrence and, consequently, a high likelihood of being erroneous (i.e., outlier).

Identifying outliers in a dataset provides important information about system performance (e.g. relative number of records classified as outliers and their relative location with respect to the optimal model as indicators). Furthermore, identifying outliers aids in determining physical causes for changes in system response and inaccuracy.

9.3.2 Algorithm formulation

Given that a dataset consists of n observations $X = \{x^{(1)}, x^{(2)}, \dots, x^{(n)}\}$ (with each observation having a number of m normally distributed features) and that a subset $\{T\}$ of X with length k has certain statistical characteristics previously known to reflect an accurate representation of the underlying random process that generated the data, it is possible to find an m dimensional multivariate normal distribution that can be considered an accurate statistical description of the random process. The equation for calculating the multivariate normal distribution is:

$$f_x(x_1, \dots, x_m) = \frac{1}{\sqrt{(2\pi)^m |\Sigma|}} \exp\left(-\frac{1}{2}(x - \mu)^T \Sigma^{-1}(x - \mu)\right) \quad (\text{Eq. 9.1})$$

where μ is a vector that contains the mean values of the m features and Σ is the $m * m$ covariance matrix.

Figure 9.3 shows a scatter plot of Feature 2 vs. Feature 1 for a hypothetical two-feature dataset with normal distributions, as shown in Figure 9.4

After calculating the distribution from the training set, test data in set X is plotted against it, and then similarities for each observation in X with respect to the resultant distribution is calculated by means of Mahalanobis Distance, as defined by the following equation:

$$D_M(x) = \sqrt{(x - \mu)^T \Sigma^{-1} (x - \mu)} \quad (\text{Eq. 9.2})$$

Threshold Th can be specified given that $D_M(x) > Th$ for the observation under study is marked as an outlier; otherwise, it is marked as a normal observation.

Figure 9.5 represents the bivariate normal distribution of the hypothetical dataset in Figure 9.3 and its corresponding elliptic contour plot.

Notably, the simple Euclidean Distance from the mean cannot be used for multivariate statistical analysis except when the contour plot is characterized by concentric circles.

Figure 9.6 shows dataset X scattered on the contour plot with outliers colored in red and normal observations in blue. The Mahalanobis Distance threshold used is $Th = 4$.

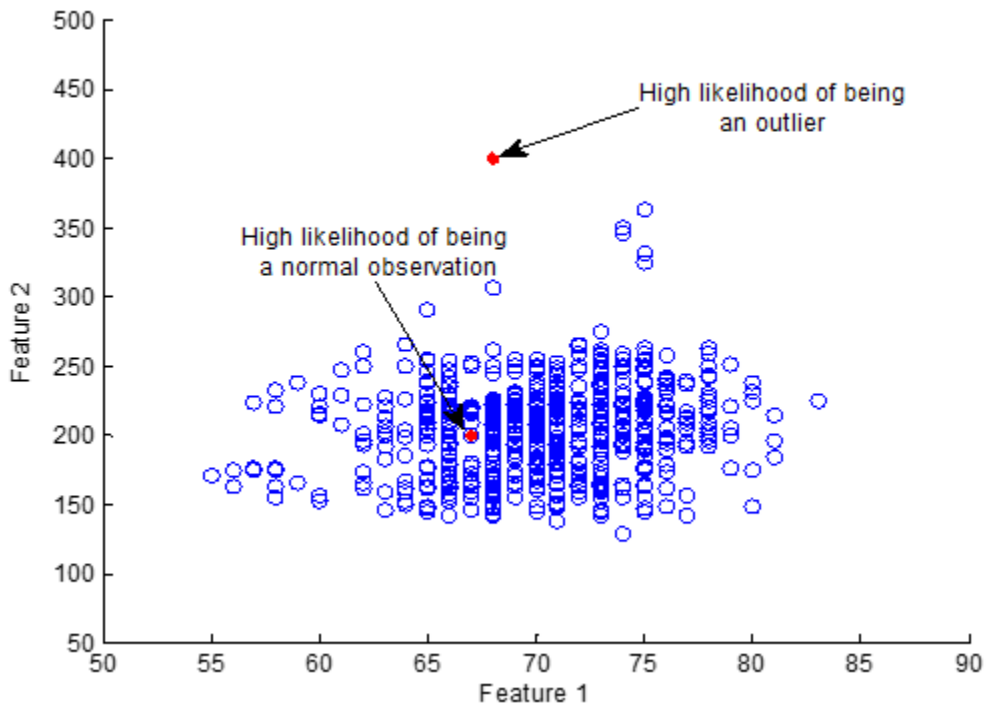


Figure 9.3 Feature 2 vs. Feature 1 scatter plot.

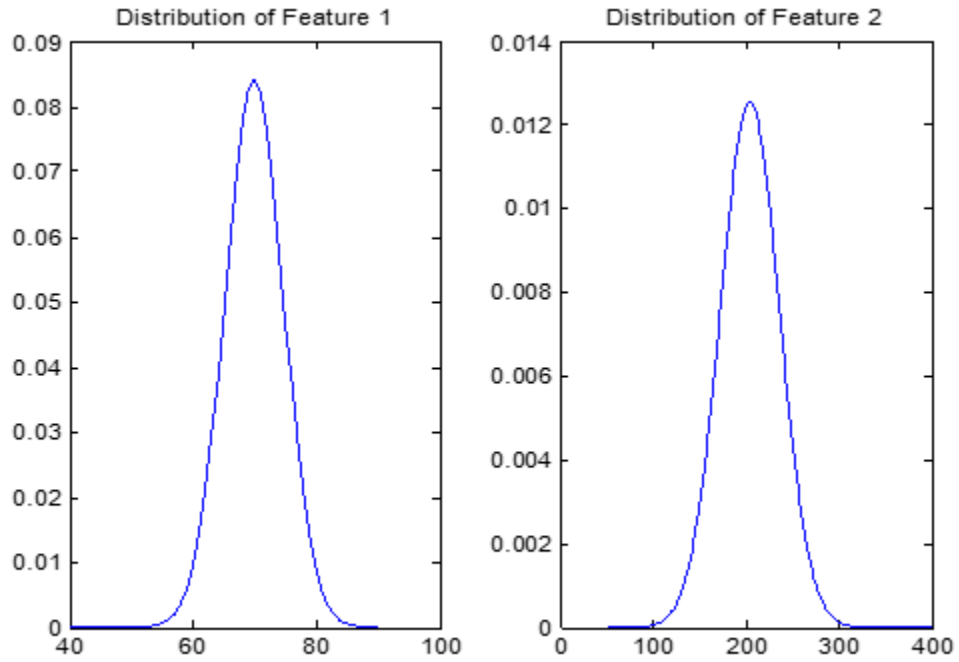


Figure 9.4 Distributions of Features 1 and 2.

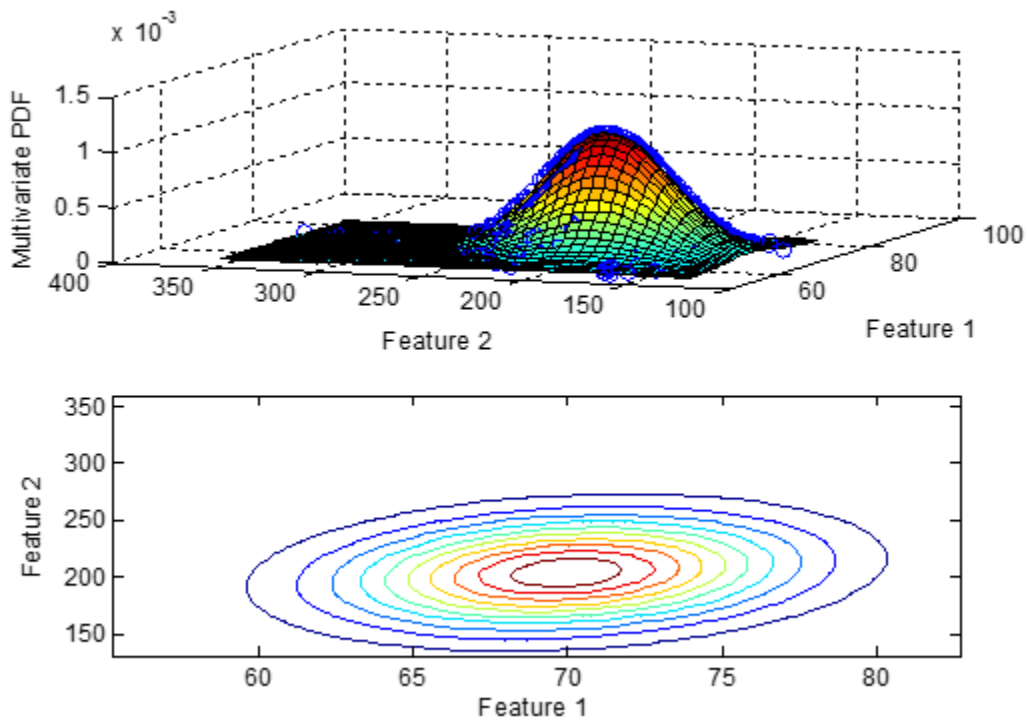


Figure 9.5 Bivariate distribution of Feature 1 and 2 and corresponding contour.

9.3.3 Detecting outliers in WIM16 data

Detecting outliers in WIM data aids in performance assessment of these systems by monitoring changes in the number of vehicles classified as outliers along with their respective location on the multivariate distribution. It can also be used as an early stage of a supervised classification algorithm for generating accurate classification training data.

To apply the algorithm for WIM16, a sufficiently large amount of system data known to be highly accurate in terms of classification and speed/weight measurements must be used to train the algorithm and find the standard multivariate normal distribution. Volume analysis shown in Figure 9.1 indicates unsurpassed performance for days immediately following re-calibration. This assumption was supported by an accuracy test that occurred October, 18 2013, and included classification and speed measurement validation using a camera and a Doppler radar. Figure 9.7 depicts histograms of class and speed obtained by WIM16, camera, and radar. It's evident that there is a slight deviation in the mean value of speed between the radar and WIM16. However, we believe the shift in radar was caused by an uncompensated cosine-effect error. This means that data collected during a two week period between 08/22/2013 and 09/05/2013 was appropriate for algorithm training.

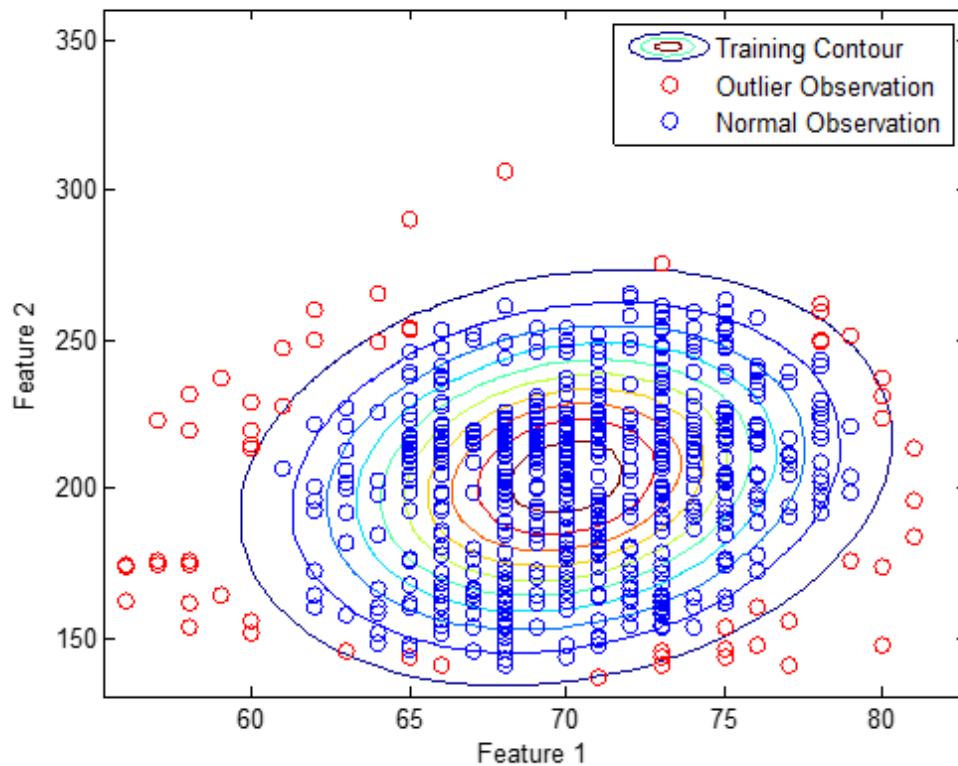


Figure 9.6 Scatter of test observations on training contour plot.

Training data included 33,695 records, 11,407 of which were Lane 0 and the remainders randomly distributed across three other lanes. Because the portable WIM system is deployed only on Lane 0, we were concerned about data recorded on that specific lane.

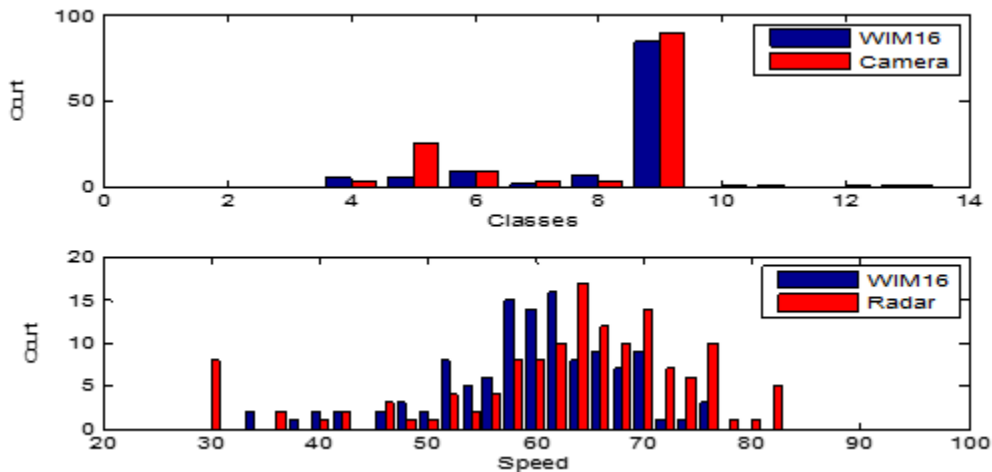


Figure 9.7 Classification and speed accuracy of WIM16.

A classification analysis of the WIM16 site showed that more than 65% of recorded vehicles were class 9. See Figure 9.8. As such, the balance of this analysis is primarily focused on class 9 vehicles.

Three main features (namely speed, GVW, and FXW) were chosen to build standard multivariate normal distribution from the training set. These three variables were chosen because their accuracy is indicative of various system component performances. For example, speed is directly related to the magnetic loop performance, and weight is directly related to piezoelectric sensor performance.

In particular, fourth axle weight was chosen because of its highly linear relationship with GVW compared to FXW. Furthermore, we previously demonstrated that portable WIM fourth axle weight measurements experience severe inaccuracies when compared to other axles. Figure 9.9 illustrates the deviation from the linear relationship between GVW and fourth-axle weight on day 25 of the deployment when compared with data from day 1. This phenomenon serves as a good indicator of declining accuracy of portable WIM sensors and implies that it would be easy to capture records causing errors by studying the distribution of “weight ratio” (i.e., creating a new feature that takes the value resulting from dividing GVW by fourth-axle weight) as opposed to studying absolute weight.

Figure 9.10 illustrates the relationship between GVW and first- and fourth-axle weights. Value of “goodness of fit” (R^2) for both regressions clearly shows that fourth axle weight and GVW are nearly linearly related.

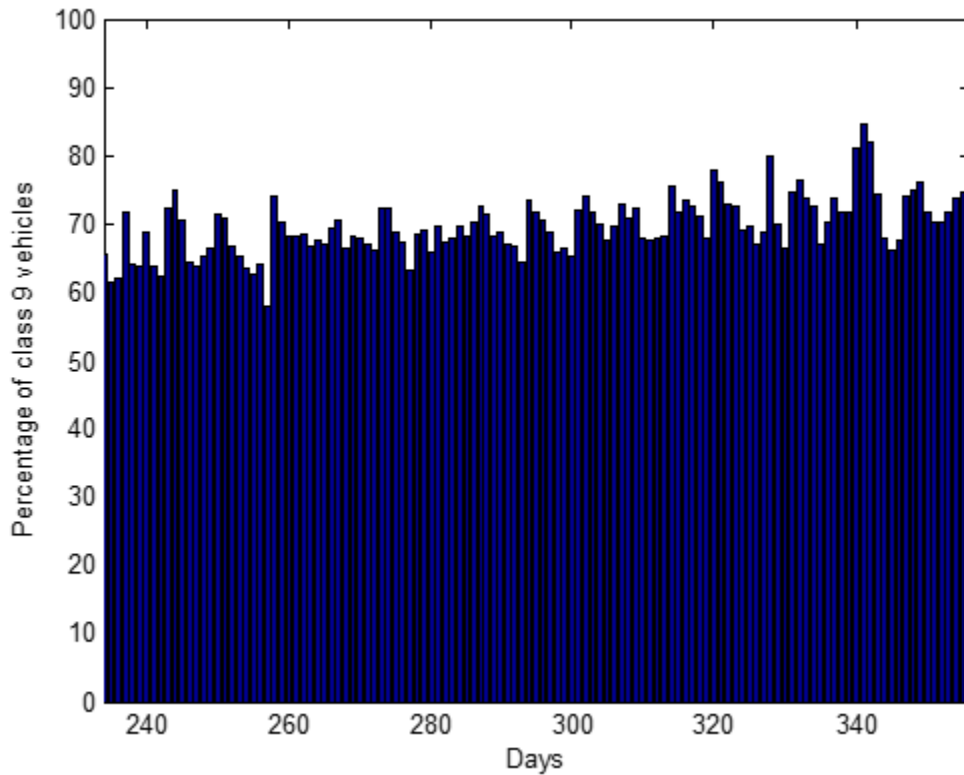


Figure 9.8 Percentage of class 9 vehicles detected following calibration.

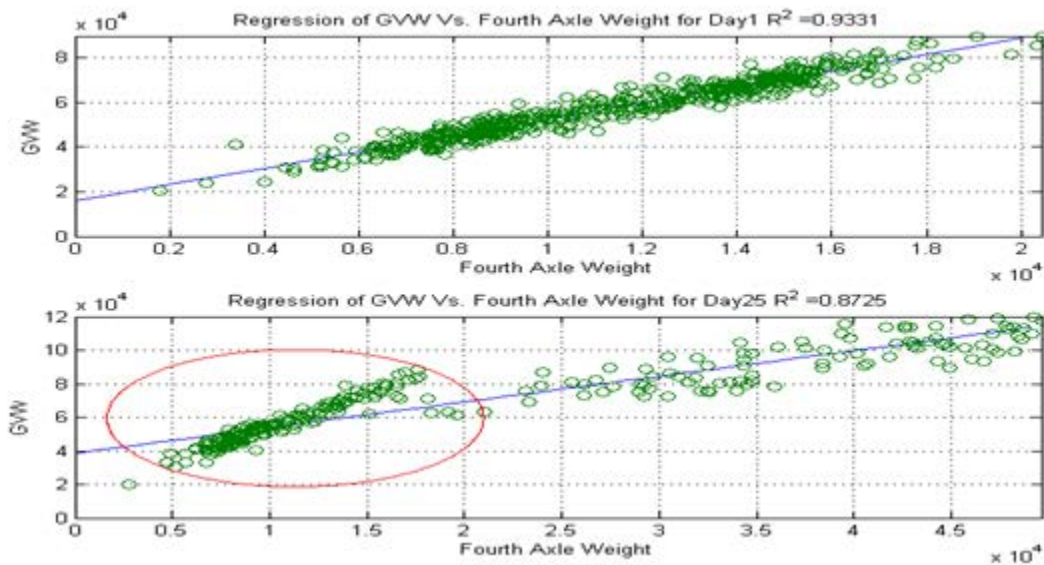


Figure 9.9 Linear regression of GVW and fourth-axle weight for days 1 and 52.

Accurate implementation of the multivariate outlier detection algorithm requires all used features to be normally distributed. However, this is not the case for class 9 GVW distribution, as can be inferred from Figure 9.11.

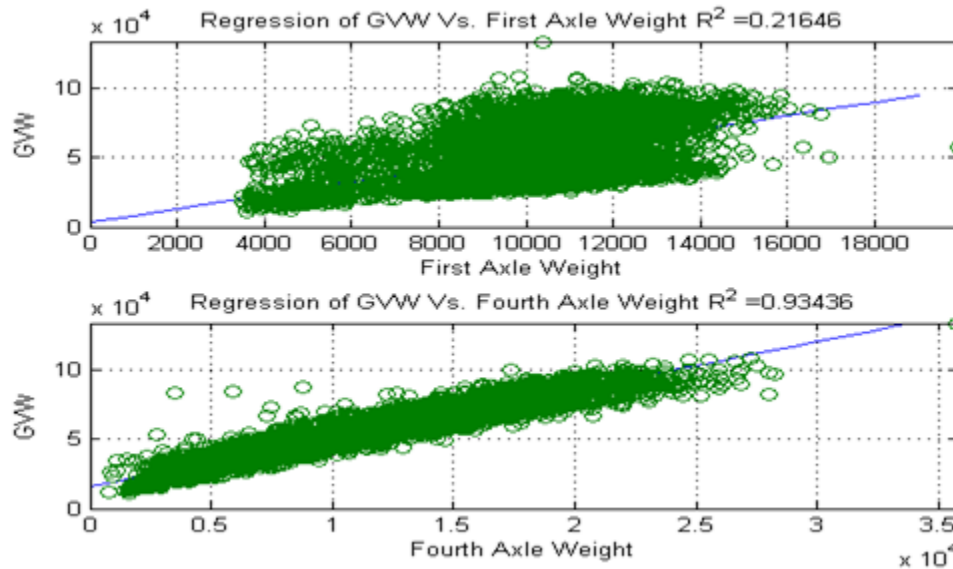


Figure 9.10 Relationship between GVW and first- and fourth-axle weights.

Expectation Maximization is a numerical algorithm for maximizing functions of several variables. The algorithm is widely used in solving a special but important problem: the estimation of parameters of a mixture of Gaussians from a set of data points [26].

Given that a set of data points is generated by multiple processes (e.g., two lines), modeling two processes necessitates estimating: 1) parameters (e.g., slope and intercept) of the two lines; and 2) the assignment of each data point to the generating process. The principle behind EM is that each step can be easily addressed assuming another is solved. Assuming each data point assignment is known, the parameters of each line can be estimated by taking into consideration only points assigned to it. Likewise, if parameters of the lines are known, each point can be assigned to the line that fits it best [27].

Thus, the basic structure of an EM algorithm can be explained:

- Start with random parameter values for the two models.
- Iterate the following until parameter values converge:
 - E step: assign points to the model that fits best.
 - M step: update the models' parameters using only points assigned to it.

Granted, the mathematical interpretation of EM is more complicated than the two aforementioned steps. However, this concern is beyond the scope of this report.

The authors of [28] proposed using EM to split class 9 GVW data into three Gaussians: the first associated with empty trucks; the second with partially-loaded trucks; and the last with fully loaded trucks. However, the observed weight-averaging behavior of the portable WIM station made makes the distinction between three Gaussians more

difficult and nearly impossible for EM to converge. Figure 9.11 compares class 9 GVW distribution among portable WIM station and WIM16.

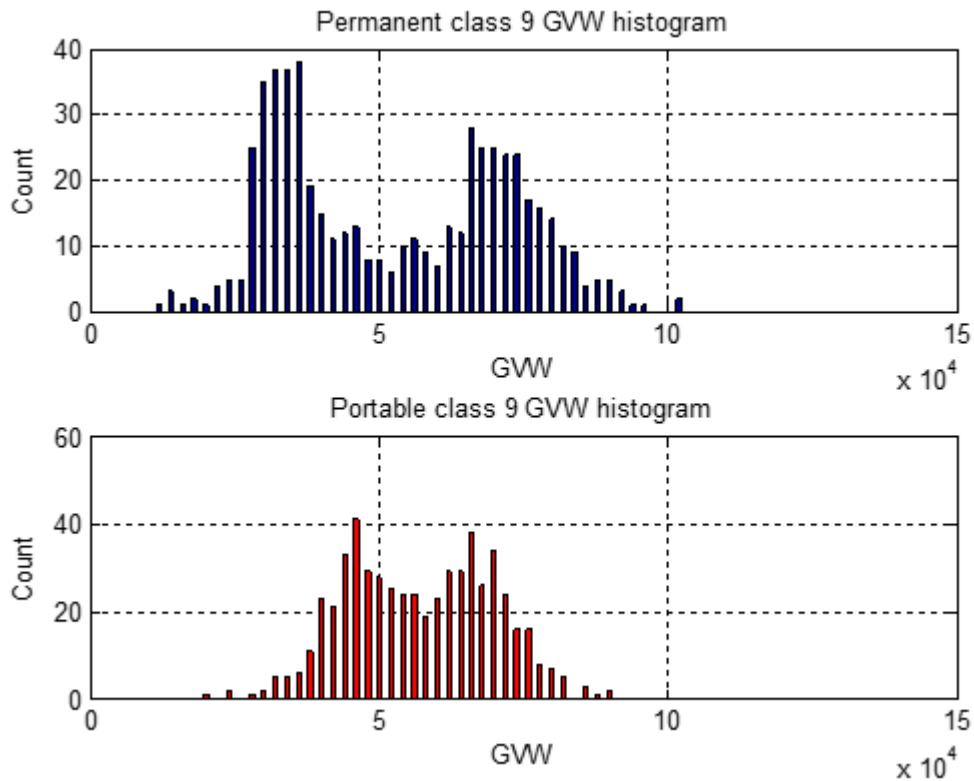


Figure 9.11 Distribution of class 9 GVW in permanent and portable WIM.

Applying EM on GVW training data resulted in two Gaussians, as illustrated in Figure 9.12, with the following parameters:

Table 9-1 Mean and standard deviation for unloaded and loaded trucks.

	Mean	Standard Deviation
Unloaded Trucks	34.911 Kips	6.531 Kips
Loaded Trucks	69.854 Kips	11.351 Kips

After splitting GVW into two Gaussians, the linear relationship between GVW and fourth-axis weight was exploited to generate a new feature by dividing the former by the latter. Two multivariate normal PDFs were generated using speed and the new feature, which will be called “weight ratio”. Dividing GVW by fourth-axis weight had two advantages. Initially dimensionality was reduced (i.e., the multivariate PDF is now calculated for two features, namely speed and weight ratio, instead of three), while the

same amount of information was maintained, hence, reduced computational complexity. Also, the generated feature had a PDF more similar to the Gaussian distribution.

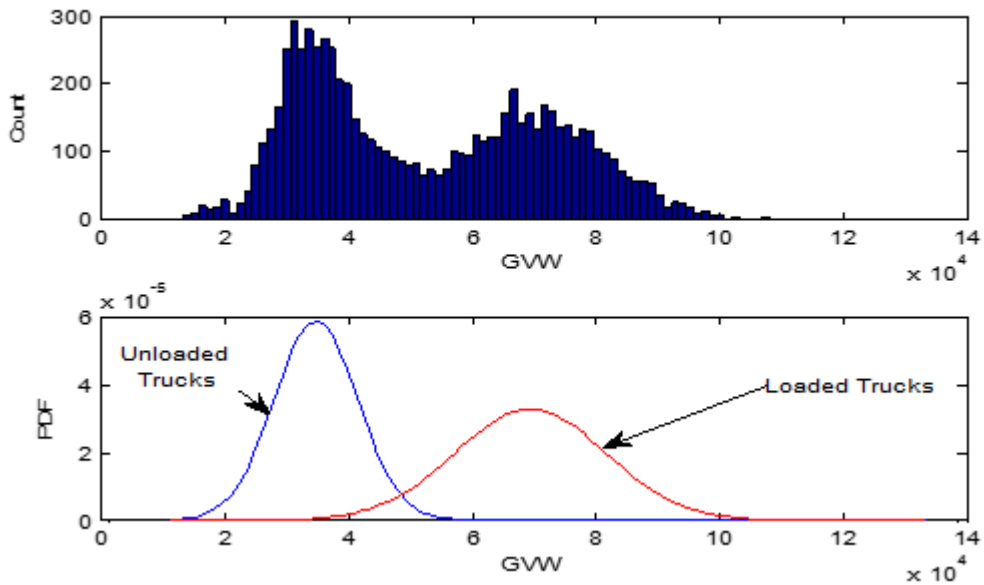


Figure 9.12 Results of Applying EM on WIM16 class 9 GWW data

Figures 9.13 through 9.16 show the resulting multivariate models for both loaded and unloaded trucks.

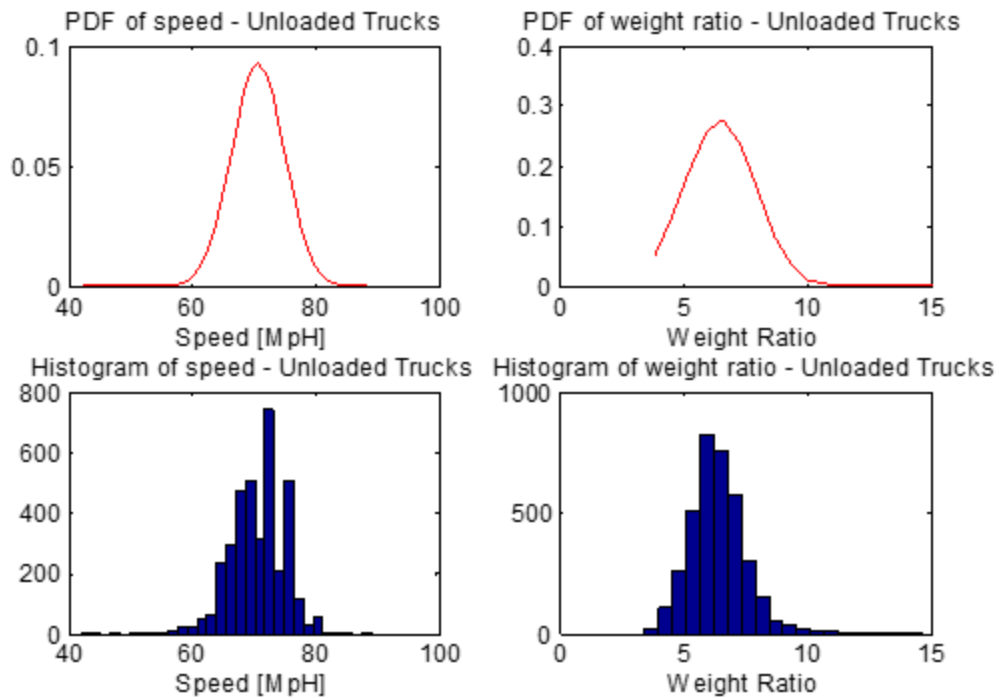


Figure 9.13 Histograms and PDFs of speed and weight ratio for unloaded trucks.

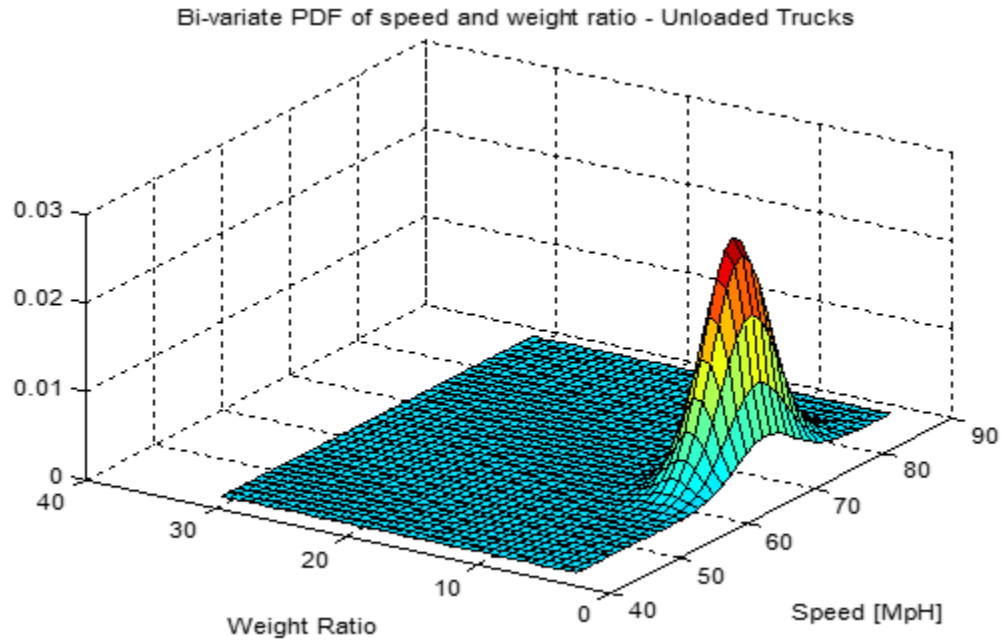


Figure 9.14 Bivariate model of unloaded trucks.

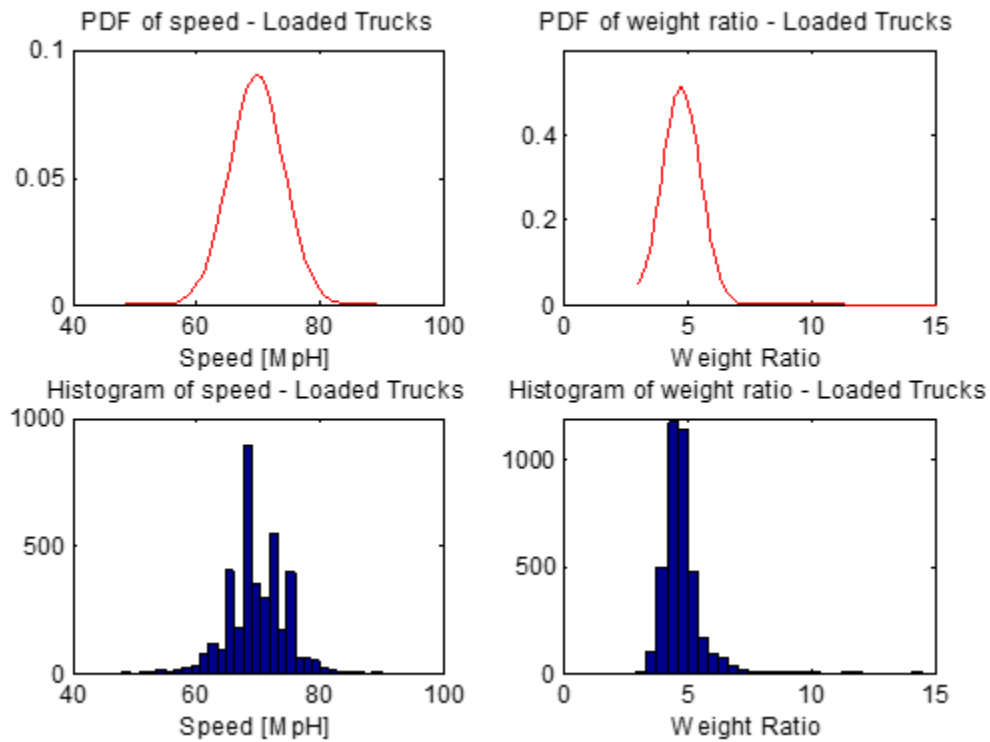


Figure 9.15 Histograms and PDFs of speed and weight ratio for loaded trucks.

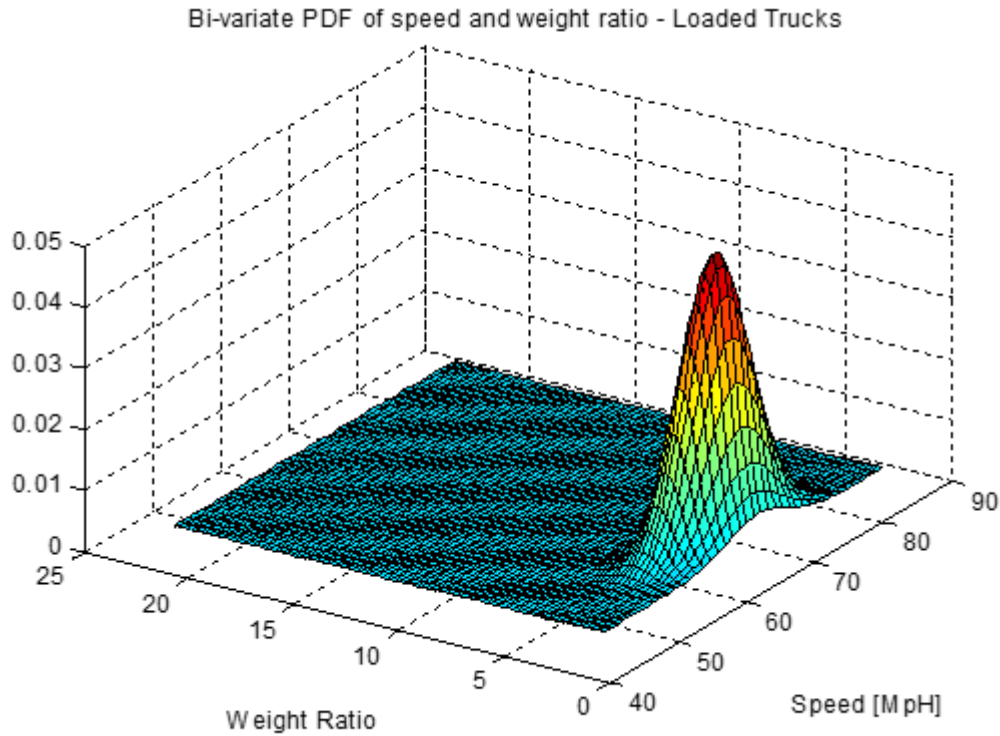


Figure 9.16 Bivariate model of loaded trucks.

Figure 9.17 depicts a basic flow diagram for analyzing WIM16 data. Analyses commenced August 1, 2013, and ended December 31, 2013.

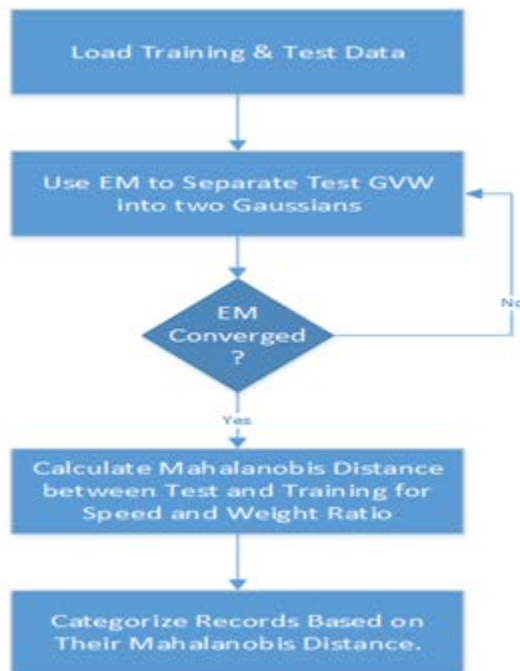


Figure 9.17 Anomaly detection flow diagram.

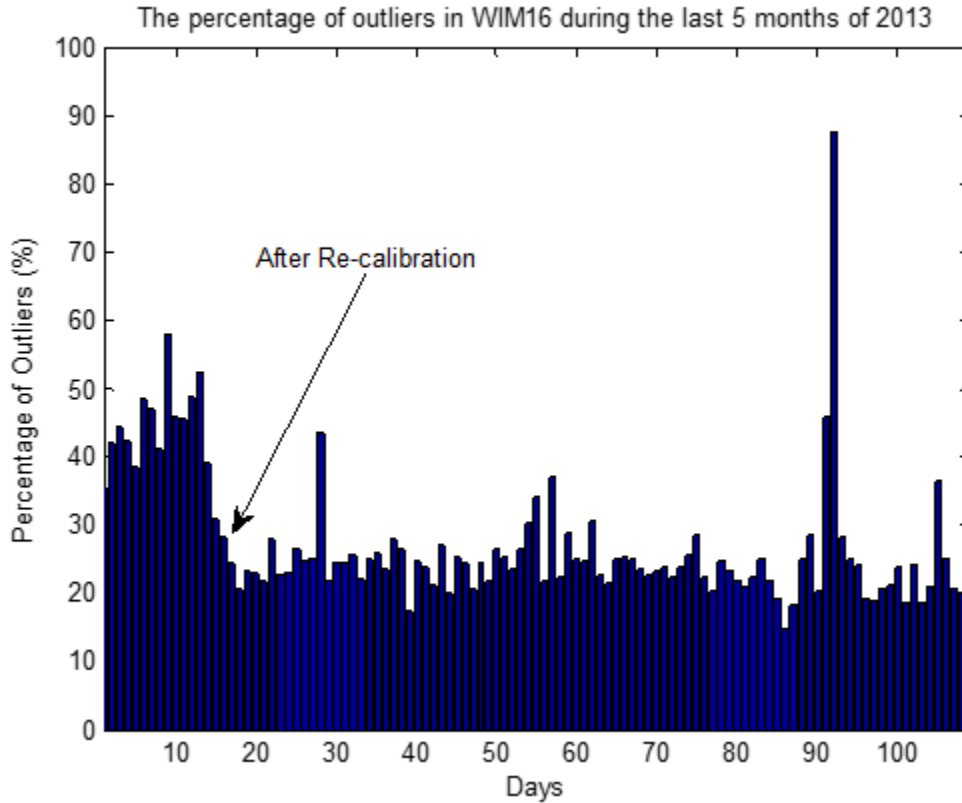


Figure 9.18 Relative number of outliers in WIM16 data.

9.3.4 Detecting outliers in portable WIM data

The model obtained in 3.3 was used to analyze portable WIM station performance. Speed, GVW, and fourth-axle weight of all class 9 and class 11 vehicles recorded at the portable site were used to fit each record to the model and subsequently determine their correlation factor. Class 11 was included because the portable WIM misclassified an inordinate amount of class 9 vehicles as class 11 after few days of deployment. Figure 9.19 shows histograms for GVW and class for selected days from deployment beginning and end. Finally, Figure 9.20 illustrates daily changes in outliers' percentage of portable WIM data, excluding holidays. The relationship of system performance with time, see Figure 9.21, was approximated by the following function with a "goodness of fit" factor $R^2 = 0.771$:

$$\text{PercentageOfOutliers} = -98.6 * \text{erfc}\left(\frac{\text{currentTime}}{\text{totalNumberOfDays}}\right) + 108.5 \quad (\text{Eq. 9.3})$$

The error function is suitable for fitting the temporal changes of outliers' percentage because the range of its absolute value is [0 1]. Thus, manipulating the error function can produce a new function with values in the range [0 100], which is the same range of the percentage values.

Eq 10.3 indicates that portable WIM inaccuracies will be more than 50% after 0.4 of the deployment period.

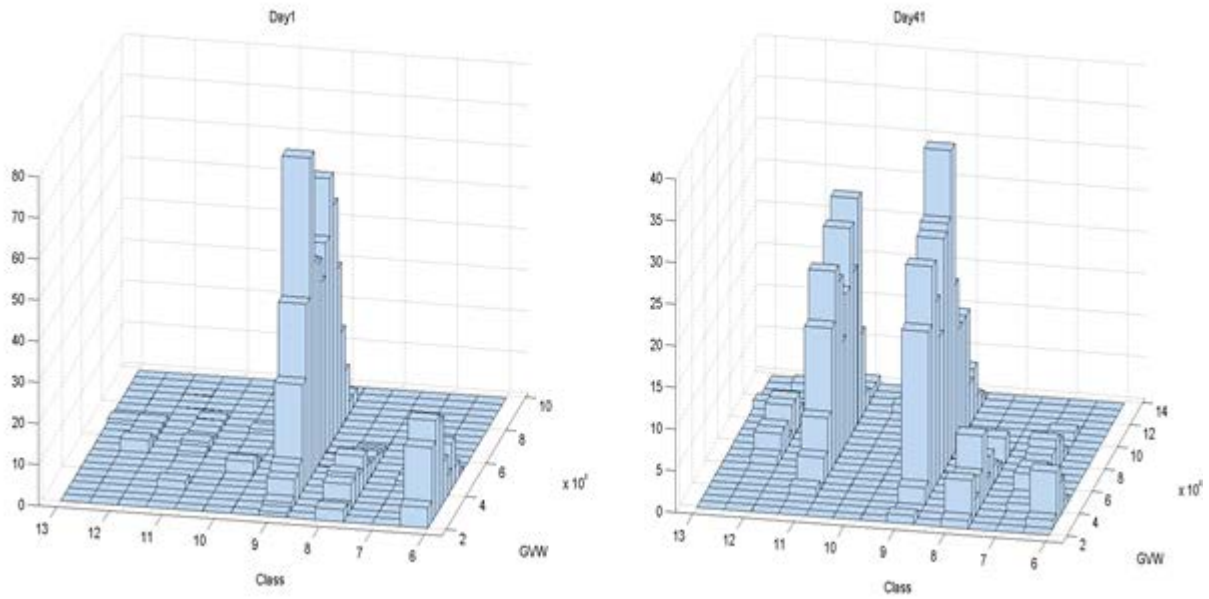


Figure 9.19 Histograms of GWW vs. class for days 1 and 41.

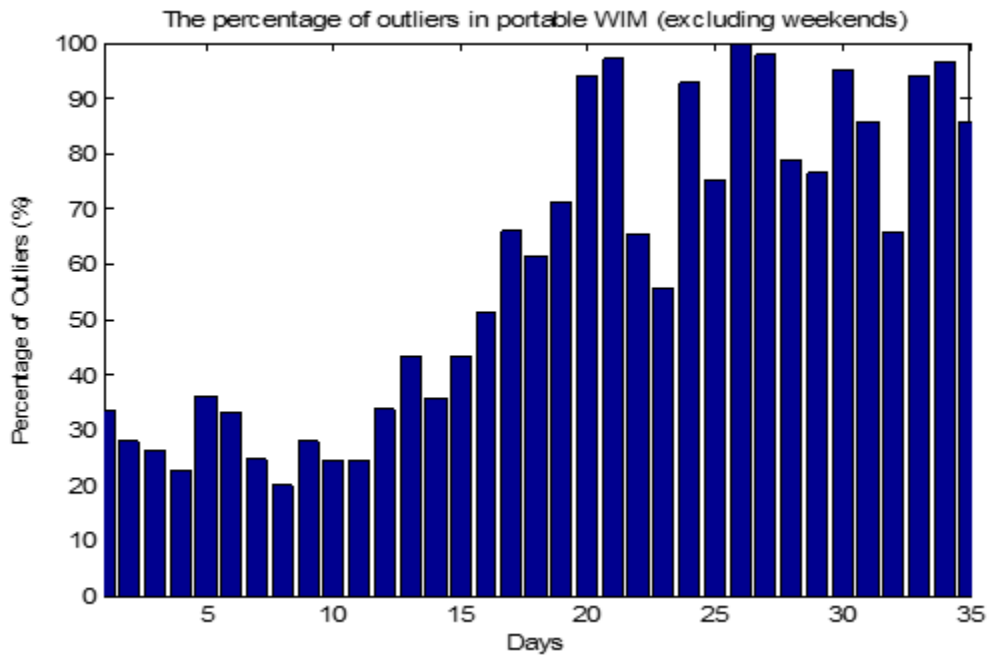


Figure 9.20 Percentage of outliers in portable WIM.

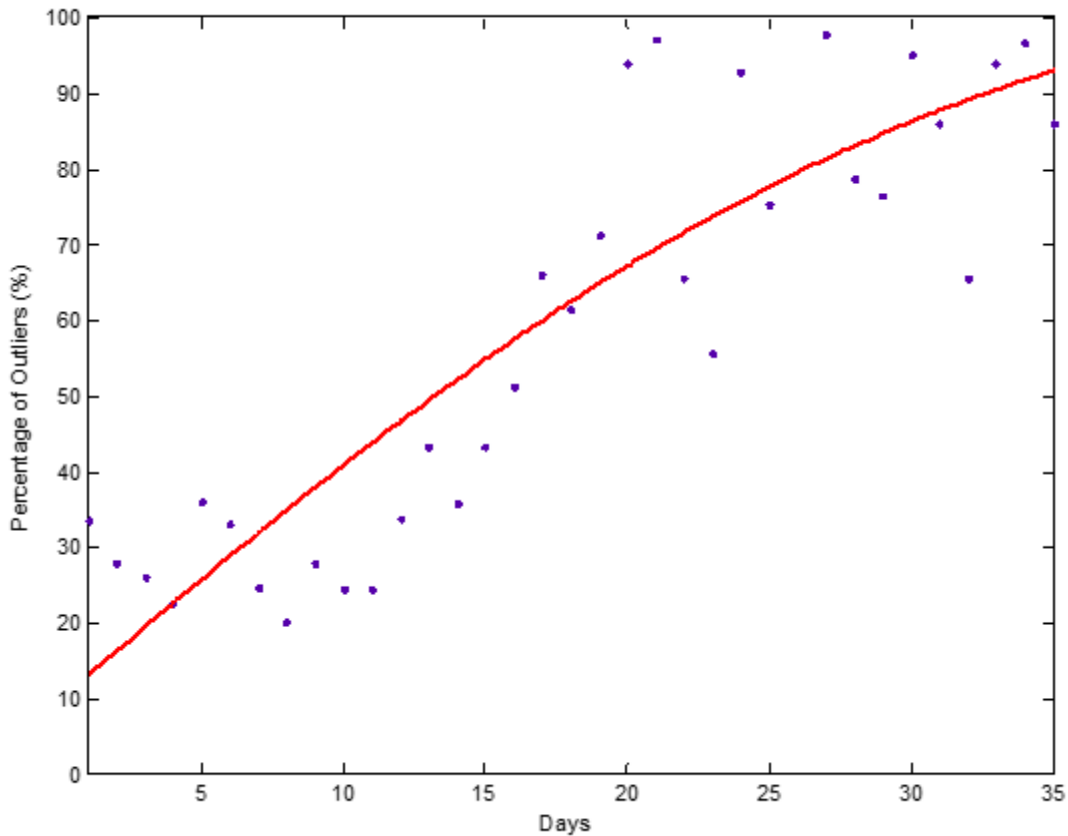


Figure 9.21 The relationship between system performance and time.

9.4 WIM data quality monitoring software

This section present the software developed to automate monitoring site calibration. Many statistical and quality assurance algorithms back this software. ODOT personnel are alerted when a site provides poor WIM data due to miscalibration.

9.4.1 Software architecture

The research team laid the full architecture of the WIM monitoring software. This software monitors data quality retrieved from WIM sites, including classification and weight validation. The software also monitors deviation of weight recorded for class 9 vehicles from the mean of its historical values. Quality of classification results recorded by the WIM site is monitored, as well. ODOT personnel are notified when WIM data quality is not sound due to miscalibration or misclassification.

A centralized software written in C# monitors WIM data quality. This is realized by reading each WIM file data generated daily by the WIM sites deployed across the state of Oklahoma. The software then extracts the daily count and weight data of each vehicle class for comparison with historical values recorded on each WIM site.

This approach is database-centric validation, where our validation software is comparing the current acquisitioned values with the historical ones to elicit and send an alert if data quality degrades.

After the WIM file is processed, there are two options for exploiting the statistical methods researched and described in previous reports to achieve WIM quality monitoring. We can either embed in our C# software the statistical control charts mathematical equations to achieve the statistical monitoring of the data quality, or alternatively, utilize existing implementation by Matlab®. Matlab is a high-level computing environment widely adopted by scientists and researchers around the world. Advantages are the richness of libraries available in one context. Statistical control charts are one among many mathematical algorithms included in the program. For example, as the statistical control chart highlights WIM site data as out-of-statistical control on a specific date, the monitoring software send alerts to designated ODOT personnel via text-messages or emails. The block diagram shown in Figure 9.22 illustrates the architecture of monitoring software. This software activity diagram describes the sequence of the monitoring software functionalities.

9.4.2 Software Implementation

The research team implemented WIM monitoring software that monitors WIM data quality, including vehicle classification and weight. The software detects deviation of weight recorded for class 9 vehicles from the mean of its historical values. This also observes the quality of vehicles classification recorded by the WIM site. The software alerts ODOT personnel when the WIM data quality is suffering due to miscalibration or misclassification.

We chose to implement the monitoring software in C#.NET because the Dynamic Link Libraries (DLLs) provided by IRD to read the iSINC generated binary files are developed in DotNet. We have previously realized reading of WIM data file within a long-running software. The software's robust performance is achieved by the operating system. The latter is responsible for observing its operations, recycling its resources, and restarting it in the event that it freezes or malfunctions.

Matlab R2012a with C# were the software used to implement calibration monitoring application. Common Object Module (COM) is a well-known technology for realizing inter-software communication. This is achieved when an application establishes a COM server (e.g., Matlab) and waits for system calls, and another software application (C#) that sends requests to the server. In order for tC# software to achieve interaction with Matlab, we added the DLL reference to our project context. The name of the application is "Matlab Application (Version 7.10) Type Library".

The next steps are:

- 1- Through the project attached Matlab DLLs, we created a single Matlab COM server. Although this step takes the most time, once it is created all Matlab Application Programming Interface (API) calls will be directed to the single established COM server.

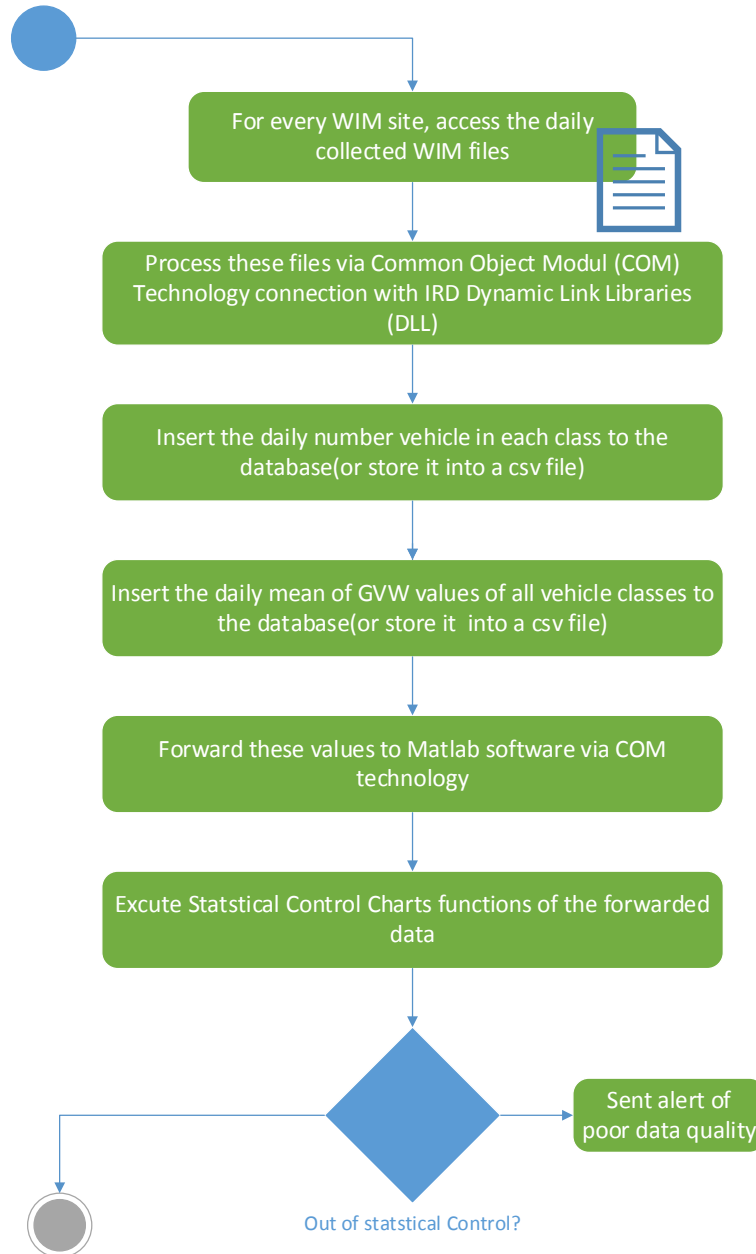


Figure 9.22 WIM quality software architectures

- 2- We created a single instance of Matlab using the *Activator* class, which is a core-system class in DotNet framework capable of creating object types either locally

- or remotely. This class is also used to acquire a reference to an object that is instantiated and allocated-in-memory.
- 3- Create a single Matlab server will tune monitoring software performance and reduce overhead in utilizing computer resources, as every instance of Matlab reserves 220 MB from the heap memory.
 - 4- Using *Put* methods is required to pass command parameters to Matlab. We selected *PutWorkspaceData* method whose signature takes three parameters. First is the chosen name of the new Matlab variable. Second is “base”, and the third is the variable value forwarded to Matlab.
 - 5- Using *GetVariable* method is necessary to acquire a computed variable from Matlab. Although C# is a strongly typed programming language, we chose to receive this value via implicitly typed variable by preceding the creation of this variable with the keyword var. This is important to achieve flexibility and reusability in our implementation of Matlab-to-C# inter-communication.

Given that the Matlab statistical control chart tags a WIM site data as out-of-statistical control, the monitoring software triggers alerts to the designated ODOT personnel. Two methods of notification were implemented: emails and text messages (i.e. Short Message Service (SMS)). Hence, an alert message will be sent to the designated ODOT employees' cell phones and email addresses. The first alerting method was developed using Simple Mail Transfer Protocol (SMTP) implementation in C#.NET. An email from WimDataQuality@gmail.com is sent to all registered ODOT recipients. Software implementation involved creating an SMTP client. The following parameters must be forwarded to the SMPT client: 1- The address and port of the SMTP server (i.e. Gmail and its port); 2- Indicating the usage of Secure Socket Layer (SSL); 3- Passing the credentials of source email account; and 4- Destination email address, message subject, and message body.

The recipient's names and contact information are stored in a database created for that reason. Figure 9.23 shows a normalized sub-database diagram to store the aforementioned information.

Through a GUI, the monitoring software has the capability to add ODOT personnel to the notification list when the WIM data quality becomes inaccurate. Figure 9.24 shows user-interface wherein the software administrator is capable of adding-removing-modifying contacts' information in the system.

Another alerting method was dependent upon Application Programming Interface (API) provided by the SMS gateway company. These APIs facilitate pushing the composed text message to the company's server, and then onto designated cellphone numbers. The provided APIs features a Hypertext Transfer Protocol (HTTP) web request, which formulates messages encoded with Universal Character Set Transformation Format with 8 bits (UTF8). The SMS gateway company will send an okay response if the SMS was successfully delivered.

Final project report

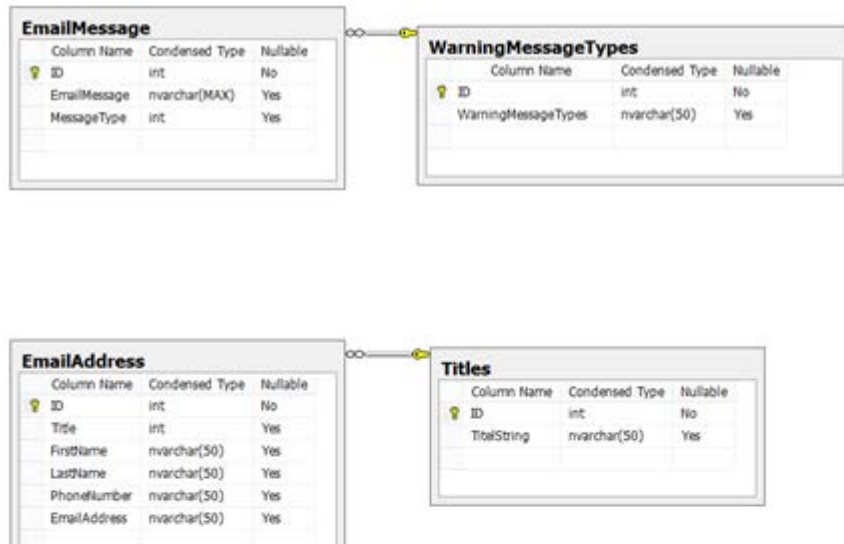


Figure 9.23 Sub-database diagram of the monitoring

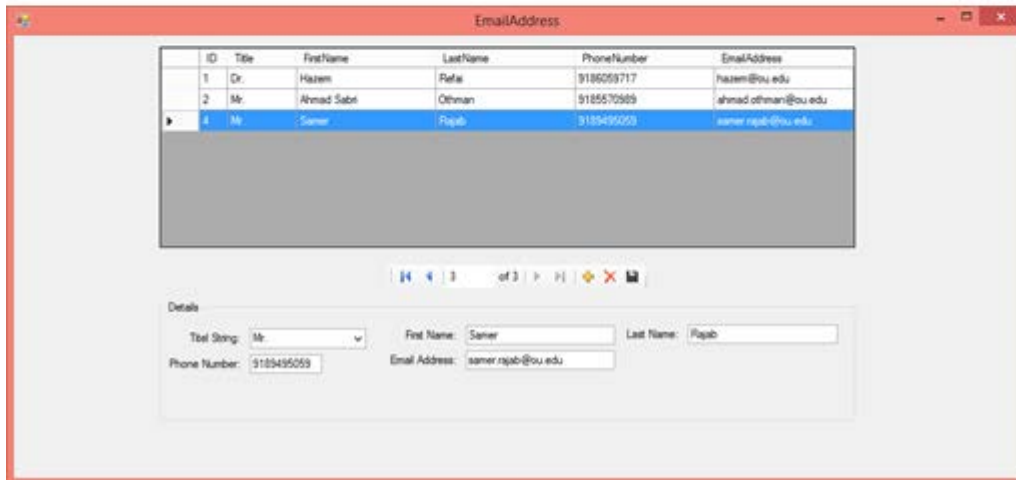


Figure 9.24 Email addresses GUI

Chapter X

10 Conclusion

This report presents results of a newly developed portable WIM system that uses off-the-shelf components and commercially available WIM controllers. The commercial WIM controller used in this project was IRD iSINC Lite. The fabricated portable system could be promoted as an alternative WIM monitoring solution to permanent WIM systems and/or static scale stations, both of which are extremely expensive to install on highways. The portable WIM uses RoadTrax BL piezoelectric class-1 sensors, galvanized metal fixtures equipped with pocket tapes to house the sensors, and a trailer with cabinet to house WIM electronics, batteries, and REECE device for real-time monitoring. The system is solar powered with three 100-Watt panels. Total cost of system is roughly \$20,000.

Many factors influence the accuracy of the WIM measurements made using a portable system. One of these is the piezoelectric BL sensor vibration was determined to be the primary factor for undetected vehicles. Improper installation of the sensor was suspected to allow the sensor to vibrate within its pocket when a vehicle axle impacted it. In turn, the WIM controller detects and registers a large number of ticks due to one axle impact. This results in either over counting or misdetection, depending on the WIM configuration—in particular, the tick filtering threshold. A method to firmly affix the sensor onto the ground was developed and proved successful. Another approach to limit vibration is to reduce the size of the piezoelectric strip (thus reducing its sensing capacity) and position the sensor to cover part of the lane area so only one tire impacts it. Six-foot sensors were found suitable for low vibration deployment. These two techniques provided extended periods of deployments with acceptable portable WIM measurement and data quality.

Default calibration factors used for sensors embedded in the roadway are not suitable for on-ground sensor installation used for portable WIM setups. Doing so causes significant weight error and inaccurate vehicle classification. Hence, portable WIM systems should be calibrated at deployment site. A new calibration is required each time the portable WIM site is changed. It is advised to use calibration factors per speed bin to increase weight accuracy.

The portable WIM system was deployed three times at two locations: US69 highway with pavement-type roadway and US412 with concrete-type roadway. System performance showed acceptable WIM measurement results with only slight variation during the first 15 days of deployment. Portable WIM data was compared to permanent WIM data collected at co-located sites. Error and regression analyses were carried out. Root mean square errors and correlation coefficient were calculated for GVW, speed, classification, FXW, and FXS for each vehicle type. Results indicated a significant error of 29% when comparing portable and permanent GVW. Correlation coefficients were found above 80% for most studied system performance parameters, indicating that portable WIM data is highly correlated with permanent site data.

References

- [1] Oregon Highway Cost Allocation Study, Office of Economic Analysis, 2009. <http://www.oregon.gov/DAS/OEA/highway.shtml>, accessed March 2013
- [2] New Trucks for Greater Productivity and Less Road Wear: An Evaluation of the Turner Proposal, Transportation Research Board Special Report 227, ISBN 0-309-04963-6, 1990.
- [3] American Association of State Highway and Transportation Officials (AASHTO), Virtual Weigh-in-Motion: A “WIM-win” for transportation agencies, <http://www.transportation.org/sites/aashtotig/docs/021907%20Short%20Version.pdf>, February 2007.
- [4] FHWA Concept of Operations for Virtual Weigh Station, 2009 http://ops.fhwa.dot.gov/publications/fhwahop09051/virtual_weigh_stn.pdf, accessed March 2013.
- [5] Standard specification for highway weigh-in-motion (WIM) systems with user requirements and test methods, American Society For Testing and Materials (1994).
- [6] McCall, B., and W. Vodrazka, Jr. States’ Successful Practices Weigh-in-Motion Handbook, Center for Transportation Research and Education, Ames, IA, December 1997.
- [7] Quinley, R. “Installation of Weigh-in-Motion Systems,” Presentation for the National Traffic Data Acquisition Conference, Albuquerque, NM, May 1996.
- [8] Dan Middleton, Ron Whi, Jason Crawford, Ricky Parker, Jongchul Song, and Carl Haas Investigation for Traffic Monitoring Equipment Evaluation Facility, FHWA Report No. 0-4664-3, January 2007. <http://www.fhwa.dot.gov/ohim/tvtw/vdstits.pdf>, accessed March 2013
- [9] Papagiannakis, T. and D. K. Senn (1995). WIM system calibration using AVI-equipped vehicles. Vehicle Navigation and Information Systems Conference, 1995. Proceedings. In conjunction with the Pacific Rim TransTech Conference. 6th International VNIS. 'A Ride into the Future'.
- [10] Rakha, H., B. Katz, et al. (2003). Field evaluation of weigh-in-motion screening on truck weigh station operations. Intelligent Vehicles Symposium, 2003. Proceedings. IEEE.
- [11] Yi, S., B. Yunfeng, et al. (2008). Study on Weigh-in-Motion System Based on Chaos Immune Algorithm and RBF Network. Computational Intelligence and Industrial Application, 2008. PACIIA '08. Pacific-Asia Workshop on.

- [12] Juncheng, X. and L. Pengmin (2009). Application of Wavelet Transform in Weigh-in-Motion. Intelligent Systems and Applications, 2009. ISA 2009. International Workshop on.
- [13] Mc Cormack, B., D. Geraghty, et al. (2005). Design and Manufacture of Surface Acoustic Wave Sensors for Real-Time Weigh-in-Motion. Instrumentation and Measurement Technology Conference, 2005. IMTC 2005. Proceedings of the IEEE.
- [14] Cebon, D2001: 'WAVE Report of WP1.1: Multiple Sensor WIM',
- [15] Hill, D. J., P. J. Nash, et al. (2002). Vehicle weigh-in-motion using multiplexed interferometric sensors. Optical Fiber Sensors Conference Technical Digest, 2002. OFS 2002, 15th.
- [16] Ronghui, Q., G. Jianxin, et al. (2008). Optic fiber-based dynamic pressure sensor. Optical Fiber Sensors Conference, 2008. APOS '08. 1st Asia-Pacific.
- [17] Leming, S. K. and H. L. Stalford (2002). Bridge weigh-in-motion system development using static truck/bridge models. American Control Conference, 2002. Proceedings of the 2002.
- [18] Leming, S. K. and H. L. Stalford (2003). Bridge weigh-in-motion system development using superposition of dynamic truck/static bridge interaction. American Control Conference, 2003. Proceedings of the 2003.
- [19] Applications of Fiber Optic Sensors in Weigh-in-motion (WIM) systems for monitoring Truck Weights on Pavements and structures, <http://nmshtd.state.nm.us/upload/images/Research/NM97ITD02WIMApplications2003.pdf>, accessed March 2013
- [20] IRD DAW300PC: http://www.irdinc.com/products/pdf/DAW300PC-Bluetooth_1108.pdf , accessed March 2013
- [21] TDC Captels: <http://www.tdcsystems.co.uk/uploads/pdfs/products/TDC-Captels-Portable-Weighing-System.pdf>, accessed March 2013
- [22] Oak Ridge National Laboratory: <http://www.ornl.gov/>, accessed March 2013.
- [23] "WEIGH-IN-MOTION RESEARCH AND DEVELOPMENT ACTIVITIES AT THE OAK RIDGE NATIONAL LABORATORY", <http://www.csiir.ornl.gov/projects/documents/wim4-1.pdf>, accessed March 2013.
- [24] R. K. Abercrombie, D. L. Beshears, L. M. Hively, M. B. Scudiere, and F. T. Sheldon with the Oak Ridge National Laboratory , James L. Schmidhammer and Jeff Vanvactor with University of Tennessee , "Prototype Weigh-In-Motion Performance", <http://info.ornl.gov/sites/publications/files/Pub5887.pdf>, accessed March 2013.

- [25] Development of a Weigh-Pad Based Portable WIM System, Prof. Taek Kwon, University of Minnesota, Duluth <http://www.dot.state.mn.us/research/TS/2012/2012-38.pdf> , accessed March 2013.
- [26] Carlo Tomasi. Estimating Gaussian Mixture Densities with EM – A Tutorial. Duke University.
- [27] Yair Weiss. Motion Segmentation using EM - a short tutorial. MIT E10-120, Cambridge, MA 02139, USA.
- [28] Chen-Fu Liao, Gary A. Davis. Traffic Data Quality Verification and Sensor Calibration for Weigh in Motion. University of Minnesota
- [29] Abryan J. Katz, Hesham A. Rakha. Field Modeling Framework and Case Study of Truck Weigh Station Operations. Virginia Tech Transportation Institute, 2012.
- [30] Miao Xie, Jiankun Hu, Biming Tian. Histogram-Based Online Anomaly Detection in Hierarchical Wireless Sensor Networks. Trust, Security and Privacy in Computing and Communications (TrustCom), 2012 IEEE 11th International Conference
- [31] Rui Zhang, Ping Ji, Dinkar Mylaraswamy, Mani Srivastava, and Sadaf Zahedi. Cooperative Sensor Anomaly Detection Using Global Information. Tsinghua Science and Technology. ISSN11007-0214/01/11pp209-219
- [32] Orna Raz, Rebecca Buchheit, Mary Shaw, Philip Koopman, Christos Faloutsos. Detecting Semantic Anomalies in Truck Weigh-In-Motion Traffic Data Using Data Mining. Carnegie Mellon University